João Pedro Matias Filipe

Licenciado em Engenharia Eletrotécnica e de Computadores

Performance Evaluation of Low Complexity Massive MIMO Techniques for SC-FDE Schemes

Dissertação para a obtenção do grau de Mestre em
Engenharia Eletrotécnica e de Computadores

Orientador: Dr. Rui Miguel Henrique Dias Morgado Dinis, Professor Associado com agregação no Departamento de Telecomunicações da Faculdade de Ciências e Tecnologia - Universidade Nova de Lisboa e Investigador Científico no Instituto de Telecomunicações (Portugal)

Co-orientador: Dr. Santiago Zazo Bello, Professor Catedrático e Investigador Científico no Grupo de Aplicações e Processamento de Sinal do Departamento de Sinais, Sistemas e Radiocomunicações da Escola Técnica Superior de Engenheiros de Telecomunicações - Universidade Politécnica de Madrid (Espanha)

Júri:

Presidente: Dr. João Francisco Alves Martins - FCT/UNL

Arguente: Dr. Luís Filipe Lourenço Bernardo - FCT/UNL

Vogal: Dr. Rui Miguel Henriques Dias Morgado Dinis - FCT/UNL

FACULDADE DE CIÊNCIAS E TECNOLOGIA
UNIVERSIDADE NOVA DE LISBOA

Setembro, 2018

Performance Evaluation of Low Complexity Massive MIMO Techniques for SC-FDE Schemes

Dedico esta obra às mais importantes pessoas da minha vida, os meus Pais, Irmão e Avós, por todo o amor e tempo dedicado, bem como pela confiança que em mim depositaram e pela ajuda e apoio que sempre me deram, proporcionando-me sempre e incondicionalmente, mais e melhores condições durante o meu percurso académico.

Agradecimentos

Quero expressar a minha gratidão à coordenação de curso do Mestrado Integrado em Engenharia Eletrotécnica e de Computadores, Professora Helena Fino, pela disponibilidade e por toda a orientação escolar que sempre me deu, especialmente nos dois últimos anos do mestrado. À equipa da Secção de Acolhimento e Mobilidade da Divisão Académica da FCT-UNL, especialmente à Dra. Ana Dallot agradeço por toda a prestabilidade e disponibilidade na resolução dos problemas, imprevistos e em todas as dificuldades que surgiram nas minhas candidaturas Erasmus, e que, com o maior profissionalismo e amizade, sempre as conseguiu contornar para tornar possível e levar a bom porto as minhas duas experiências internacionais, respetivamente no ano de 2016 e em 2017/2018. Agradeço também à Direção Geral do Ensino Superior (DGES) e aos Serviços de Ação Social (SAS) da Universidade Nova de Lisboa (UNL) pela atribuição das bolsas de mobilidade Erasmus que me foram concedidas para as minhas estadias no estrangeiro no contexto dos programas de mobilidade internacional 'Erasmus+, Student Mobility for Studies', os quais foram experiências que em muito me enriqueceram e que contribuíram para a minha formação e evolução enquanto indivíduo, ao nível do meu crescimento pessoal, académico e, creio, futuramente a nível profissional, tendo mudado a minha perceção e visão sobre o mundo e sendo, definitivamente, dois marcos muito importantes na minha vida.

Aos professores, amigos e demais pessoas integrantes nos dois percursos de intercâmbio pelo estrangeiro, com quem entrei em contacto e partilhei imensas experiências enriquecedoras, nomeadamente em Budapeste – Hungria (2016) e em Madrid – Espanha (2017/2018).

O meu especial agradecimento ao meu orientador, Prof. Rui Morgado Dinis, e ao meu co-orientador, Prof. Santiago Zazo Bello, por toda a disponibilidade, ajuda e dedicação que sempre tiveram para comigo na elaboração desta Tese de Mestrado.

Finalmente, a todos aqueles que sempre lutaram por mim e que me ajudaram a alcançar o que consegui até hoje, a minha mãe Lídia, o meu pai José e o meu irmão Diogo. À minha restante família e aos amigos mais próximos do denominado "Grupo do SAL". A todas as pessoas que considero importantes e essenciais na minha vida pessoal. A todos os amigos, colegas e companheiros da Universidade Nova de Lisboa, com quem tive o prazer de partilhar muitas e boas convivências ao longo da vida académica, os quais foram pessoas francamente determinantes nos momentos de maior resiliência, contribuindo para o que sou hoje e para o meu futuro e sucesso.

Abstract

Massive-MIMO technology has emerged as a means to achieve 5G's ambitious goals; mainly to obtain higher capacities and excellent performances without requiring the use of more spectrum. In this thesis, focused on the uplink direction, we make a study of performance of low complexity equalization techniques as well as we also approach the impact of the non-linear elements located on the receivers of a system of this type. For that purpose, we consider a multi-user uplink scenario through the Single Carrier with Frequency Domain Equalization (SC-FDE) scheme. This seems to be the most appropriate due to the low energy consumption that it implies, as well as being less favorable to the detrimental effects of high envelope fluctuations, that is, by have a low Peak to Average Power Ratio (PAPR) comparing to other similar modulations, such as the Orthogonal Frequency Division Multiplexing (OFDM). Due to the greater number of antennas and consequent implementation complexity, the equalization processes for Massive-MIMO schemes are aspects that should be simplified, that is, they should avoid the inversion of matrices, contrary to common 4G, with the Zero Forcing (ZF) and Minimum Mean Square Error (MMSE) techniques. To this end, we use low-complexity techniques, such as the Equal Gain Combining (EGC) and the Maximum Ratio Combining (MRC). Since these algorithms are not sufficiently capable of removing the entire Inter-Symbol Interference (ISI) and Inter-User Interference (IUI), we combine them with iterative techniques, namely with the Iterative Block with Decision Feedback Equalizer (IB-DFE) to completely remove the residual ISI and IUI. We also take into account the hardware used in the receivers, since the effects of non-linear distortion can impact negatively the performance of the system. It is expected a strong performance degradation associated to the high quantization noise levels when implementing low-resolution Analog to Digital Converters (ADCs). However, despite these elements with these configurations become harmful to the performance of the majority of the systems, they are considered a desirable solution for Massive-MIMO scenarios, because they make their implementation cheaper and more energy efficient. In this way, we made a study of the impact in the performance by the low-resolution ADCs. In this thesis we suggest that it is possible to bypass these negative effects by implementing a number of receiving antennas far superior to the number of transmitting antennas.

Keywords: Massive MIMO; SC-FDE; 5G; Low resolution ADCs; Energy efficiency; Low complexity equalizers.

Resumo

O esquema MIMO Massivo surge como um meio para atingir os objetivos do 5G, cuja principal característica é o alcance de maior capacidade e excelentes desempenhos, sem para tal requerer mais espectro. Nesta tese simulamos um cenário uplink e fazemos um estudo de desempenho de técnicas de equalização de baixa complexidade. É ainda abordado qual o impacto na performance por parte dos elementos não lineares presentes nos receptores de um sistema deste tipo. Para este propósito, consideramos um cenário uplink multi-utilizador implementado através de uma mono portadora com equalização no domínio da frequência (SC-FDE). Esta modulação é a mais adequada devido ao seu baixo consumo energético e menor propensão aos efeitos prejudiciais das altas flutuações de envolvente, ou seja, por ter um baixo rácio entre a potência-máxima e a potência-média (PAPR) comparando com a multiplexação por divisão de frequências ortogonais (OFDM). Devido ao maior número de antenas e complexidade, a equalização para esquemas MIMO Massivo deve ser simplificada, ou seja, deve evitar a inversão matricial contrariamente ao que ocorre no 4G com equalização linear: Zero Forcing (ZF) e Minimum Mean Squared Error (MMSE). Para tal, nesta tese usamos técnicas de baixa complexidade, tais como o Equal Gain Combining (EGC) e o Maximum Ratio Combining (MRC). Uma vez que estes algoritmos não são capazes de remover toda a interferência inter-simbólica (ISI) e inter-utilizador (IUI), combinámos estes algoritmos com técnicas iterativas, nomeadamente a Equalização Iterativa por Feedback implementada no Dominio da Frequência (IB-DFE) para assim, remover a interferência residual. Os efeitos negativos da distorção não-linear causada pelos Conversores Analógico-Digital (ADCs) é outro aspecto importante dos receptores. Fortes degradações de desempenho estão associadas aos altos níveis de ruído de quantização quando se implementam ADCs de baixa-resolução. No entanto, apesar destes elementos com baixas resoluções se tornarem prejudiciais ao desempenho da maioria dos sistemas, são, todavia, considerados uma solução viável em cenários de MIMO Massivo visto que tornam a sua implementação mais barata e eficiente. Deste modo, fazemos um estudo do impacto na performance pelos ADCs de baixa-resolução, sendo sugestivo e verificável que é possível contornar estes efeitos negativos implementando um número de antenas receptoras muito superior ao número de antenas transmissoras.

Palavras-chave: MIMO Massivo; SC-FDE; 5G; ADCs de 1 bit; Eficiência energética; Equalização de baixa complexidade.

Content

List of figures

Acronyms

1G - First Generation of Mobile Communications

2G - Second Generation of Mobile Communications

3G - Third Generation of Mobile Communications

4-PSK - Quadrature Phase Shift Keying

4G - Fourth Generation of Mobile Communications

5G - Fifth Generation of Mobile Communications

8-PSK - Octogonal Phase Shift Keying

ADC - Analog to Digital Converter

ADSL - Assymetric Digital Subscriber Line

AMPS - Mobile Phone System

AWGN - Additive White Gaussian Noise

BER - Bit Error Rate

BS - Base Station

CDMA - Code Division Multiple Acess

CEPT - Confederation of European Posts and Telecommunications

CP - Cyclic Prefix

CSI - Channel State Information

DAC - Digital to Analog Converter

DFE - Decision Feedback Equalization

DFT - Discrete Fourier Transform

DL - Downlink

DS - Delay Spread

EDGE - Enhanced Data Rates for GSM Evolution

EGC - Equal Gain Combining

FD - Frequency Domain

FDD - Frequency Division Duplex

FDE - Frequency Domain Equalization

FDM - Frequency Division Multiplexing

FDMA - Frequency Division Multiple Acess

FFT - Fast Fourier Transform

GMSK - Gaussian Minimum Shift Keying

GSM - Groupe Speciale Mobile

IB-DFE - Iterative Block with Frequency Domain Equalization

ICI - Inter Channel Interference

IDFT - Inverse Discrete Fourier Transform

IFFT - Inverse Fast Fourier Transform

IID - Independent Identically Distribution

IS-95 - Interim Standard 95

ISDN - Integrated Services Digital Network

ISI - Inter Symbol Interference

IUI - Inter User Interference

IoT - Internet of Things

IP - Internet Protocol

LLR - Log Likelihood Ratio

LTE - Long Term Evolution

MFB - Matched Filter Bound

MIMO - Multiple Input Multiple Output

MISO - Multiple Input Single Output

MLSE - Maximum Likelihood Sequence Estimation

MMSE - Minimum Mean Squared Error

MRC - Maximum Ratio Combining

MSB - Most Significant Bit

MSE - Mean Squared Error

MT - Mobile Terminal

MU - Multi-User

MU - MIMO - Multi User Multiple Input Multiple Output

NSR - Noise to Signal Ratio

OFDM - Orthogonal Frequency Division Multiplexing

OFDMA - Orthogonal Frequency Division Multiple Access

PA - Power Amplifier

PAPR - Peak-to-Average Power Ratio

QAM - Quadrature Amplitude Modulation

QPSK - Quadrature Phase Shift Keying

QoS - Quality of Service

R - Number of receivers

RF - Radio Frequency

Rx - Receiver Antennas

SC - Single Carrier

SC-FDE - Single Carrier with Frequency Domain Equalization

SC-FDMA - Single Carrier Frequency Domain Multiple Access

SIMO - Single Input Multiple Output

SINR - Signal to Interference and Noise Ratio

SISO - Single Input Single Output

SNR - Signal-to-Noise Ratio

SQNR - Signal-to-Quantization Noise Ratio

SU - Single-User

T - Number of Transmitters

TD - Time Domain

TDD - Time Division Duplex

Tx - Transmitter Antennas

UL - Uplink

UMTS - Universal Mobile Telecommunications System

WCDMA - Wide-Band Code-Division Multiple Acess

WLAN - Wireless Local Area Network

ZF - Zero Forcing

1. Introduction

1.1 Context and Motivation

Over the past generations, there has been a significant evolution in mobile communications and in the transmission techniques applied in each of these generations. The block transmission techniques, as Orthogonal Frequency Division Multiplexing (OFDM) and the Single Carrier with Frequency Domain Equalization (SC-FDE), have been employed regularly in scenarios whose transmission channel is severely time-dispersive. The implementation of such techniques have been combined with schemes where multiple antennas are used in the transmitter side and in the receiver side. These Multiple Input Multiple Output (MIMO) systems were developed to perform higher rates and overcome the need for fast and reliable communication links. These models become especially interesting due to the fact that there is an exponential increase in the speed of transmission and in the capacity of telecommunications systems, a characteristic that is more and more requested due to the current level of technological evolution to which electronic devices are subject daily, as well as the applications that are proving to be more and more expensive in the processing resources. In today's world, the number of devices that are connectable to the communication networks in operation, increases exponentially day by day. The need for high data transmission rates, has also increased the impact of multipath propagation effect as well as the Inter Symbol Interference (ISI), facts which make the development of more evolved equalization methods necessary. Before 1990s, the multipath propagation effect has been considered one of the main obstacles to achieve higher transmission rates. This undesirable, but natural effect, occurs due to the different delays originated with the severall different reflections and interferences in the propagation of the signal through out the transmission channel. The different delays, due to the obstacles and interferences, provoke the so called ISI. Expressing this effect in the Time Domain (TD), we can consider that the Delay Spread (DS) is the time measure between the first and the last arriving signals. This measure is used to calculate the necessary Cyclic Prefix (CP), which consists in the guard time interval needed to be introduced between the transmitted symbols to prevent the occurrence of ISI. The use of the CP between the transmitted symbols leads to more limitations in the transmission data throughput **[1]**. The multipath propagation effect, occurred in time domain, can lead the system to be sensitive to frequency selective fading, when the bandwidth of the signal is larger than the coherence bandwidth.

In this thesis we will focus on the Uplink (UL) transmission. It is of major importance to take into account the energy efficiency in the transmission process, since it is a critical aspect in cell-phones, the onwards called Mobile Terminals (MT). Taking this fact into account, although usual because of his great performances, the OFDM modulation technique is not suitable to be used in the UL direction, due to its high complex envelope fluctuations that lead to a high Peak to Average Power Ratio (PAPR) **[2]**. Therefore, the SC-FDE, which avoids the undesirable PAPR, surges as an option to the UL since it has similar results to OFDM **[3]**.

The next generation of wireless communication systems is expected to reach even larger speeds and capacity of users, as well as it is intended to perform transmissions with less latency. In order to achieve these 5th Generation (5G) objectives, the Massive Multiple Input Multiple Output (Massive-MIMO) architecture is assumed to be the ideal strategy, already with some proven results of great performances **[4] [5]**. The implementation of Massive-MIMO systems, where hundreds or even thousands of transmitter and receiving antennas are used, brings a lot of advantages but, despite that, it can also imply a greater complexity and become especially problematic at the level of the receivers, during the signal equalization. In MIMO systems, during the equalization process, the operation of removing the channel effect, usually implies the inversion of the received data matrix. Thus, when the scale of a MIMO system is increased to a Massive-MIMO system, the channel matrices will be of a much larger size, so that the "normal" inversions in a MIMO system become something very undesirable and impractical in this type of system. The efficient equalization techniques such as Zero Forcing (ZF) and the Minimum Mean Squared Error (MMSE) become algorythms that are impractical in this scenarios. Thus, the need arises to develop distinct approaches that do not entail so much difficulty of execution with this evolved scenario. In this view, the use of low complexity receivers such as the Maximum Ratio Combining (MRC) and Equal Gain Combining (EGC) becomes as suitable options since they are simpler, even being these techniques less efficient than the previously refered. These equalization methods avoid carrying out these matrix inversion operations which entail enormous processing costs. Then, this thesis focus in the application of these low complexity equalization techniques, coupled with the association of iterative feedback schemes which are good in deal with the ISI and Inter User Interference (IUI). The Iterative Block Decision Feedback Equalization (IBDFE) works in an iterative fashion that leads to an enhancement in the performance as the iterations number increases. The objective is to put the capabilities of the IBDFE together with the low complexity algorythms MRC and EGC doing a joint solution. Since this thesis is focused in the receiver side, it also becomes pertinent to approach the Analog to Digital Converters (ADCs) that are needed in the receivers. These elements introduce Nonlinear Distortion Effects in the transmitted signals consonant the adopted number of bits of resolution. However, this distortion penalty tends to be

minimized when considering a scenario where we employ a much larger number of receiving antennas than the transmiting ones **[6]**.

1.2 Objectives

In this document, a general approach will be made to the characteristics inherent to the mobile generations of the recent past and, in detail, a sequential description of transmission and reception technologies using the most advanced techniques and schemes.

We intend to provide a detailed description of possible approaches to implement the next generation of mobile communications: the so-called 5G. A distinct set of receiving techniques are described through a MIMO system. In evolving the scale of implementation of MIMO systems, it is pertinent to describe Massive-MIMO systems where there is a significant increase in the number of the used antennas. A detailed study will be conducted for a Massive-MIMO system considering the UL with the SC-FDE modulation. We will approach the main characteristics, advantages, disadvantages, potentialities and limitations of these models. The main objective is to compare the different types of receivers and understand the potential they have in the Massive-MIMO context. Emphasis is placed on low complexity receivers, namely the Maximum Ratio Combiner (MRC), and the Equal Gain Combiner (EGC). However, other algorithms, such as the Zero Forcing (ZF) and MMSE (Minimum-Square Error), as well as the Iterative Block Decision Feedback Equalizer (IB-DFE) based on the MMSE algorithm, are studied and analyzed because they are part of the implementation of a joint solution that can be applicable in perfect and imperfect channels in Massive-MIMO scenarios. The combination of the low complexity algorithms with the iterative algorithms is addressed and is the main focus of this thesis. It is intended to make a study of a multi-user scenario in which each user only has one broadcast antenna, and the receiver is a Base Station (BS) with several receiving antennas. A performance and comparison evaluation will be done between the different receivers, contrasting different scenarios where the number of transmitter and receiver antennas that are employed is varied, as well as other factors inherent to the equalization algorithms themselves, such as the number of iterations used in the iterative equalization. Firstly, an analysis is made without the impact of non-linear elements, considering only the signal sending, the modulation and the reception (where the equalization is done). Subsequently, it is considered the implementation of the ADCs in the receivers, elements which causes the introduction of non-linear distortion effects on the sent signals. The ADCs incorporated in the receivers are of great importance in all data processing, and in this thesis, a greater emphasis will be given to the study of how standard saturation levels, as well as the number of resolution bits of each element, may or may not influence the transmission performance of

signals that are received and need to be preprocessed prior to equalization. The study of impact of the nonlinearities on the transmitted signals is done in an analogous way to the study where they are not considered, i.e., they are considered in several types of scenario where the variation in the number of transmitter and receiver antennas is made. All the performance results are obtained through Monte-Carlo simulations, where we obtain a Bit Error Rate (BER) graphic in function of the Signal-to-Noise Ratio (SNR). Finally, the objective is to show the importance that the high ratio between receiving and transmitting antennas has in the compensation of the negative effects of nonlinear distortion, thus showing that low-resolution ADCs are plausible for Massive-MIMO scenarios.

1.3 Organization

This thesis is organized in 8 different chapters. After this first chapter of introduction, the Chapter 2 contains the State of the Art where we approach the charachteristics of the Mobile Networks. We emphasize the modulations used in the Long Term Evolution (4G) that serves as a basis to the future 5G, namely the OFDM and the SC-FDE, the basis to this thesis. In the Chapter 3 is described how important are the diversity techniques and is also made a detail about the transmission and reception of signals in the broadband wireless systems. The MIMO and Massive-MIMO technologies are conveniently addressed, since, this last, is the main theme of work in this thesis. In Chapter 4 are described the proposed equalization techniques, namely the low complexity algorithms, of major importance to this work, associated with the iterative equalization schemes. In chapter 5 we present the Non-linear effects and the hardware elements, in this case the ADCs, which are known by provoke a negative impact in the systems performance, with their implementation made in the receivers. In the Chapter 6 we present all the performance experimental results, firstly without considering the imposing of non-linear distortion effects, and after, with that imposition, doing a variation in severall parameters, as the number of antennas, number of iterations by the iterative equalization techniques, or the number of resolution bits and the clipping level effects. Finally, in Chapter 7 we present the conclusions about this thesis and the possible future work to explore in this addressed matter.

2. State of the Art

2.1 Fourth Generation of Mobile Communications (LTE) - 4G

The 4G appears on scene presenting herself as a set of standard measures and is proposed with very specific objectives to succeed the 3G. The Long Term Evolution (LTE) by itself suggests that the goals to be achieved in this generation will not be achieved from the start in a single time, but gradually, rather the years ahead and the development of new emerging technologies. LTE has come about because of the natural, fast and constantly revolutionary evolution of technology. Applications designed for mobile devices are increasingly reminiscent of data resources, and users are increasingly craving for faster and better Internet services to respond to those same applications. In this way, mobile communications systems have had to adapt to developments in the technological world in a way that can respond effectively to this huge demand of data-rates. The new 4G system was proposed to evolve the existing Universal Mobile Telecommunications System (UMTS) network, allowing communications over the Internet through the Internet Protocol (IP), as already existing in previous generations, although in a much faster, reliable and secure way. Services such as video chat, streaming, high-definition television on the mobile phone and the many other services available on the Internet should also be achieved on mobile devices. Some of the proposed objectives for the 4G were:

- Enhancement of the dynamic capacity of the system, allowing the allocation of more users simultaneously in a cell;

- Coexistence with existing systems, i.e., combining narrow band systems (200 kHz GSM) and broadband systems (5MHz Wide-Band Code-Division Multiple Acess (WCDMA));

- Reduce the latency between communications, providing a faster response in the communication between users and the network;

- Increase or even attempt to maximize spectral efficiency;

- Flexibility and dynamism in the assignment of the frequency band available according to the services that are required by the users at a given moment;

- A fully IP network, with packet-only switching and thus more simplified;

- Optimization of the power efficiency of the mobile terminals with consequent saving in terms of energy levels of the batteries;

The development of the LTE system began with the approach taken in a 3rd Generation Partnership Project (3GPP) study in 2004 in Canada. This joint collaboration of the mobile communications industry organizes and manages the development of standards for mobile communications systems. The new system should have a distinct and more comprehensive / manipulable architecture with the existing radio Technologies, in terms of multiple access and multiplexing. The evolution of WCDMA was not enough, due to the large bandwidth that would be used and the complexity that this would entail, so it became imperative to design a whole new system **[7].**

Thus, two new technologies emerge to the sceene and would come to be implemented; the first one for Downlink (DL), the Orthogonal Frequency Division Multiple Access (OFDMA), based on OFDM and the another one to do the UL transmission, namely the Single Carrier Frequency Domain Multiple Access (SC-FDMA), based on SC-FDE. The terms Multiple Access arise in the LTE because of the strategy adopted to increase system capacity by multiplexing more users by dividing the frequency assignment (groups of frequency bandwidths) in the case of SC-FDE and individual sub-carriers in the case of OFDM, respectively at different time intervals and in different channels, thus giving a more dynamic and maximized use of the system. OFDM and SC-FDE are the "single user" or the "basis" versions.

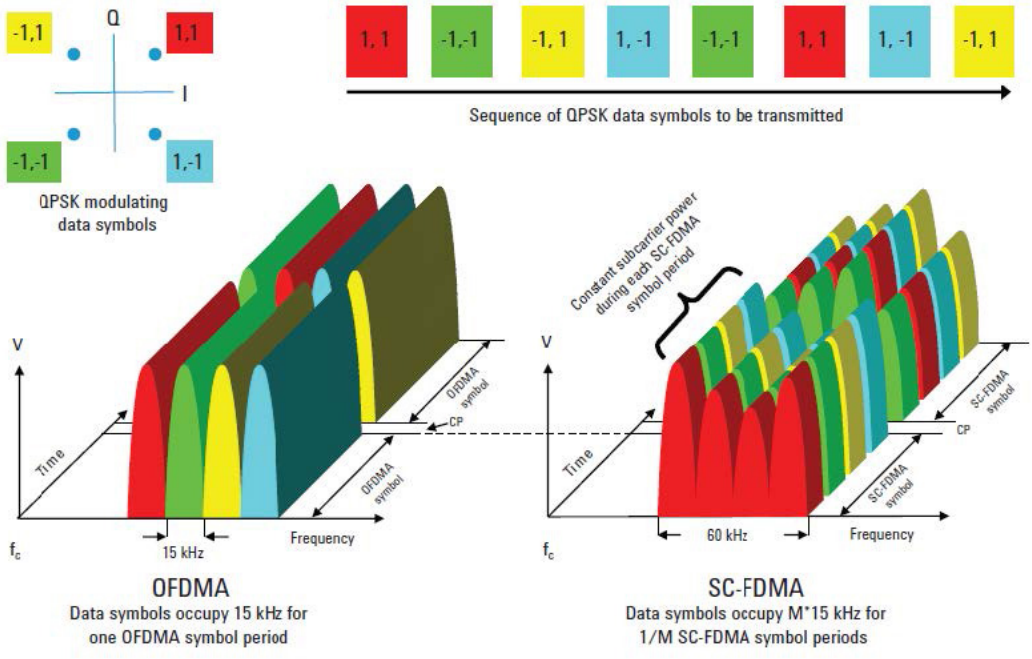

Fig. 2.1: Representation of a OFDMA transmission versus a SC-FDMA transmission.

(Source: [8])

2.2 OFDM - Orthogonal Frequency Division Multiplexing

The OFDM consists of a frequency division multiplexing technique in which the spectrum of the subcarriers frequencies is partially overlapping one another, rather than being positioned consecutively, side by side (parallel) to one another, as in Frequency Division Multiple Acess (FDMA). The main objective with this technique of overlapping carrier waves is to save or to take the maximum advantage of the frequencies of the available bandwidth. Although this overlap occurs, the subchannels are associated with frequencies that are orthogonal to each other, thus making it possible to make a complete and efficient recovery of the signal that was sent, and that finally reaches the receiver, without compromising the quality of the signal.

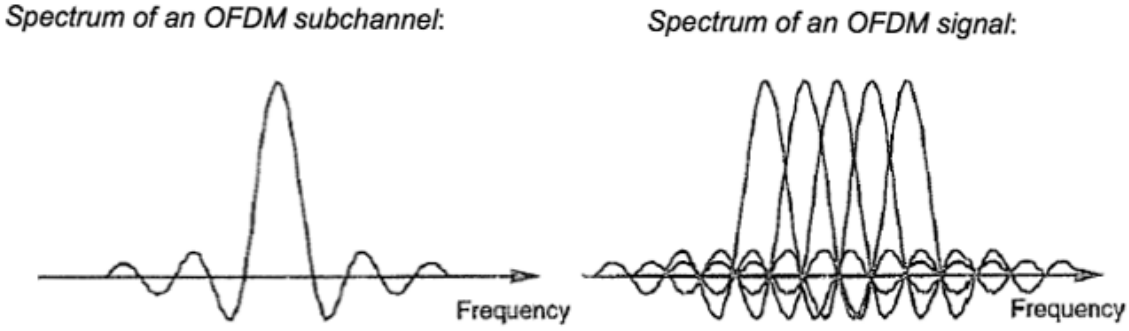

Fig. 2.2: OFDM Spectrum.

(Source: [9])

The orthogonality between the different *N* subcarriers corresponding to a sent signal is achieved and guaranteed by the emission of pulses of rectangular shape (binary digital transmission). Thus, the discrete time domain signal is converted to the frequency domain by the Fourier Transform operation, where the N generated subcarrier waves are to be viewed individually as Sinc signals whose central frequency corresponds to the frequency of the corresponding subcarrier and whose zeros of those Sinc signals are spaced apart by a factor of $\frac{K}{T_s}$ (where K is an integer). According to the mathematical properties of the frequency domain analysis (Fourier Analysis), it is crucial to ensure that the simultaneous spacing between all N subcarriers corresponds to a factor of $\frac{1}{T_s}$ (T_s being the value corresponding to the time of symbol duration or interval time between symbols) so that there may be no overlapping of the center frequencies of each carrier with the adjacent carriers. The subcarrier frequencies are equally spaced and hence the subcarriers separation is constant. Thus, without overlaps, it is possible to guarantee the orthogonality and consequently it is possible to recover the signal at the receiver when demodulating and equalizing in the frequency domain.

Furthermore, one of the big advantages of this type of scheme is that it allows to obtain notable gains in terms of saving the use of the available spectrum (a scarce and important resource) when compared with simple Frequency Division Multiplexing (FDM) systems, that is, this type of application becomes more efficient at the spectral level because of the partial overlapping between subcarriers. **[10]**

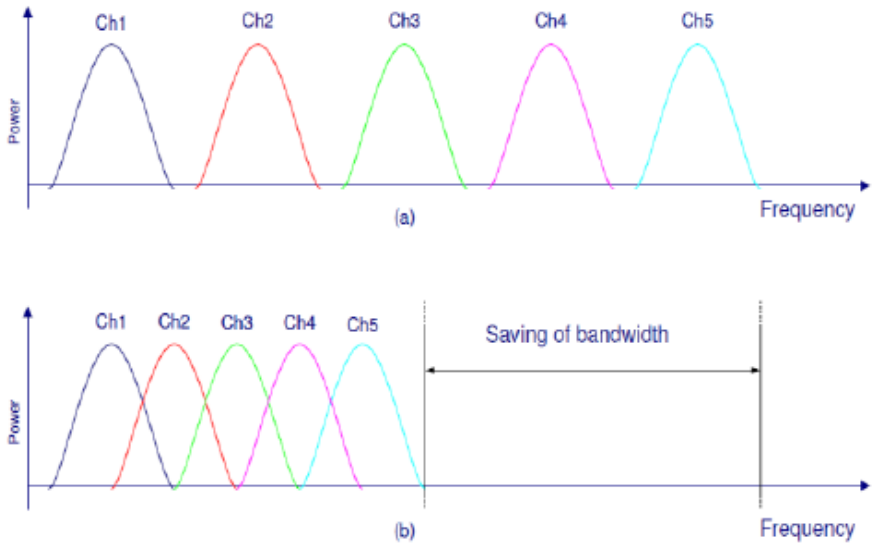

Fig. 2.3: Comparison of the bandwith use between a FDM system (a) and a OFDM system (b) and the respectively savings.

(Source: [11])

OFDM is the technique applied in 4G/LTE, mainly in the DL connection, due to severall advantages it presents. OFDM techniques are intended to be a way of transmission data-streams of a single user in all the available subcarriers in a certain moment or through-out consecutive time periods. It is possible for other users to transmit simultaneously (i.e., during the same symbol times) but on different sub-carriers or in different subcarrier sets (so, in parallel). The simplest situation is when all the available subcarriers are allocated to a user for all of the time.

The data symbols are transmitted independently over many closely spaced orthogonal subcarriers making use of Quadrature Phase Shift Keying (QPSK) or Quadrature Amplitude Modulation (QAM) as 4-QAM (2 bits per time-symbol), 16-QAM (4 bits per time-symbol) or 64-QAM (6 bits per time-symbol) Modulations, depending on the quality conditions of the transmission channel. The combination of a time-slot (T_u time period) with a certain subcarrier or set of subcarriers, corresponds to a source where each symbol (the usefull part) is modulated in a certain modulation. Finally, gathering everything, the modulated waveform is composed of *N* orthogonal subcarriers with each narrowband subcarrier.

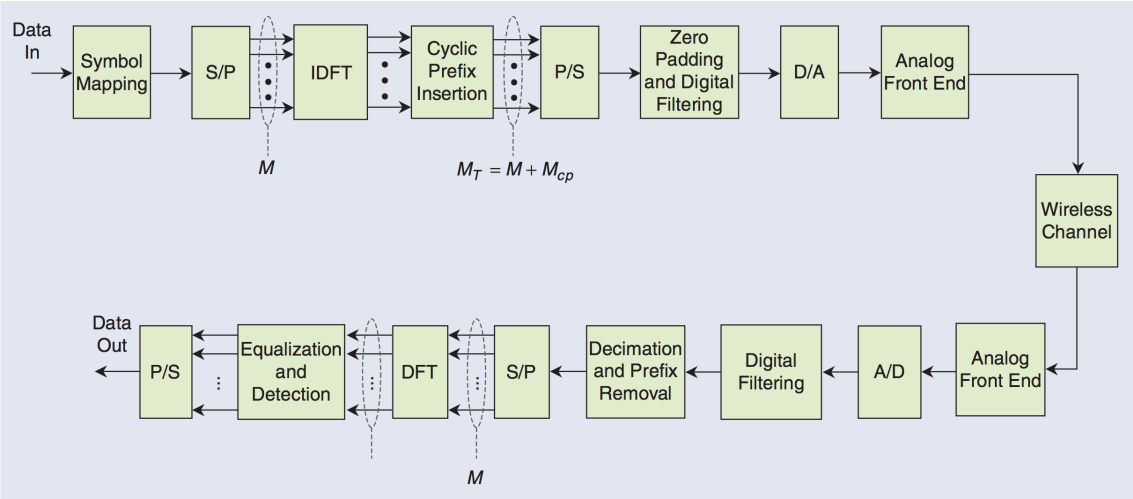

Fig. 2.4: OFDM block diagram.

(Source: [12])

The M-point time-domain blocks obtained from the IFFT (after the serial to parallel conversion of all the modulated symbols) are then serialized to create a time-domain signal after the add of CP. The CP is added to each symbol to minimize the ISI caused by the time dispersive channels (due to the delay spread created by the multipath propagation). The CP duration (T_g) should be sufficient to cover the delay spread energy of a radio channel impulse response. After the insertion of the CP, the OFDM symbol duration (T_s) should be:

$$T_s = T_g + T_u \tag{1}$$

As it can be seen in the following figure:

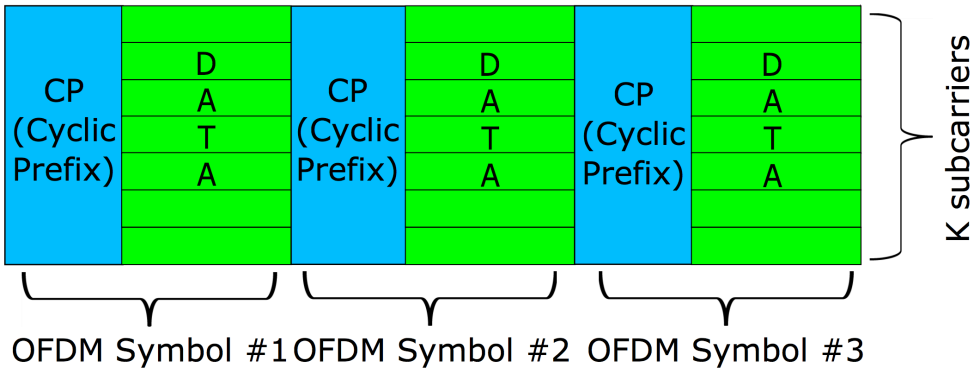

Fig. 2.5: Duration of OFDM symbols.

(Source: [13])

2.2.1 Continuous-Time Implementation

A modulated signal in OFDM consists of a sequence of data blocks whose mathematical expression, representative of this signal in the time domain, is given by the following equation in the complex form:

$$s(t) = \sum_{n=-\infty}^{\infty} \left(\sum_{k=0}^{N-1} S_{n,k} g_k (t - nT_s) \right) \quad (2)$$

where:

$$g_k(t) = \begin{cases} e^{2\pi f_k t}, & t \in [0, T_s] \\ 0, & otherwise \end{cases} \quad (3)$$

and:

$$f_k = f_0 + k \times \frac{1}{T_s} \; with \; k = 0,1,2, \dots, N-1 \quad (4)$$

where $S_{n,k}$ is the symbol that is transmitted in the n_{th} time slot by the k_{th} subcarrier.

$S_{n,k}$ is a complex number such that $S_{n,k} = a_{n,k} \pm j b_{n,k}$ is associated with a point of the considered constellation (QAM, QPSK, etc.).

T_s is the variable which represents the symbol time interval. N is the variable representing the number of subcarriers used for transmission, while f_k is the frequency of the k_{th} subcarrier, where f_0 is the frequency value of the first subcarrier.

Thus, the term in brackets in (2) corresponds to the OFDM block sent in the n_{th} interval, represented by $S_n(t)$.

The signal $S_n(t)$ which is actually transmitted corresponds to the real part, described by:

$$S_n(t) = Re\left[\sum_{k=0}^{N-1} S_{n,k} g_k (t - nT_s) \right] \quad (5)$$

Taking into account (2) comes:

$$S_n(t) = Re\left[\sum_{k=0}^{N-1} S_{n,k} \, e^{2\pi f_k t} \right] \quad (6)$$

decomposing $e^{2\pi f_k t}$, arises:

$$S_n(t) = \sum_{k=0}^{N-1} \{ a_{n,k} \cos(2\pi f_k t) - b_{n,k} \sin 2\pi f_k \, t \}, t \in [nT_s, (n+1) T_s]. \quad (7)$$

Thus the OFDM block appears as a sequence of $S_n(t)$ blocks:

$$s(t) = \sum_{n=-\infty}^{\infty} S_n(t) \quad (8)$$

The demodulation of the signal is made based on the orthogonality present in the subcarriers,

through the following operation:

$$\int_{T_s} g_k(t)\, g_{k'}^*(t)dt = T_s\delta(k-k') \tag{9}$$

And the received signal is then obtained by the following relation:

$$S_{n,k} = \int_{nT_s}^{(n+1)T_s} s(t) g_{k'}^*(t)\, dt \tag{10}$$

2.2.2 Discrete-Time Implementation

The implementation of OFDM systems in the Continuous-Time domain becomes impracticable due to the extreme complexity that this entails, thus giving rise to the implementation of this system in the Discrete-Time domain as the viable alternative. This implementation is based on the operation of the Fast Fourier Transform (FFT).

By sampling the signal to be transmitted in OFDM [described in (2) and (5)], at a frequency N times greater than the symbol rate of the $\frac{1}{T_s}$ subcarriers and assuming f_0 = 0, we obtain the following:

$$S_n(m) = \sum_{k=0}^{N-1} S_{n,k} g_k(t - nT_s)\,, t = (n + \frac{m}{N})\, T_s \; and \; m = 0,1,\ldots,N-1. \tag{11}$$

By doing the substitution of (3), appears the following:

$$S_n(t) = \sum_{k=0}^{N-1} S_{n,k} e^{2\pi f_k t} = N.IDFT\{S_{n,k}\} \tag{12}$$

Thus, it is possible to generate the signal $S_n(t)$ equivalent to a block of the baseband signal $s(t)$ from its samples, since these correspond to the IDFT of the complex numbers $S_{n,k}$ less than one factor *N*-scale. For this to be possible, the sampling frequency $\frac{N_1}{T_s}$ must be equal to or greater than the Nyquist frequency.

Finally, the demodulation of the signal is performed through the Discrete Fourier Transform (DFT), obtaining $S_{n,k}$.

The exemplary scheme of modulation and demodulation of an OFDM system with QPSK/4-QAM can be seen in the following block diagrams:

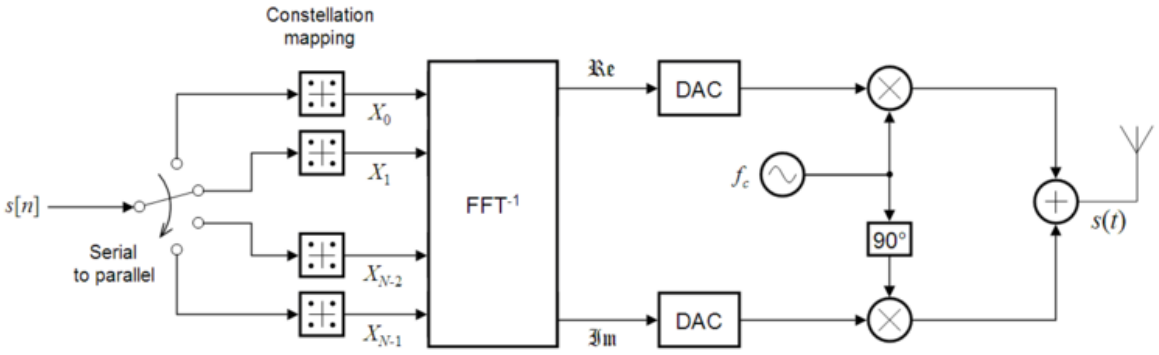

Fig. 2.6: OFDM Transmission Scheme (Modulator).

(Source: [14])

It is possible to verify that to implement this type of transmission structure it is necessary to make use of N different oscillators, each one of them associated to each one of the different subcarriers, that is, for N different frequencies, N different oscillators must exist, as well as N analog filters (which from the point of view of implementation costs can be very expensive).

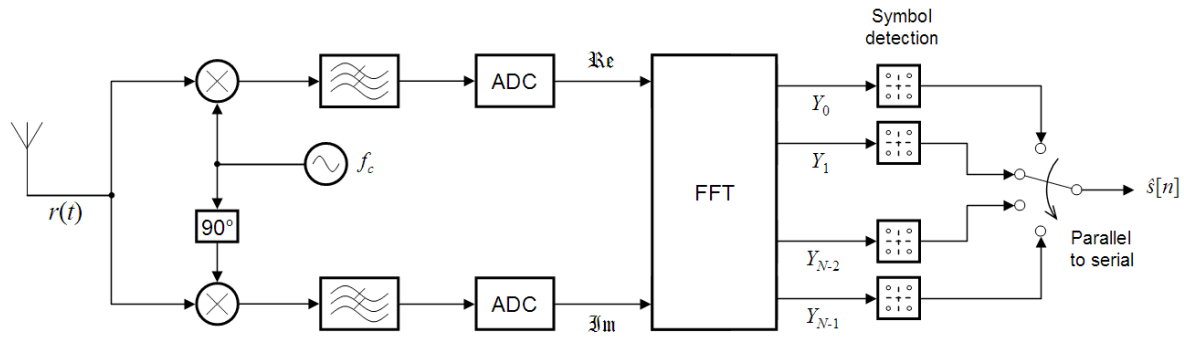

Fig. 2.7: OFDM Receiver Side (Demodulator).

(Source: [14])

2.2.3 On the Reception of Data Streams

An OFDM-modulated signal can traverse a highly time-dispersive (high Delay Spread) channel $h(t)$, thus the transmitted signal can be affected by random noise $n(t)$. In this situation, the received signal $y(t)$, is given by:

$$y(t) = s(t) * h(t) + n(t) \quad (13)$$

In most situations, the channel used to transmit the signal is highly Delay-Dispersive because of the multipath propagation phenomenon that triggers a sequence of extraordinary elements affecting the original transmitted signals. The multipath propagation yields signal paths of different paths with different times of arrival at the receiver.

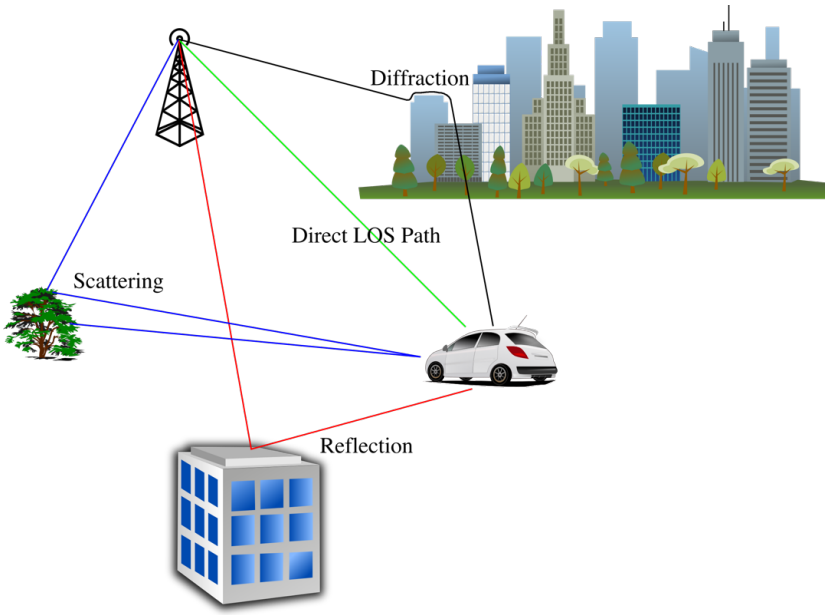

Fig. 2.8: Multipath Propagation Scheme.

(Source: [15])

This situation is very problematic because, due to it, there is the so-called Inter-Symbol Interference (ISI) phenomenon and, in the case where the channel is heavily delay-dispersive, this phenomenon can affect the adjacent data blocks between each other. That is, the consecutive symbols from a data-stream sent by a user, run the risk of overlapping each other upon arrival at the receiver.

Considering the discrete time domain, the channel can be characterized by the discrete time impulse response $h[i], with\ i\ =\ 0,\ldots,L$, where L is the value corresponding to the Channel Delay Spread, i.e., the maximum value of delay imposed by the channel on the received signal, whereby the following equations can be written:

$$y(m) = s(m) * h(m) + n(m) \tag{14}$$

$$y(m) = \sum_{i=0}^{L} h[i].\, s[m-i] + n[m] \tag{15}$$

From (15) it can be concluded that the response at any instant *m* depends on *m-i* previous values, which, in turn, can give rise to the ISI phenomenon.

One way to combat this problem is to basically copy a set of samples from the final part of the OFDM block and enter them at the beginning of the block, that is, to repeat them. These samples are repeated in the time domain and have, at most, a size equal to the maximum delay spread of the channel.

The orthogonality between subcarriers is maintained, and this set of data which is repeated at the beginning of the OFDM block is the CP, as illustrated in the following figure:

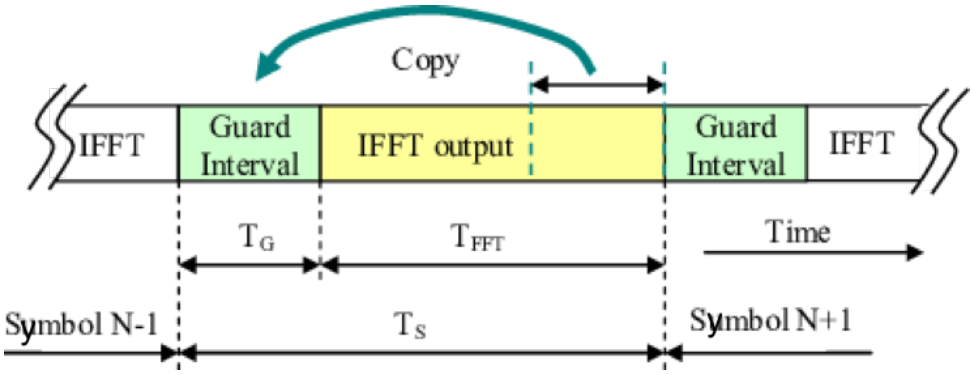

Fig. 2.9: Guard Interval between symbols, as know as Cyclic Prefix.

(Source: [16])

This highly efficient process consists of copying symbols from the end of the OFDM block and inserting these same symbols before the beginning of the block, which in a certain way will be a repetition at the beginning of the data block.

The CP must have a length (duration) greater than or equal to the channel's maximum delay spread.

The introduction of the CP is important for bridging the negative consequences, namely the ISI due to the multipath effect, which affect the signal processing at the receiver. These phenomenon, that occurs in multipath propagation and that cause delays in arriving at the receiver, are, in particular: the phenomenon of reflection, diffraction and dispersion of the signal in the various obstacles of the channel.

Below is possible to identify the situation where there is not implemented the CP and the consequent occurrence of ISI in the receiver:

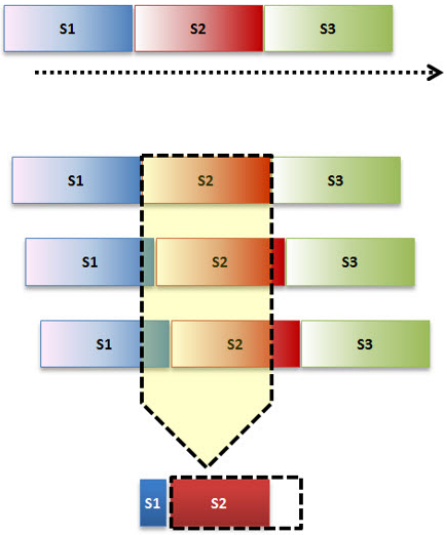

Fig. 2.10: Data Scheme without CP.

(Source: [17])

However, as we can see, with the insertion of the CP between the transmited symbols, we obtain the following structure where the ISI is totally avoided:

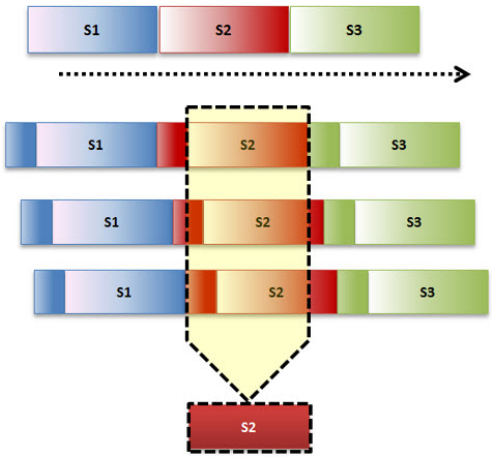

Fig. 2.11: Data Scheme with CP.

(Source: [17])

The CP, when copied from the final part of the block and introduced at its beginning, causes the symbol to "close itself", that is, the symbol that was previously a discrete linear convolution, is now seen as a circular convolution (also discrete in time).

Thus, the received data can be analyzed as a result of a circular convolution between the channel impulse response and the data block, together with the addition of the noise interference.

At the receiver side, it is then possible and feasible to perform the equalization in the frequency domain. In this way, the received signal can be represented as follows:

$$y[m] = s[m] * h[m] + n[m] = IDFT(X_{n,k}) \otimes h[m] + n[m] \quad (16)$$

Upon receipt of this signal, the DFT is applied, passing the TD signal to the FD:

$$Y_{n,k} = DFT(y[m]) = DFT\left[IDFT(X_{n,k}) \otimes h[m] + n[m]\right] \quad (17)$$

$$\Leftrightarrow Y_{n,k} = DFT(y[m]) = (S_{n,k}).(DFT(h[m])) + DFT(n[m]) \quad (18)$$

$$\Leftrightarrow Y_{n,k} = S_{n,k}.H_k + N_k \quad (19)$$

with:
$$H_k = DFT\,(h[m]) \quad (20)$$

and
$$N_k = DFT\,(n[m]) \quad (21)$$

In fact, (20) corresponds to the channel frequency response function, sampled at the frequency of the k_{th} sub-carrier.

The equation (21) corresponds to the noise that is added in the transmission and which obeys a Gaussian distribution with zero mean.

From (19) it can be concluded that there is no Inter Channel Interference (ICI) and it can

also be concluded that the orthogonality between the sub-carriers remains, even after the introduction of the channel effect.

Upon arrival of the signal to the receiver, it becomes necessary to do the equalization of the signal, i.e., to remove the effect of the channel on the signal that was originally transmitted to obtain the transmitted data. This equalization process will be addressed later in ($section$ 4).

The $Fig.$ 2.12 shows an OFDM system diagram, making emphasis on the transmitter and receiver. In this systems, each user transmits symbols in the time-domain and in a 'parallel scheme', that is, each user has a certain portion of the total existing bandwidth. For the sake of simplicity and to give an example, let us consider that each user has one dedicated frequency. This implies that, for each one of the users, the transmission of their respective data-streams is made only at one frequency allocated to each one of them and in each time period (sequence of time-slots). This division of the bandwidth results in an increase in the duration of the time-symbol for each of the different flows of data (for each user) in order to compensate the 'limitation' of frequencies allocation that was made to each user. The available bandwidth to use is given by:

$$BandWidth = \frac{1}{T_s} \tag{22}$$

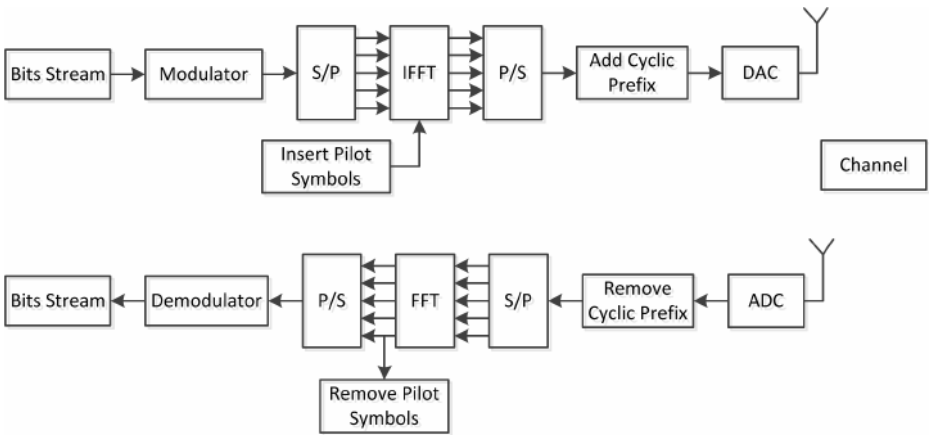

Fig. 2.12: OFDM transmiter and receiver.

(Source: [18])

With the symbol duration increased in this type of parallel transmission, when compared to a serial transmission, it is verified that the OFDM system is more robust to the multipath propagation effect. Then, with the insertion of the CP, the hypothetical occurrence of ISI is decreased.

The Multiple Acess Scheme applying the OFDM basics is called Orthogonal Frequency Division Multiple Acess (OFDMA) and it provides a better usage of the Frequency and Time

availabilities or accessibility. Despite OFDM can be applied in a multi-user situation, the OFDMA is more dedicated and suitable for that type of scenario due to a better management of the demand by the users, as represented in the $Fig.\,2.13$ and $Fig.\,2.14$.

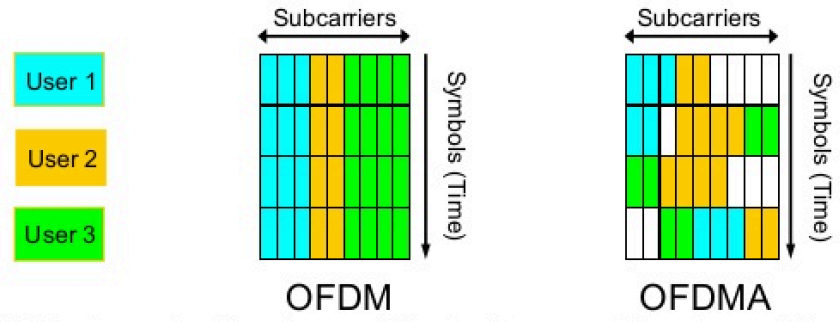

Fig. 2.13: OFDM versus OFDMA transmission schemes.

(Source: [19])

The OFDMA is largely used in the most recent Mobile Communications, as LTE/4G, because of their great dynamism in the resources management and consequent better capacity.

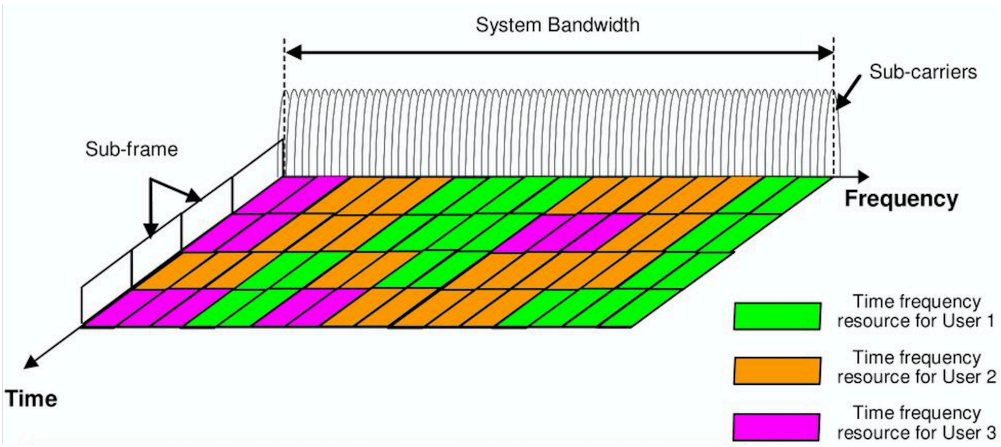

Fig. 2.14: OFDMA, used in the DL Multiple Acess.

(Source: [20])

The LTE architecture and system itself focuses on energy efficiency and thus implies some requirements in its operation by the MTs. The transmission power of the mobile phones must be below certain limits to avoid the high energy consumption (due to signal amplification). This translates into the, as small as possible, Peak to Average Power Ratio (PAPR) values:

$$PAPR = \frac{POWERaverage}{POWERpeak} \tag{23}$$

where *POWERpeak* corresponds to the peak power of the symbol and the *POWERaverage* corresponds to the average power of all transmitted blocks of symbols. This ratio is usually high in OFDM/OFDMA, since the complex symbols associated with each subcarrier are distributed according to an Independent Identically Distribution (IID), and in addition being the IDFT operation associated with each one of the subcarriers independently. This is a linear transformation process on a large number of complex symbols modulated in QAM (Quadrature Amplitude Modulation) according to an IID. This makes the amplitude of the symbols, that are transmitted, depend directly on the constellation points of the modulation scheme concerned. Thus, and considering the Central Limit Theorem, an OFDM-based signal, in TD, can be approximated by a Gaussian distribution. This Gaussian distribution should show large amplitude variations for each of the transmitted symbols, thus causing a high PAPR (not desirable in MTs). This high PAPR has negative consequences since it causes high energy consumption due to the fluctuations of the signal envelope, thus forcing the electronic amplifiers of the MTs to work in non-linear (i.e., high load/saturation) regimes. In the DL, this type of situation is not so problematic since the transmitter is a BS, however, in the UL it is not desirable because the transmitter is a MT, which runs through batteries to be energetically powered. To overcome this critical drawback of OFDM, the next section approaches another similar technology to OFDM, whose's better to deal with the UL transmissions of the MTs.

2.3 SC-FDE - Single Carrier with Frequency Domain Equalization

As was refered previously, the OFDM algorithm has some disadvantages to implement in the UL context. To avoid this problematic facts, a similar system to OFDM is presented which only differs in the way how the sequence of procedures is implemented, namely the IFFT block. All the negative aspects from the OFDM can be circumvented through a single-carrier approach called Single Carrier – Frequency Domain Equalization (SC-FDE) **[21][22][23][24]**.

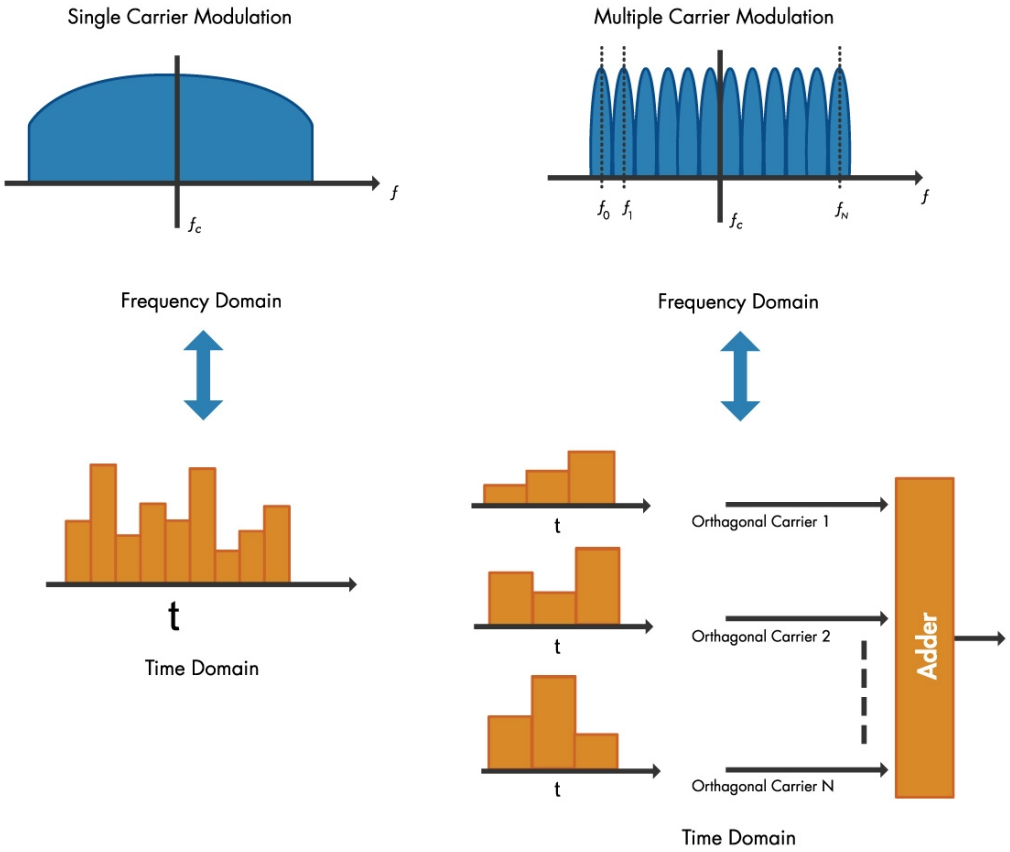

Fig. 2.15: Single-Carrier Modulation (used in SC-FDE) vs Multi-Carrier Modulation (applied in OFDM).

(Source: [25])

To avoid complexity in the architecture of the MTs, and a consequent saving of the use of batteries power, the SC-FDE algorithm works in a way where the transmited signals do not require the presence of a IFFT block in the UL transmitter device. In this UL focused context, the IFFT block is implemented in the SC-FDE receiver (the BS, where the power supply is not so critical) maintaining the complexity in the BS side. The difference between OFDM and SC-FDE

basically consists in the position of the IFFT block in the "procedures chain". This method is highly efficient and maintains the same high performances of OFDM with the big advantage of low PAPR fluctuations **[23]**. The equalization in SC-FDE is also made in the frequency-domain.

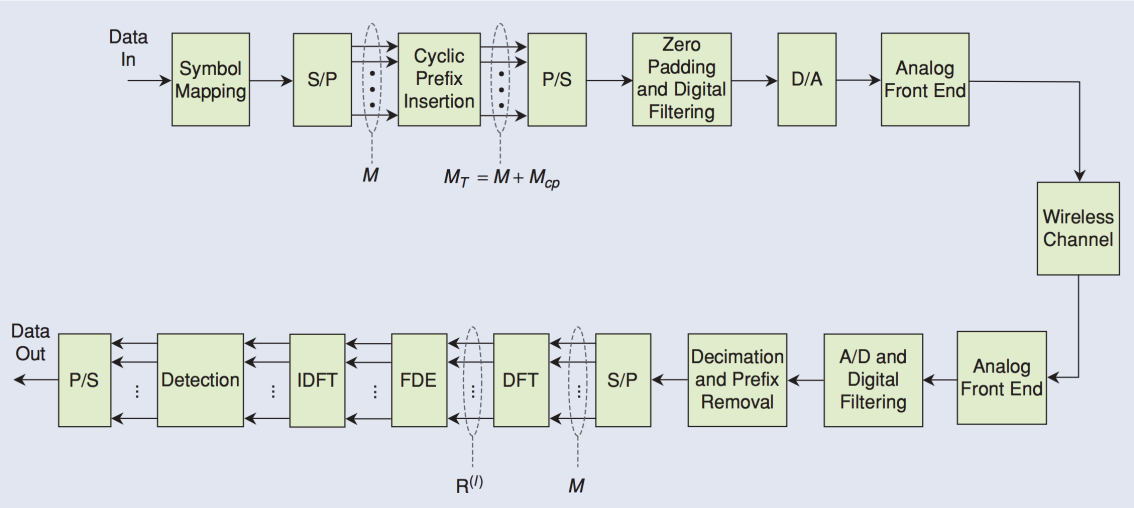

Fig. 2.16: SC-FDE block diagram.

(Source: [12])

While OFDM uses the different available subcarriers in the available bandwidth to transmit different simbols in different channels, the SC-FDE, in another way, uses all the available banwidth to a certain user to transmit blocks. So, instead of the OFDM where the different symbols (user data-stream) are transmited simultaneously (each symbol in a different sub-carrier through-out the time), the SC-FDE transmition scheme consists in transmit the symbols belonging to each user, each symbol in a time-slot and making use of all the available frequencies (a certain portion of band of the total bandwidth) in that period of time to each symbol transmission. In this way, all the available frequency resources, to one certain user, are dedicated to each symbol (or group of symbols) at a time-slot or sequence of time-slots, as we can see in $Fig.\,2.17$.

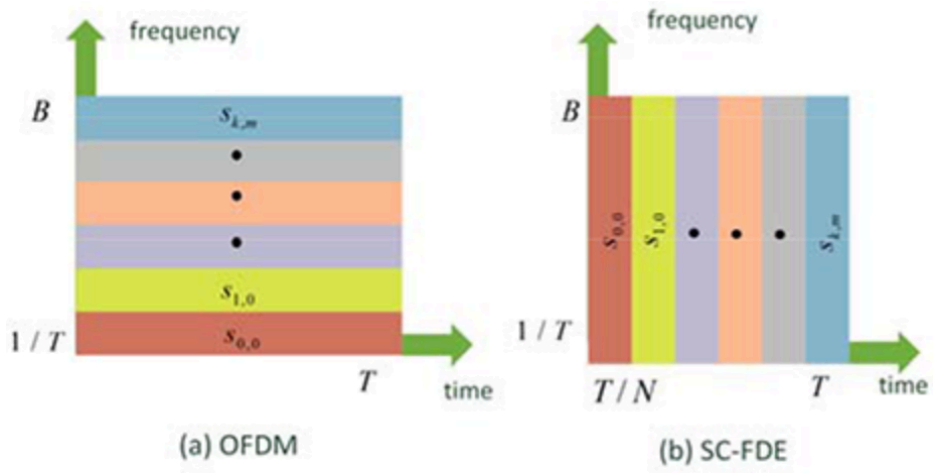

Fig. 2.17: a) OFDM versus b) SC-FDE frequency allocation.

(Source: [26])

The SC-FDE is called Single Carrier Frequency Division Multiple Acess (SC-FDMA) in a multiple acess situation, where severall different users can be, respectivelly each one, allocated to transmit in a portion of the total available bandwidth. The SC-FDMA, as well as OFDMA, can be concerned as a more dynamic version of SC-FDE, as it is possible to observe in $Fig.$ 2.18.

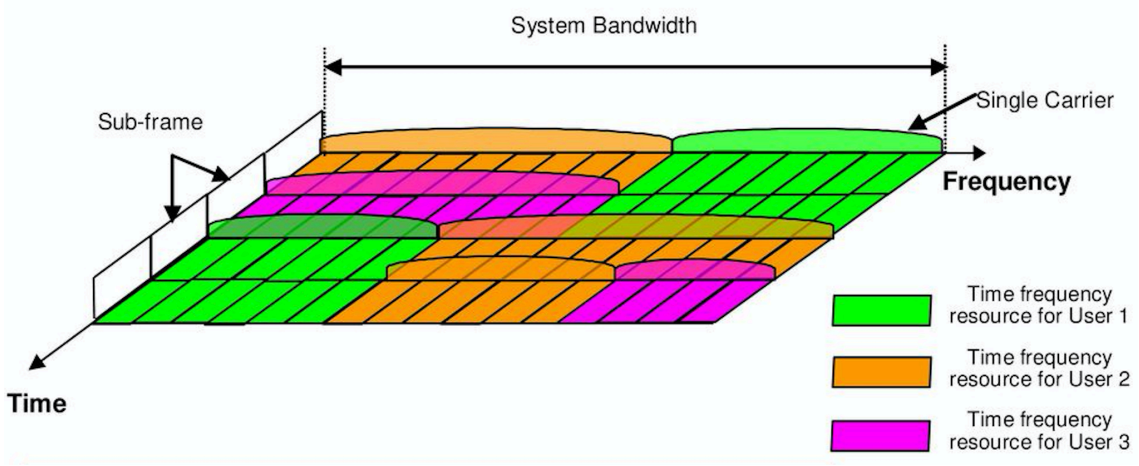

Fig. 2.18: SC-FDE (SC-FDMA), used in the UL Multiple Acess.

(Source: [20])

This modulation method avoids complexity, presents advantages and also has comprovedly equal or even better UL performances when compared with OFDM **[12]** reasons why it is used in the LTE/4G uplink. The absence of IFFT in the UL transmitter (MT) results in a less complex system, making the transmission mechanism much simpler and consequently saving power.

The SC-FDMA can be interpreted as a linearly precoded OFDMA scheme, in the sense that it has an additional DFT processing step preceding the conventional OFDMA processing as referred previously and as can be seen in $Fig.2.19$.

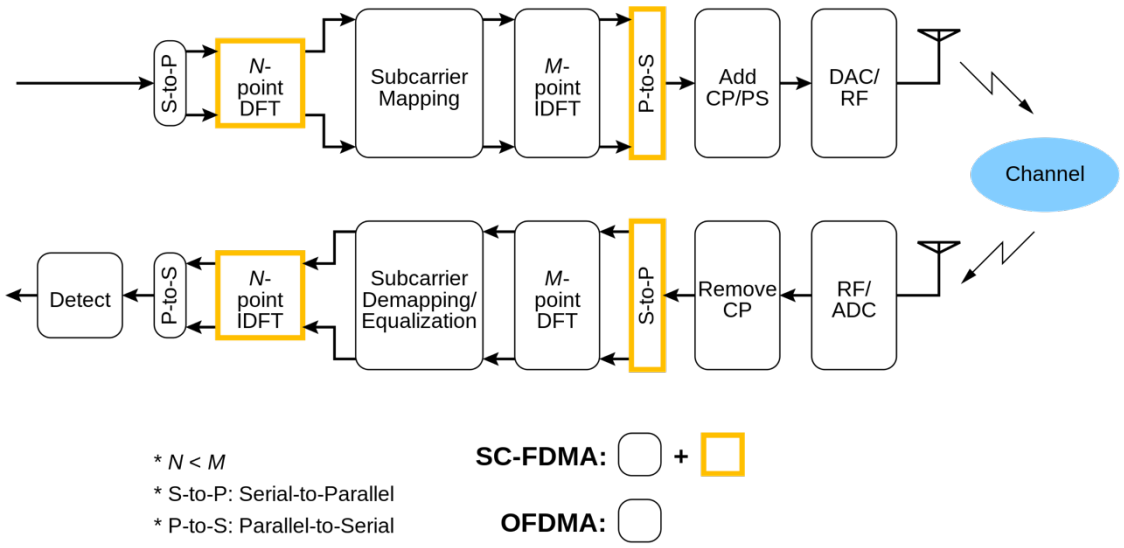

Fig. 2.19: SC-FDMA versus OFDMA blocks chain.

(Source: [27])

This few diferences in the characteristics of both systems becomes particulary interesting to adapt the devices to be a tipical OFDM or a SC-FDE transmiter/receiver doing just the necessary change of the position of the IDFT block. The SC system transmits a single carrier, modulated at a high symbol rate (instead of OFDM with low symbol rate). The Frequency Domain Equalization (FDE) in a SC system is simply the FD analog of what is done by a conventional linear Time Domain Equalizer (TDE). For channels with severe Delay-Spread, the FDE is simpler than corresponding TDE, for the same reason that OFDM is simpler: the FFT operations and the simple channel inversion operation. The use of SC modulation and FDE by processing the FFT of the received signal has several attractive features, namely:

• The SC modulation has a reduced PAPR requirements when compared to OFDM, thereby allowing the use of less costly power amplifiers **[22]**.

• The SC system performance with FDE is similar to OFDM performance, even for very long channel delay spread. The receiver complexity is similar to OFDM, proportional to the Logarithm of the multipath spread. Coding, while desirable, is not necessary for combating frequency selectivity, as it is in nonadaptive OFDM systems.

• SC modulation is a well-proven technology in many existing wireless and wireline applications,

and its RF system linearity requirements are well known.

Both systems can be enhanced by coding (which is in fact required for OFDM systems), adaptive modulation and per space diversity. In addition, OFDM can be incorporate peak-to-average reduction signal processing to partially (but not completely) alleviate its high sensitivity to power amplifier nonlinearities. SC-FDE can be enhanced by adding Decision Feedback Equalization (DFE) or Maximum Likelihood Sequence Estimation (MLSE) **[28]**.

Comparable SC-FDE and OFDM systems have the same block length and CP lengths. Since their main hardware difference is the location of the IFFT, a modem can be converted as required to handle both OFDM and SC signals by switching the location of this block between the transmitter and receiver, as it can be seen in $Fig.2.20$.

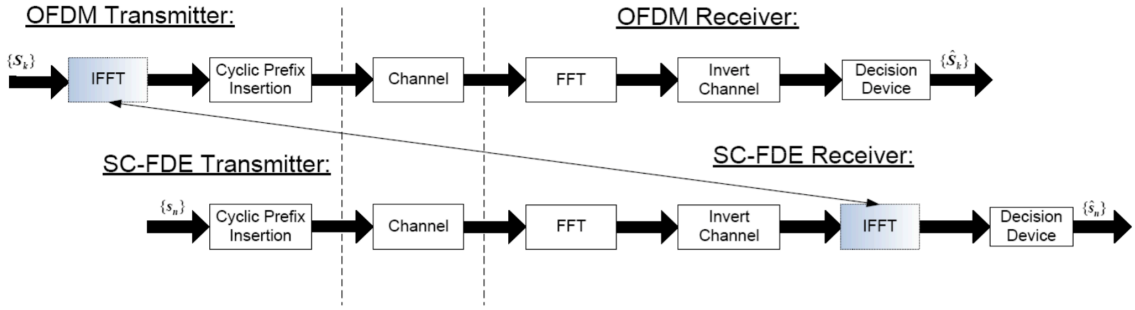

Fig. 2.20: IFFT block position in OFDM vs SC-FDE.

3. Schemes of Diversity, Transmission & Reception of Signals

3.1 Diversity Schemes to Improve the Bit Error Rates

As previously mentioned, the transmission of data through the air interface can be done through techniques with some degree of sophistication. These type of techniques for increasing the transmission gains aren't itself enough to achieve the maximum benefit of what technology can offer nowadays. Then, it is possible to improve the Bit Error Rates (BER) of the data transmissions between two points. In order to maximize the performance of telecommunication systems, we take advantage of some techniques, the so-called diversity techniques. These techniques, whose are very important in achieving higher performances **[29][30]**, can be combined with each other to approach even better results. They are represented in the $Fig.3.1$:

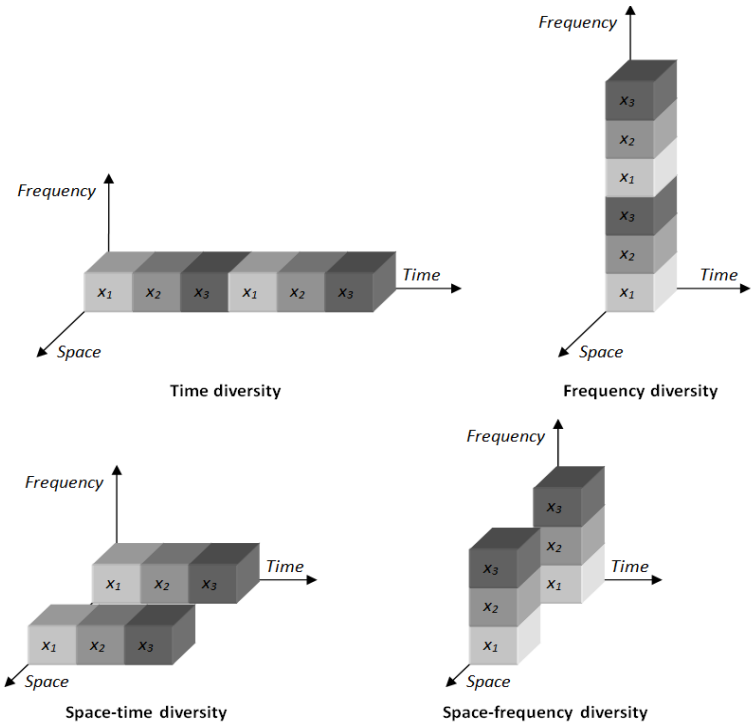

Fig. 3.1: Different types of Diversity Techniques.

(Source: [31])

• Time Diversity - Corresponds to a transmission scheme, whose core business is related to the transmission of data in different time intervals (i.e.: consecutive), in order to combat the selectivity in time by the physical environment where the transmission takes place (the channel).

• Frequency Diversity - Consists in the transmission of a data block in a set of distinct frequencies within a certain bandwidth, in order to avoid channels that are selective in the frequency, that is, channels that cancel certain frequencies. This type of diversity technique only applies to non-flat-fading channels (non-frequency selective channels);

• Spatial Diversity - In this type of technique, several transmitting and receiving antennas are used to increase the multiplexing of communication "channels" between the transmitting and receiving ends, i.e.: achieving a greater amount of transmission possibilities and combinations between transmitting antennas and receiving antennas simultaneously, to transmit a given signal. This technique is very important in nowadays telecommunication systems, presenting a significant impact in the performance **[32][33]**.

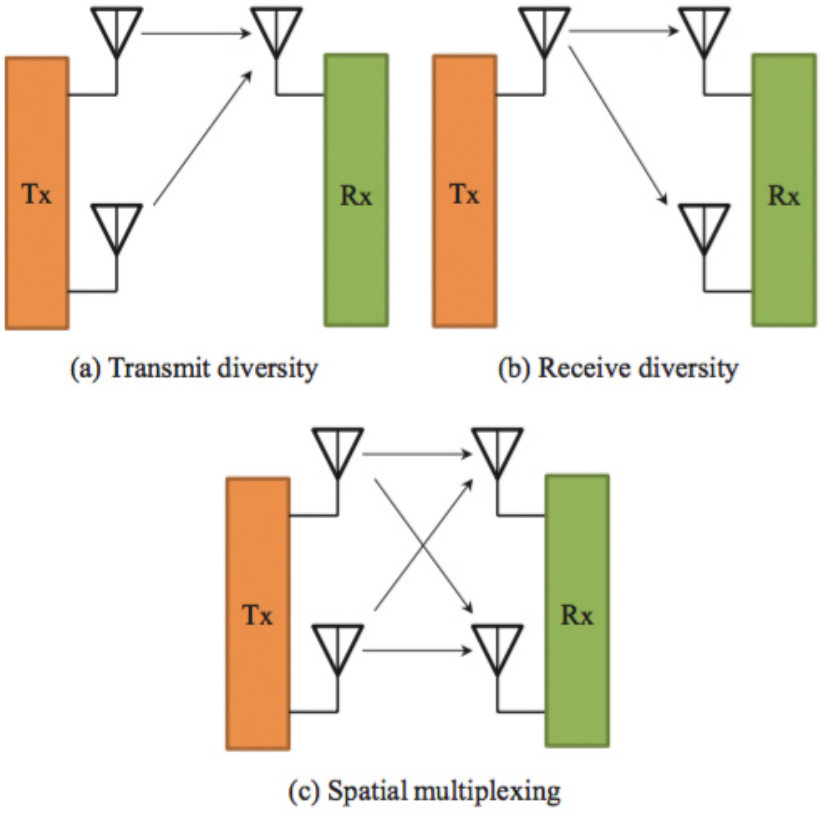

Fig. 3.2: Types of Spatial Diversity.

(Source: [34])

3.2 Transmission Schemes

3.2.1 MIMO – Multiple Input Multiple Output

Taking advantage of the spatial diversity, as we can see in $Fig.3.3$, is possible to use different types of schemes to transmit signals between an array of Transmitter Antennas (Tx) and an array of Receiver Antennas (Rx). The more multiplexing between Tx and Rx, more speed and reliability will be present in the transmission between the terminals ($Fig.3.4$). The most efficient scheme used in telecommunications is the MIMO where severall Tx transmit to severall Rx, thus resulting in a high performance communication system. This type of scheme can be designed to be used with 2x2, 2x4, 4x2, 4x4, 6x6, 6x4, or another type of structures, depending only in the available capacity to implement more or less Tx and Rx antennas. Over the last 20 years, MIMO technology has proven its excellent performance **[35]** and has been commonly integrated in systems from 3G to LTE/4G with the aim of increase their capacity. LTE-Advanced (4.5G) and 5G are also two generations that use this kind of configurations to achieve higher rates of data transmission and to increase their capacities. The performance of telecommunication systems, in general, is proportional to the minimum number of necessary antennas used in the 'Transmit/Receive' relation. However, despite the milestones achieved to date with MIMO technology, according to **[1],** the number of antennas currently employed in this type of configuration is still insufficient to provide the desired rates for 5G. One can note that MIMO scenarios can be described also in two different ways, related to a Single-User (SU) transmission or to a Multi-User (MU) transmission.

Nowadays, MIMO Techniques are used in the Wi-Fi networks as well as in the WLAN networks due to his efficiency in the presence of severall users. In MIMO schemes, the different Tx can be used to transmit Spacial Diversity (using the diferent Tx to transmit the same data package in simultaneous, resulting thus on a better system redundancy, and thus achieving better BERs, consequence of the higher reliability. By another way, MIMO systems are able to create a multiplexing scenario where each of the different Tx transmits different parts of the same data package with focus on the achievement of higher data rates.

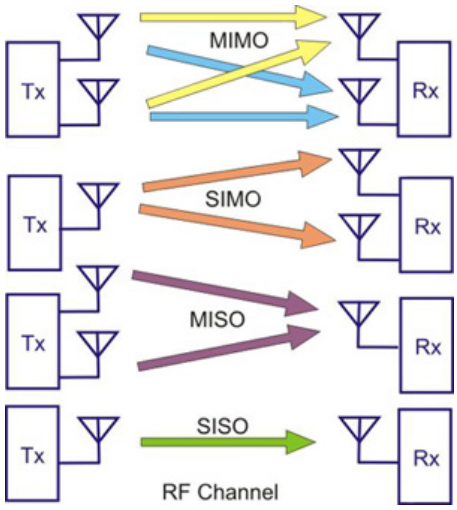

Fig. 3.3: Types of Spatial Diversity in Transmission and Reception.
(Source: [36])

3.2.2 SIMO - Single Input Multiple Output

The Single Input Multiple Output (SIMO) model corresponds to a diversity reception system, in which the system has two or more Rx and only one Tx. This type of structure has its maximum performance when using combinatorial equalization techniques, that is, in order to use the information that reaches the receivers more efficiently.

3.2.3 MISO - Multiple Input Single Output

The Multiple Input Single Output (MISO) model, is a type of system that consists of transmit diversity, by implementing two or more Tx and using only one Rx. In this type of structure, it is imperative to implement precoding algorithms to process the redundant information to be sent, so that there can be an efficient combination of the data at the equalization. Alamouti techniques are well suited for this type of application **[37]**.

3.2.4 SISO - Single Input Single Output

The Single Input Single Output (SISO) model does not present any diversity. This type of configuration is the simplest one, but at the same time, the one who offers less advantages in

terms of being effective.

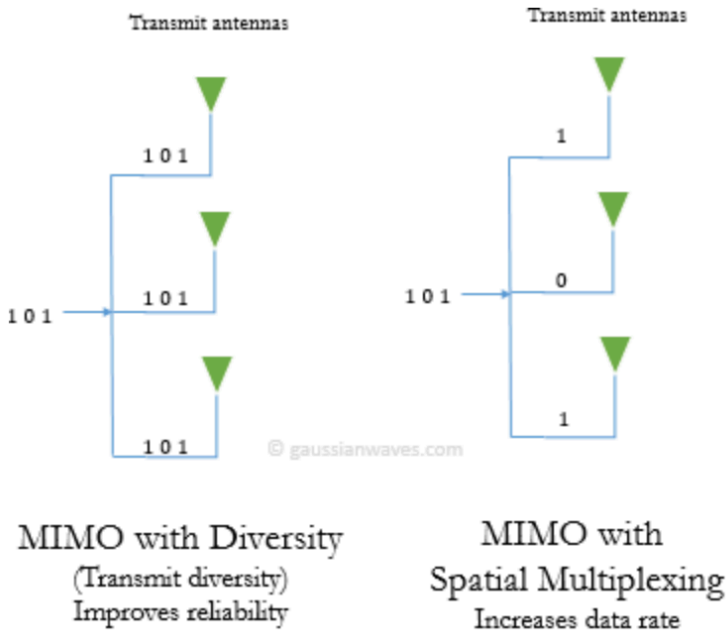

Fig. 3.4: Diversity vs Multiplexing in MIMO systems.

(Source: [38])

3.2.5 Massive MIMO

On the next generation of Mobile Communications, the 5G, massive arrays of antennas are intended to be used in the base stations with the objective of maximize this type of scheme and reach high data-rate transfer. This type of implementation is called Massive Multiple Input Multiple Output (Massive-MIMO) and pretends to be revolutionary to achieve some speciffic targets of 5G. The live holograms and other aplicatives whose consumes a lot of data resources as well as the lower latency are some of the examples **[39]**.

The Massive-MIMO can be seen as an expansion of the current MIMO in some orders of magnitude, especially as regards the number of antennas used in the Tx/Rx pair. This magnitude can go to the order of tens or even hundreds of antennas depending on the configurated situation. The main goal of Massive-MIMO is to achieve greater performances than the MIMO technology and specialy increase the system capacity. Massive-MIMO can increase the capacity 10 times or more and simultaneously, improve the radiated energy-efficiency in the order of 100 times **[40]**. Increasing the number of involved antennas, Massive-MIMO configurations can figure even a larger spatial multiplexing. This implies that the BS should have an excellent knowledge of the transmission channel, the Channel State Information (CSI) **[39]**. The UL channel estimation is

done by the BS through the pilot data, which are sent by the MTs to the BS. In this way, is possible to obtain an approximate estimate of the channel assigned to each user. In the case of the DL, the inverse situation occurs, that is, the MTs carry out the channel estimation and send the information that they processed to the BS. It should be noted that DL channel estimation may be too difficult to implement in Massive-MIMO configurations in scenarios whose mobile terminals are highly mobile, that is, in scenarios whose Doppler effect is high. Since the number of antennas present in this type of configuration is very high, it is not feasible to the level of time used in the processing and to the level of the frequency resources that will be highly consumed, being necessary an availability of both these resources when much more antennas are employed. Also by the fact that each handset would have to estimate tens or hundreds of distinct channels for all Tx/Rx pairs, again such an implementation would be impractical. To circumvent these technical obstacles, the Time Division Duplex (TDD) mode is a more viable option, implying in this way the initial assumption that the channel in use is the same in both DL and UL. However, the Frequency Division Duplex (FDD) mode can also be employed in some more specific cases **[41]**.

In Massive-MIMO, TDD system protocol operation is preferable. During a coherence interval, there are three operations: channel estimation (including the UL training and the DL training), UL data transmission, and DL data transmission **[42]**. A TDD Massive-MIMO protocol is shown in the figure below:

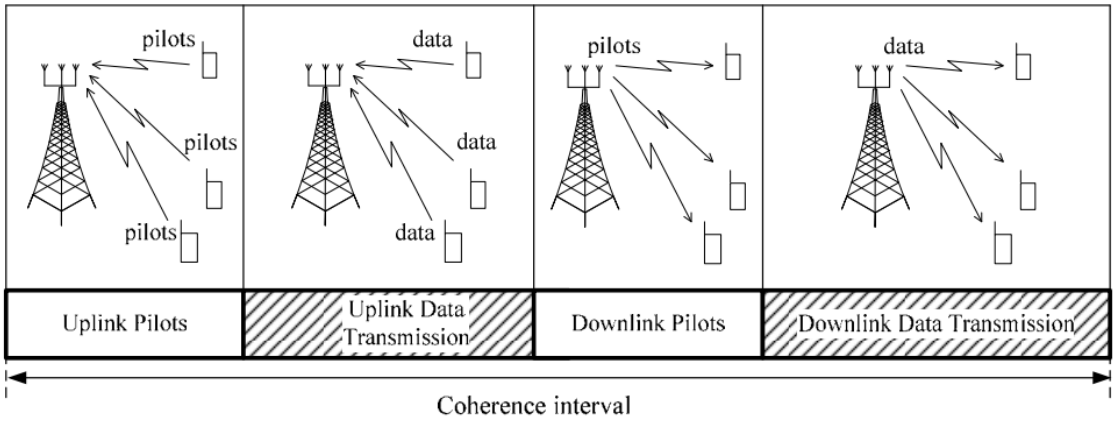

Fig. 3.5: TDD system Protocol for Massive-MIMO.

(Source: [43])

3.3 Signal Transmission

In this section is described the Signal Transmission in a UL scenario using the SC-FDE modulation scheme.

When using the SC-FDE technique, the sent information is organized in blocks of data, which

are containing N symbols, each. The transmitted blocks $\{s_n; n = 0, \cdots, N-1\}$, which in this case are fixed in $N = 256$, are generated from a Quadrature Phase Shift Keying (QPSK) constellation. The complex envelope of an N-size symbol block can be written as:

$$s(t) = \sum_{n=0}^{N-1} s_n r(t - nT_s) \tag{24}$$

where $r(t)$ represents the support pulse, and T_s represents the symbol duration.

After that, an M-point DFT is employed with the objective of reproduce a frequency domain representation of the information symbols. Applying the DFT on both sides of the equation (27), we obtain:

$$S(f) = F\big(s(t)\big) = \sum_{n=0}^{N-1} s_n R(f) e^{(-j2\pi f n T_s)} \tag{25}$$

Before the transmission of the data symbols, the Cyclic Prefix (CP) is added in the beggining of each data block.

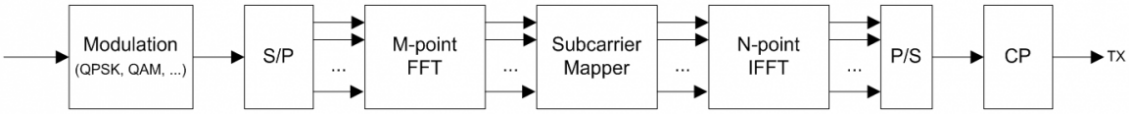

Fig. 3.6: SC-FDE transmission structure.

After this, the discrete signal is separated into a in-phase (S_n^I) and quadrature (S_n^Q) components. Posteriorly, the original digital signals are converted to continuous-time signals through a Digital to Analog Converter (DAC) **[44]**. These signals are then combined to generate the time-domain transmitted signal which travels through the propagation medium.

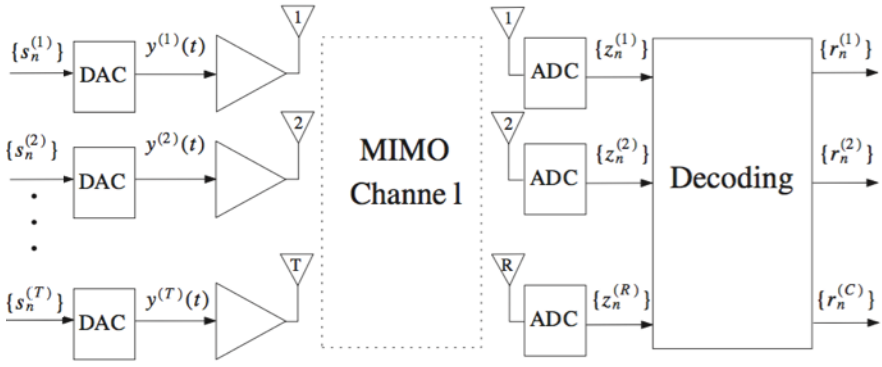

Fig. 3.7: Multi- user UL in Massive-MIMO.

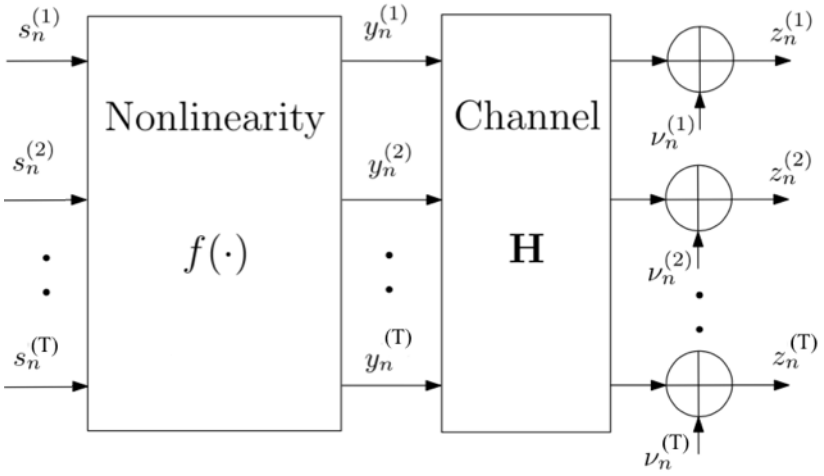

Fig. 3.8: Transmitter side.

In the $Fig.3.7$ and $Fig.3.8$, is possible to see a sketch where T diferent Mobile Terminals (MT) are represented as being the transmiters, with one DAC process for each transmitter. Is also possible to observe a R-array of different Rx Antennas, each branch with a pair of Analog to Digital Converter (ADC), in the receiver, i.e., the BS.

Behind this scheme, is H_k which represents the channel realization of $R \times T$ (in the frequency domain), for each one of the different k_{th}subcarrier involved in the transmission scheme:

$$H_k = \begin{bmatrix} H_k^{(1,1)} & H_k^{(1,2)} & \cdots & H_k^{(1,T)} \\ H_k^{(2,1)} & \cdots & \vdots & H_k^{(2,T)} \\ \vdots & \vdots & \ddots & \vdots \\ H_k^{(R,1)} & \cdots & \cdots & H_k^{(R,T)} \end{bmatrix} \tag{26}$$

3.4 Signal Reception

In this section is described the Signal Reception for a SC-FDE scheme employed in the UL of a Massive-MIMO scenario.

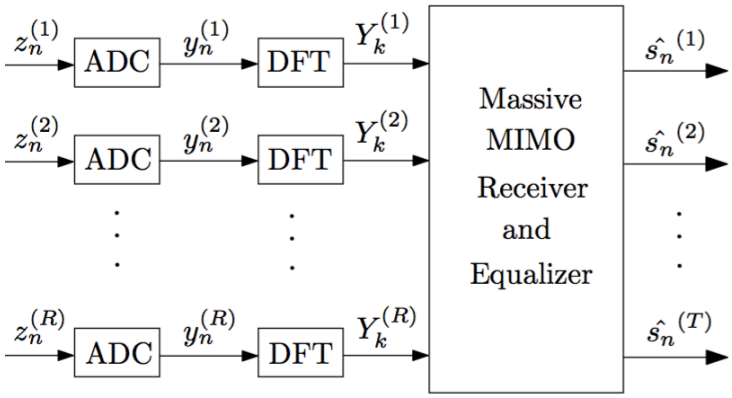

Fig. 3.9: Receiver side.

When the signals arrive the receiver, the continuous time signal is sampled by an ADC, and then the CP is removed from the received block, where the TD samples:

$$\{y_n\,; n = 0, \cdots, N-1\} \tag{27}$$

are obtained and then submitted to a N-size FFT operation resulting in a desired FD block:

$$\{Y_k\,;\ k = 0, \ldots, N-1\} \tag{28}$$

of the received signal, where Y_k is given by:

$$Y_k = H_k S_k + N_k \tag{29}$$

being H_k the frequency response of the channel at the kth subcarrier. S_k represents the transmitted symbols and N_k the Additive White Gaussian Noise (AWGN) samples.

It is important to note that, to simulate a real Channel we should add the White Gaussian Noise (AWGN) to the received signal in each one of the R_{th} Antennas. So, we obtain:

$$Y_k^r = [Y_k^1, Y_k^2, Y_k^3, \ldots, Y_k^{(R)}]^T = H_k S_k + N_k \tag{30}$$

With:

$$S_k = [S_k^1, S_k^2, S_k^3, \ldots, S_k^{(T)}]^T \tag{31}$$

Since the CP is a copy of the last part of the block, it converts a discrete time linear convolution into a discrete time circular convolution. Therefore, the transmitted data propagating through

the channel can be modelled as a circular convolution between the channel impulse response and the transmitted data block, which in the FD is a point-wise multiplication of the DFT frequency samples as shown in (29).

The equalization is then performed on the FD of the received signal, where the equalized samples ($\tilde{S}_k = F_k Y_k$) are obtained depending on the type of the used equalizer (F_k), whose equalization vector is defined by:

$$\{F_k; k = 0, \cdots, N-1\} \tag{32}$$

After the equalization process, the data symbols are converted back to the TD through an IFFT to perform the symbol detection.

4. Equalization Techniques

In this section, severall different types of receivers able to be employed in the 5G communication systems are proposed and described.

First we board the most sophisticated techniques as Zero Forcing and the Iterative Block Decision Feedback Equalization (IB-DFE) that are known to be very effective in combat the ISI and IUI however entailing very high costs in Massive-MIMO schemes due to their high mathematical complexity in matrix inversions **[45]**.

After, we approach the low complexity techniques as Maximum Ratio Combining (MRC) and Equal Gain Combining (EGC), which are techniques that don't need to perform matrix inversions, being then more suitable for Massive-MIMO scenarios. Despite that fact, it should be noted that these techniques are not able to eliminate all the ISI **[46]**. Finally, we associate the low complexity techniques with the iterative algorythms to try to combine the good charachteristics of each one and employ them taking into account the Massive-MIMO architecture requirements.

4.1 Zero Forcing (ZF)

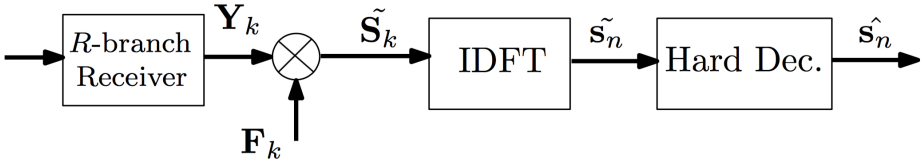

Fig. 4.1: Frequency Domain Equalization.

The Zero Forcing technique (ZF) consists in a linear FDE technique, and corresponds to the simplest equalization method. Basically is done by multiplying the received FD signal Y_k that arrives the receiver, by the equalization matrix F_k associated with each one of the k_{th} subcarriers, thus obtaining the signal ready to be detected by the receiver detector. After the equalization procedure, the obtained signal sequence is:

$$\tilde{S}_k = F_k Y_k \tag{33}$$

Which can be seen as the following decomposition:

$$\tilde{S}_k = [\tilde{S}_k^{(1)}\ \tilde{S}_k^{(2)}\ \tilde{S}_k^{(3)}\tilde{S}_k^{(4)} \cdots\ \tilde{S}_k^{(T)}]^T \in \mathbb{C}^N \quad (34)$$

The resulting signal, $\tilde{S}_k$, will then be translated to the TD (by the IFFT) before the decision process. The ZF equalization function should attend the following condition:

$$I_k = F_k H_k \quad (35)$$

From where it arises the equalization matrix for the Zero Forcing technique:

$$F_k = H_k^H (H_k H_k^H)^{-1} \quad (36)$$

Then, through (36), is possible to conclude that the more the 'weight' of the channel H_k, the more difficult will be the detection and decision processes due to the negative impact of the noise amplification $\frac{N_k}{H_k}$ **[47]**.

Despite this fact, the ZF method is still considered a very effective technique to avoid the ISI. Nevertheless, the MMSE algorithm overcomes this undesirable problem of ZF, as described below.

4.2 Minimum Mean Squared Error (MMSE)

The MMSE is a equalization technique where the main objective is to find a matrix F_k that minimizes the Mean Squared Error θ_k. The Mean Squared Error θ_k, which is the 'distance' or 'difference' between the signal $\tilde{S}_k$ and the transmited signal S_k, is described by:

$$\theta_k = \frac{1}{N^2} \sum_{k=0}^{N-1} \theta(k) \quad (37)$$

that, is equivalent to:

$$\theta_k = E\left[\left|\tilde{S}_k - S_k\right|^2\right] \Leftrightarrow \quad (38)$$

$$\Leftrightarrow\ \theta_k = E[|Y_k F_k - S_k|^2] \quad (39)$$

The MMSE equalization function, F_k, is obtained by minimizing the MSE function, i.e.:

$$min_{f_k}(E[|Y_k F_k - S_k|^2]), \qquad k\ \in [0,1,\dots,N-1] \quad (40)$$

And so arises F_k:

$$F_k = (H_k H_k^H + \beta I)^{-1} H_k^H \quad (41)$$

where:

$$\beta = {}^1/_{SNR} \quad (42)$$

The MMSE method is not so efficient to avoid the ISI negative effects for the low values of

the SNR, however, in general it presents better results than the ZF method for higher values of the SNR. The two aforementioned techniques can be easily employed when we are considering a small number of antennas in the system. However, for Massive-MIMO systems, where there are a lot of Rx and Tx, their implementation becomes unworkable, once they require the inversion of very large matrices for each subcarrier. Therefore, low-complexity equalization techniques should be considered to implement in Massive-MIMO. Two example of such techniques are the MRC and the EGC, both described below.

4.3 Maximum Ratio Combiner (MRC)

The MRC is an equalization method which uses combining techniques to equalize the received signals that does not require matrix inversions, what is a excelent characteristic to the high complexity in Massive-MIMO configurations where the big relation Tx/Rx generate a big multiplexing scenario that, in turn, requires highly values of processment resources.

This equalization technique combines the different gains of the different arrival signals and correlates them to avoid the negative effects of the fading channels and get the better performance results **[48]**.

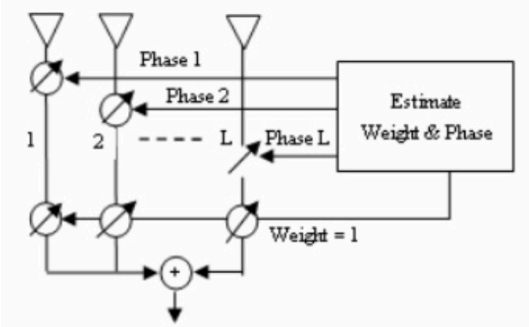

Fig. 4.2: MRC blocks diagram.

The matrix of the gain coefficients is the equalization matrix, F_k, which contains all the different weights according with each of the different Rx branch. It can be written as:

$$F_k = H_k^H \tag{43}$$

This low-complexity receiver is not so effective to combat the multipath fading and interference, so it comes desirable the combination of this algorithm with an iterative feedback solution. By this way, arises a possibility to achieve a reasonable performance in severe frequency selective channels since the MRC by its own, can't totally remove the ISI and IUI. The iterative

receivers, as we shall see next, are able to perform a Number of Iterations (I), whose gradually promotes the removal of the interferences.

4.4 Equal Gain Combiner (EGC)

The EGC is a very similar technique to the MRC, except for the fact that it is less complex once it only imposes a unitary gain in each of the arriving signals (contrasting with MRC where different gain weights are needed to compensate the magnitude variation of the different arriving signals, caused by the fading effect).

The EGC considers the phase components introduced, in the signals, by the channel effects during the transmission, and compensates their deviations.

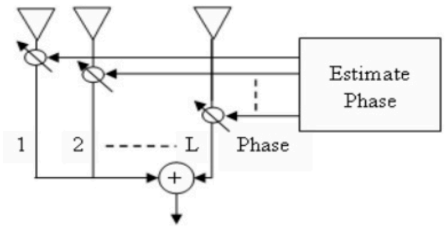

Fig. 4.3: EGC equalizer diagram.

The equalization matrix of the EGC is:

$$F_k = e^{(j*\arg(H_k^H))} \tag{44}$$

This type of equalization method is less complex than the MRC because it inputs the same gain in each Rx branch. Such as the MRC equalization method, the EGC technique by it's own is also not enough to overcome the need of good performances in the presence of Massive-MIMO scenarios. Therefore, the iterative solution is also needed to put together with the EGC itself, where the creation of a feedback loop, will mitigate the residual interference in an iterative fashion. This iterative cancelation of interference can be done I times, as previously refered. It is also important to note that when imposing $I = 1$, we are still facing a linear FDE receiver. The Iterative Block – Decision Feedback Equalizer (IB-DFE) arises as an plausible basis and, in fact, it will be the basis to do a joint solution, both for MRC and EGC implementations, as we shall see next.

4.5 Iterative Block – Decision Feedback Equalizer (IB-DFE)

The *IB-DFE* is an iterative receiver, which presents generally better results than the linear receivers **[49]**. The feedback loop serves as a method to eliminate the ISI and the IUI which the linear receivers can't completely eliminate.

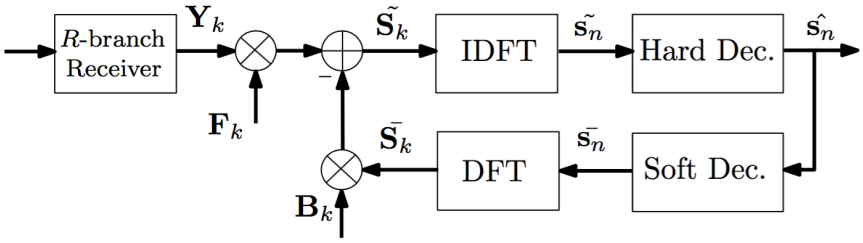

Fig. 4.4: IB-DFE equalizer diagram.

It should be noted that the iterative techniques employed in MIMO systems are highly suitable in the context of broadband wireless systems **[21]**.

In the $Fig.4.4$ we can observe an *IB-DFE* blocks diagram where is described a receiver with *R* antenas, a Hard Decisions module in the main branch and a Soft Decisions module in the feedback loop.

The F_k and B_k are, respectively, the FeedForward and FeedBack coefficients matrix corresponding to the I_{th} iteration.

These two matrix are generated with the objective of maximize the Signal to Interference and Noise Ratio (SINR), a useful method to quantify the performance.

For the I_{th} iteration, the FD data block, at the output of the equalizer, associated to the kth subcarrier, is expressed by:

$$\tilde{S}_k = \left[\tilde{S}_k^{(1)}\ \tilde{S}_k^{(2)}\ \tilde{S}_k^{(3)}\ \cdots\ \tilde{S}_k^{(I-1)}\right]^T \in \mathbb{C}^N, \tag{45}$$

So, at each iteration occurs:

$$\tilde{S}_k{}^I = \sum_{r=1}^{R}\left[F_k^{(r,I)}Y_k^{(r)} - B_k^{(I)}\tilde{S}_k^{(I-1)}\right] \tag{46}$$

The feedforward filter coefficients matrix, associated to the rth receive antenna is:

$$\left[F_k^{(r,I)}; k = 0,\cdots,N-1\right]:(r = 1,\cdots,R) \tag{47}$$

The feedback coefficients matrix is:

$$\left[B_k^{(r,I)}; k = 0,\cdots,N-1\right]:(r = 1,\cdots,R) \tag{48}$$

The equalized symbols, in the FD, from the previous iteration are:

$$\left[\tilde{S}_k^{(I-1)}; k = 0, \cdots, N-1\right] \tag{49}$$

whose are then converted back to the TD through a N-point IDFT operation, resulting in a TD equalized block, $\tilde{s}_n^{(I-1)}$:

$$\left[\tilde{s}_n^{(I-1)}; k = 0, \cdots, N-1\right] \tag{50}$$

After, the signal passes through an hard-decisions detector, which operation can be described by:

$$\hat{s}_n = sign(Re\{\tilde{s}_n\}) + jsign(\tilde{s}_n) \tag{51}$$

originating the TD version of the received data block:

$$\left[\hat{s}_n^{(I)}; k = 0, \cdots, N-1\right] \tag{52}$$

Once the detection process is made on a iterative basis, one iteration after another the detection of the last iteration will provide a reliability increasing in the detection for the next iteration and onwards. This, of course, only occurs if the detected data of the previous iteration is reliable. Of course, if the initial detected data is too poor, the iterative process may not be able to cancel the ISI. Coding and interleaving techniques on the transmitted data, may be solutions to apply with the objective of overcome this problem. Regarding the $Fig.4.4$, we can see the multiplication of the feedback coefficients by $\bar{S}_k$ such that:

$$[\bar{S}_k; k = 0,1, \cdots, N-1] \tag{53}$$

which represents the frequency-domain average values conditioned to the FDE output, of the previous iteration (also known as Soft-Decisions).

After the first iteration, if the residual BER is not too high, the feedback coefficients can mitigate a significant part of the residual interference. Then, is possible to rewrite the output of the equalizer, associated to the k_{th} subcarrier, as:

$$\tilde{S}_k{}^{(I)} = \sum_{r=1}^{R} \left[F_k^{(r,I)} Y_k^{(r)} - B_k^{(I)} \bar{S}_k^{(I-1)}\right] \tag{54}$$

where:

$$\bar{S}_k^{(I-1)} = \rho^{(I-1)} \hat{S}_k^{(I-1)} \tag{55}$$

After a few iterations, $\rho \approx 1$, which means that we have almost complete the cancellation of the residual ISI, while the feedforward coefficients perform an approximate matched filtering. Since $\rho^{(I-1)}$ can be regarded as the blockwise reliability of the previous iteration $\hat{S}_k^{(I-1)}$, $\bar{S}_k^{(I-1)}$ is the overall block average of $S_k^{(I-1)}$ at the FDE's output. Here, the blockwise averages

are replaced by symbol averages, applying a DFT operation at the output TD block of the receiver. The transmitted symbols are selected from a QPSK constellation under a Gray mapping rule, i.e.:

$$s_n = \pm 1 \pm j = s_n^{\boldsymbol{I}} + j s_n^{\boldsymbol{Q}} \tag{56}$$

where:

$$s_n^{\boldsymbol{I}} = Re\{s_n\} \tag{57}$$

and:

$$s_n^{\boldsymbol{Q}} = Im\{s_n\} \tag{58}$$

The last two definitions can also be applied to $\tilde{s}_n$, $\bar{s}_n$and $\hat{s}_n$.

Assuming a Gaussian distribution of the symbols, it can be shown that the mean value of s_n, conditioned to the FDE output TD symbols $\tilde{s}_n$, is:

$$\bar{s}_n = \tanh\left(\frac{L_n^{\boldsymbol{I}}}{2}\right) + jtanh\left(\frac{L_n^{\boldsymbol{Q}}}{2}\right) = \left(\rho_n^{\boldsymbol{I}} \hat{s}_n^{\boldsymbol{I}}\right) + \left(j\rho_n^{\boldsymbol{Q}} \hat{s}_n^{\boldsymbol{Q}}\right) \tag{59}$$

where $L_n^{\boldsymbol{I}}$ corresponds to the Log Likelihood Ratio (LLR) of the in-phase bit of the n_{th} symbol:

$$L_n^{\boldsymbol{I}} \frac{2\tilde{s}_n^{\boldsymbol{I}}}{\sigma_p^2} \tag{60}$$

and $L_n^{\boldsymbol{Q}}$ corresponds to the in-quadrature bit of the n_{th} symbol:

$$L_n^{\boldsymbol{Q}} \frac{2\tilde{s}_n^{\boldsymbol{Q}}}{\sigma_p^2} \tag{61}$$

where:

$$\sigma_p^2 = \frac{1}{2}\,\mathbb{E}[|s_n - \tilde{s}_n|^2] \approx \frac{1}{2N}\sum_{n=0}^{N-1} \mathbb{E}[|\hat{s}_n - \tilde{s}_n|^2] \tag{62}$$

and $\rho_n^{\boldsymbol{I}}$ and $\rho_n^{\boldsymbol{Q}}$ are regarded as the reliabilities associated to the in-phase and quadrature bits of the n_{th} symbol, expressed by:

$$\rho_n^{\boldsymbol{I}} = \frac{\mathbb{E}[s_n^{(\boldsymbol{I}*)} \hat{s}_n^{\boldsymbol{I}}]}{\mathbb{E}[\left|s_n^{(\boldsymbol{I})}\right|^2]} = \left|\tanh\left(\frac{\left|L_n^{(\boldsymbol{I})}\right|}{2}\right)\right| \tag{63}$$

and:

$$\rho_n^{\boldsymbol{Q}} = \frac{\mathbb{E}[s_n^{(\boldsymbol{Q}*)}\hat{s}_n^{\boldsymbol{Q}}]}{\mathbb{E}[\left|s_n^{(\boldsymbol{Q})}\right|^2]} = \left|\tanh\left(\frac{\left|L_n^{(\boldsymbol{Q})}\right|}{2}\right)\right| \tag{64}$$

where, as similar to the hard-decisions, for the first iteration ($I = 1$), we have the correlation coefficients $\rho_n^{\boldsymbol{I}} = 0$ and $\rho_n^{\boldsymbol{Q}} = 0$ and $\bar{s}_n = 0$, whereas the feedforward coefficients are the same as the hard-decisions presented in the equations (47) and (76), but with the following correlation coefficients:

$$\rho^{(I)} = \frac{1}{2N}\sum_{n=0}^{N-1}\left[\rho_n{}^{\boldsymbol{I}(I)} - \rho_n{}^{\boldsymbol{Q}(I)}\right] \tag{65}$$

This receiver structure employs hard-decisions in the direct loop where the estimation reliabilities of the previous iteration $\rho_n{}^{(I-1)}$are related to an entire block of received information, whereas in the feedback loop, the soft-decisions uses independent reliability factors related to each of the in-phase and quadrature symbols of the selected constellation $\rho_n{}^{\boldsymbol{I}}$ and $\rho_n{}^{\boldsymbol{Q}}$.

As mentioned before, for a given iteration of the IB-DFE for the detection of the t_{th} MT, the receiver is characterized by the feedforward F_k and feedback B_k coefficients, associated to each of the k_{th} frequency $[k = 0,1,2\cdots, N-1]$.

For the QPSK constellation with Gray mapping used throughout this thesis, the BER is given by:

$$P_e \approx Q\left(\sqrt{\frac{1}{\theta_k}}\right) \tag{66}$$

where $Q(x)$ denotes the Gaussian error function and θ_k is represented by equation (37).

Regarding the FD estimated symbols from equation (48) and the MSE of each k frequency of θ_k, we arrive at expression:

$$\begin{aligned} min_{\theta(k)} &= \mathbb{E}\left[\left|\tilde{S}_k - S_k\right|^2\right] \Leftrightarrow \\ \Leftrightarrow min_{\theta(k)} &= \mathbb{E}[|Y_k F_k - S_k|^2] \Leftrightarrow \\ \Leftrightarrow min_{\theta(k)} &= \mathbb{E}[|F_k Y_k - B_k \bar{S}_k - S_k|^2] \end{aligned} \tag{67}$$

designating the MSE on the FD samples $\tilde{s}_k$ **[48]**.

Clearly, the bit error probability will be minimized if we minimize the MSE at each subcarrier θ_k, resulting in a set of F_k and B_k coefficients.

The F_k and B_k coefficients are obtained applying the Lagrange function to equation (67). The Lagrange function is defined as:

$$J = \theta_k + \lambda(\gamma_k - 1) \tag{68}$$

where the optimum coefficients F_k and B_k being the solution of the following system of equations:

$$\begin{cases} \Delta_F J = 0 \\ \Delta_B J = 0 \\ \Delta_\lambda J = 0 \end{cases} \tag{69}$$

The solution for this system of equation can be found on **[50]**.

Solving the system in order to F and B, and assuming:

$$\Delta_\lambda J = 0, \gamma_t = 1 \tag{70}$$

and after some straightforward manipulations, we obtain:

$$F = k\Lambda H^H e_t \tag{71}$$

and:

$$B = \alpha HF - e_t \tag{72}$$

with

$$\Lambda = (H^H(I_p - P^2)H + R_N R_S^{-1}|\alpha|^{-2})^{-1} \tag{73}$$

where the Λ definition is described in **[50]**. Then the F_k and B_k coefficients surge naturally and are defined by:

$$F_k^{(r,I)}, (r = 1,2, \dots, R) \tag{74}$$

$$B_k^{(I)} = \rho^{(I-1)} \left(\sum_{r=1}^{R} F_k^{(r,I)} H_k^{(r)} - 1 \right) \tag{75}$$

The equalization function is described below:

$$F_k^{(r,I)} = \frac{k_F^{(I)} H_k^{(r)^*}}{\beta + [1 - (\rho^{(I-1)})^2] \sum_{r=1}^{R} |H_k^{(r)}|^2} \tag{76}$$

Whith the Noise to Signal Ratio (NSR) denoted by β is given as:

$$\beta = \frac{1}{SNR} = \frac{\mathbb{E}[N_k^{(r)}]}{\mathbb{E}[S_k^{(r)}]} \tag{77}$$

And the correlation factor, used to measure the blockwise reliability of the decisions used in the feedback loop is defined by:

$$\rho^{(l)} = \frac{\mathbb{E}[s_n^* \hat{s}_n^I]}{\mathbb{E}[|s_n|^2]} = \frac{\mathbb{E}[S_k^* \hat{S}_k^I]}{\mathbb{E}[|S_k|^2]} \tag{78}$$

The parameters of the receiver are calculated based on a channel frequency response which is represented by:

$$\sum_{r=1}^{R} F_k^{(r,I)} H_k^{(r)} \tag{79}$$

The residual ISI component in the FD is related with the difference between the channel frequency response given by (79) and the following, equation (80):

$$\gamma(I) = \frac{1}{N} \sum_{k=0}^{N-1} \sum_{r=1}^{R} F_k^{(r,I)} H_k^{(r)} \tag{80}$$

where $\gamma(I)$ can be regarded as the average channel frequency response at the I_{th} iteration, after combining the outputs of the R output filters.

From and (71) and (76), k is selected to ensure that $\gamma(I) = 1$.

From each iteration, there is a resulted equalized samples from the received block where the iterations are done, in order to eliminate the residual ISI from this same block.

In the FD, these equalized samples are given by:

$$\tilde{S}_k{}^{(I)} = \gamma(I) S_k + \epsilon_k^{(I)} \tag{81}$$

Where the global error consisting of the residual ISI and IUI plus the channel noise is given by:

$$\epsilon_k^{(I)} = \tilde{S}_k{}^{(I)} - \gamma(I) S_k \tag{82}$$

As mentioned before, the F_k and B_k coefficients are obtain as to maximize the desired signal against noise and interference, i.e.: the SINR, which is expressed by:

$$SINR = \frac{|\gamma(I)|^2 \mathbb{E}[|S_k|^2]}{\mathbb{E}[\left|\epsilon_k^{(I)}\right|^2} \tag{83}$$

For the first iteration, that is ($I = 0$), no information exists about the transmitted data S_k, and the correlation coeficient ($\rho = 0$), and from (75) comes $B_k^{(0)} = 0$ and therefore $F_k^{(r,0)}$ comes as:

$$F_k^{(r,0)} = \frac{H_k^{(I)^*}}{\beta + \sum_{r=1}^{R} |H_k^{(r)}|^2} \tag{84}$$

resulting in a linear FDE receiver. It is worth mentioning that although the equations above are directed to an R order receiver, the IB-DFE parameters are easily obtained from the same equations assuming that $R = 1$.

The equalized signal in the I_{th} iteration is given by:

$$\tilde{S}_k = F_k Y_k - B_k \bar{S}_k \tag{85}$$

The IB-DFE referred to above only contemplates receivers of the MMSE type, but it is possible to apply this type of technique to other types of less complex equalizers, such as the MRC or the EGC. This expansion of IB-DFE to simpler receivers is a plus when thinking of technologies such as 5G where the complexity of systems is much higher due to the number of antennas involved.

In this way, the use of equalizers that do not involve mathematical inversions of matrix and that at the same time can separate the data of each user, should be considered and used even if it does not lead to so great performances (due to the weak capacity in reducing the ISI and IUI) because it can be compensated with the complement of iterative equalizers. When simple receivers are combined with iterative approaches in a scenario where $R \gg T$, the performance increases substantially, approaching the Matched Filter Bound **[51]**.

4.6 Combined MRC+IBDFE (low complexity iterative receiver)

The outputs of the Maximum Ratio Combiner, R_v are given by:

$$R_v = \sum_{d=1}^{D} a_d r_{dv} e^{j\emptyset d} \tag{86}$$

where v is the number of independent transmitted signals, and D is the diversity order. When feedback equalization is considered, the equalized signal associated to the k_{th}subcarrier $\tilde{S}_k$ is given by:

$$\tilde{S}_k = \psi F_k Y_k - B_k \bar{S}_k^{l-1} \tag{87}$$

with $B_k \bar{S}_k^{l-1}$ denoting the soft-decision equalized symbol of the previous iteration. The $R \times R$ feedback coefficients matrix B_k is given by:

$$B_k = \psi F_k Y_k - I \tag{88}$$

where ψ is a $T \times T$ diagonal matrix which works as a normalization parameter that ensures that the average power of the signals do not change due to the combined effect of the channel and equalization. *T*he t_{th} element is defined as:

$$\psi^{(t,t)} = \frac{1}{\sum_{k=0}^{N-1} \sum_{r=1}^{R} |H_k|^{(r,t)}} \tag{89}$$

4.7 Combined EGC+IBDFE (low complexity iterative receiver)

The R_m outputs of the Equal Gain Combiner are expressed by:

$$R_m = \sum_{d=1}^{D} r_{dm} e^{j\emptyset d} \tag{90}$$

The only difference between the two low complexity iterative receivers, i.e., between the Combined-MRC (MRC+IBDFE) and the Combined-EGC (EGC+IBDFE), resides in the use of a different matrix F_k in the iterative process, that in this EGC+IBDFE case, is given by:

$$F_k = e^{(j * \arg(H_k^H))} \tag{91}$$

5. Nonlinear Effects at Reception

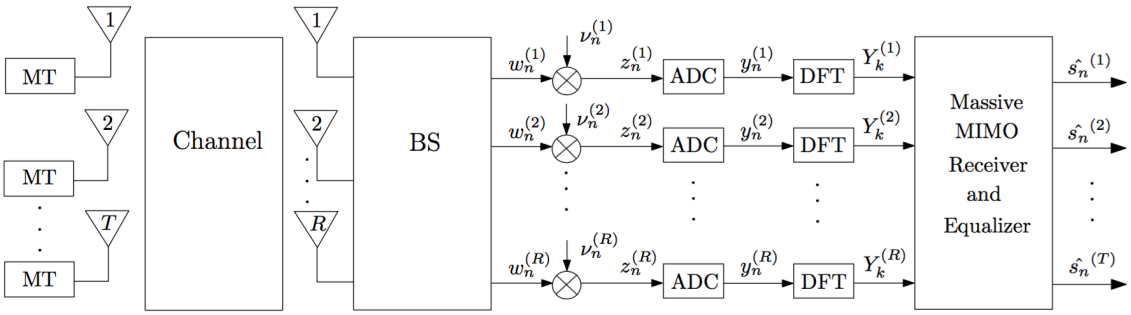

Fig. 5.1: Massive-MIMO Scheme, receiver side detailed.

The sending of information between two distinct points (in this case a transmitter and a 'set' of receivers) is made by the most evolved telecommunication systems in a sophisticated way, whose methods of sending and processing data is mostly handled by advanced computer systems. After processing the data (which are represented in the form of bits), the signals are sent in a purely analogue way, through the physical space. Before the sending of these TD signals, the data present in the MTs (or the BSs), is binary information (that is, 0's or 1's). In order to send the signal via the space propagation medium, it is necessary to convert them from its digital domain to the analogue domain, that is, to transform digital signals from the discrete time to analog signals of continuous time. This conversion process from Digital to Analog occurs at the transmission level and has its homologue at the signal reception level, i.e.: the conversion from Analog to Digital, so that the receivers can process the signals and then equalize them. These two conversion processes are carried out, respectively, by electronic components called Digital to Analog Converters (DACs) and Analog to Digital Converters (ADCs). These elements are particularly relevant in this case study because of their impact on the quality/performance of telecommunications systems, due to the non-linearities they may introduce in the original sended signals (in the case of transmission) or in signals that have already been propagated by the space and are, now, at their input terminals (in the case of reception).

In MIMO systems, with OFDM or SC-FDE modulations, it is necessary to implement these nonlinear elements in each sender or receiver. Hence, due to this increase in the complexity of the systems, it is interesting to analyse their impact when the number of Tx or Rx involved is larger than in a typical MIMO scenario. It becomes a special object of study, since the more antennas involved, the more ADCs or DACs have also to be implemented. The main objective is

to understand the impact of these non-linear elements on the overall performance of data transmission. Since this work focus in the reception of information in the Base Stations (with several receiving antenna schemes) when uplinking information, emitted by individual transmitters of 1 single antenna, it becomes particullary important to analyse the effect of the ADC's in the reception. In Massive-MIMO systems, the implementation of low resolution ADC's, a priori, is a very considerable option because of their low energy consumption (whose becomes relevant in a 'large scale' system). However, the harmful nonlinearity these elements introduce in the systems, depends directly on their capabilities and characteristics. A low resolution ADC is generaly cheaper and consums less energy, but, the negative side is that it has a worse performance. On the other side, an ADC with a higher resolution is more expensive but theoretically has a better performance. The ideal in future telecomunication systems would be to implement severall low resolution ADCs in the large reception antenna-arrays of Massive-MIMO schemes, in the prespective of reducing the global implementation costs, but never losing the sense of necessity to maintain a relative Quality of Service (QoS) in the discret signals at their output.

Next, the main aspects of the ADCs, namely their mode of work and operation, will be addressed. Finally, an analysis of the impact of these elements on the performance of the system will be made, taking into account several variables such as the resolution bits (b) and the normalized saturation level, also known as the Normalized Clipping Level (S_M) **[52][53]**.

5.1 Hardware Impairments Characterization

For the digital modulators and demodulators, the front-end components may not completely respect the orthogonality between the in-phase (I) and in-quadrature (Q) components, resulting in an IQ imbalance characterized by an amplitude offset (ϵ) and a phase offset ($\Delta\phi$).

Both amplitude and phase mismatches are assumed to be symmetric between the real part and the imaginary part of the transmitted signal.

Lets consider an input signal (S_{in}) of an ADC at the receiver, which suffering from IQ imbalance, yields the output signal (S_{out}) given by:

$$\begin{gathered} S_{out} = S_{in}[\cos(\Delta\phi) + j\epsilon\, sin(\Delta\phi)] + S_{in}^{*}[\epsilon\cos(\Delta\phi) - j\, sin(\Delta\phi)] \Leftrightarrow \\ \Leftrightarrow\ S_{out} = S_{in}\,\alpha + S_{in}^{*}\,\beta \end{gathered} \tag{92}$$

This implies that the signal S_{in} is interfered by its own complex conjugate S_{in}^{*}. The desired signal and the interference signal are weighted by α and β, which are given by:

$$\begin{aligned} \alpha &= \cos(\Delta\phi) + j\epsilon\, sin(\Delta\phi) \\ \beta &= \epsilon\cos(\Delta\phi) - j\, sin(\Delta\phi) \end{aligned} \tag{93}$$

Obviously, smaller amplitude and phase mismatches yield larger $|\alpha|$ and smaller $|\beta|$, and therefore, the impairment from IQ imbalance is less severe. The interference from S_{in}^{*} causes attenuation and rotation of the original signal S_{in}, leading to ISI in the SC-FDE transmissions.

As indicated above, both DAC and ADC introduce IQ imbalances in the signals **[54]**.

To this end, the TD transmited signal (S_{in}) at the transmitter and the received signal S_{out} at the receiver side, are both interfered by their respective complex conjugates, as shown in $Fig.35$ by a simplified block diagram:

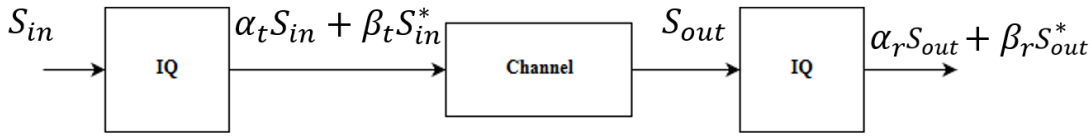

Fig. 5.2: Simplified block diagram for illustration of incorporating IQ imbalance at both the transmitter and the receiver.

where, α_i and β_i, i $\in$ {t, r}, represent the weighting factors at either the transmitter or at the receiver.

As described in **[54]**, assuming s_{in} the transmit signal vector, the noise-free receive signal vector $\hat{s}_{in}$ after equalization, in a SC-FDE transmission technique, is given by:

$$\hat{s}_{in} = \alpha_r \alpha_t s_{in} + \beta_r \beta_t^{*} HFH^{*} S_{in} + \alpha_r \beta_t s_{in}^{*} + \beta_r \alpha_t^{*} HFH^{*} S_{in}^{*} \quad (94)$$

where H and F denote, respectively, the diagonal channel matrix and the equalization matrix.

As a result, a high gain subcarrier may interfere on a low gain subcarrier located at the other side of the spectrum, thus totally corrupting the signal detection there.

In digital communication systems, DACs and ADCs with finite resolution are applied at the transmitter and receiver, respectively. On one hand, using more quantization bits offers higher precision for signal conversion between the digital and analog domains. On the other hand, the power dissipation of ADC scales exponentially with the resolution, i.e., adding one more quantization bit doubles the energy costs of the Quantizer **[54]**.

To this end, is desirable practical ADCs designs with less quantization bits, while preserving the system's performance. This issue is especially important for communications at mmWave range because a large number of antennas as well as RF chains and beamforming are assumed for Massive-MIMO schemes, leading to prohibitive hardware energy cost with high-resolution ADC/DACs. Since in this thesis we focus our work in the receiver side, in the next section we board the ADCs main characteristics and their impact in the performance.

5.2 Analog to Digital Converters

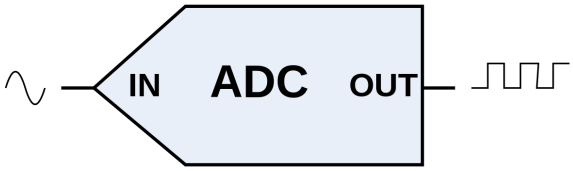

Fig. 5.1: Analog to Digital Conversion.

There are severall types of different Analog to Digital Conversion technologies. However, all of them resides in a basic principle: the conversion of the input analog signal to a certain number of bits (N). The sequence of bits represents a code number and, each bit has the double of the weight of the next one, starting from the Most Significant Bit (MSB) up to the Least Significant Bit (LSB). In a nutshell, it is intended to find the sequence of bits (b_{N-1}, b_{N-2}, ..., b_0) that represents the analog input value V_{in}, which can be described as:

$$V_{in} = \sum_{i=0}^{N-1} b_i \, 2^i \left(\frac{V_{ref}}{2^N}\right) \tag{95}$$

The MSB has weight $\frac{V_{ref}}{2}$, the next $\frac{V_{ref}}{4}$, etc., and the LSB has weight $\frac{V_{ref}}{2n}$.

Therefore, more bits lead to more precision in the digital representation of a analog signal. Here we simplify the dynamic range to be between $V_{in} = 0$ and V_{ref}, although the range may vary between any other two different values.

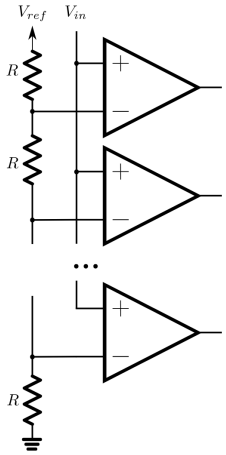

Fig. 5.4: Example of a Flash ADC, with threshold V_{ref}.

The converters have a resistive ladder that divides the reference voltage in 2^N equal parts. For each part, a comparator compares the input signal with the voltage supplied by that part of

the resistive ladder. The output of all the comparators is like a thermometer: the higher the input value, more comparators have their outputs high from the bottom to the top. A dedicated component called "Priority Encoder" translates this gauge into a binary code, which corresponds to the position of the last comparator with the high output, counting from the bottom up.

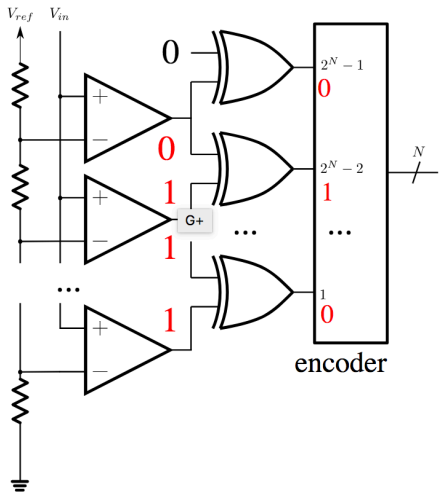

Fig. 5.5: Priority Encoder working example.

The Priority Encoder has to find the position of the last comparator with high output, starting from the bottom. That means that it should find the position where neighboring comparators have different outputs (all below have output high and all above have output low).
That can be simply done by XORing the outputs of neighboring comparators and feeding their outputs to a digital encoder. Only one XOR has its output active and the encoder will translate that position into a binary representation. If there are 2^N comparators, the encoder outputs a N-bit number.

As ADC technologies evolved, it was possible to categorize ADCs because of their characteristics (like speed, power consumption, number of used comparators, etc), which are more interesting in some cases than in others.

In general, it can be stated that the power dissipated by the ADC is directly influenced by the predefined sampling frequency (f_s) and the number of quantization bits (b) **[52]**. The greater the evidence of either of these two factors, the greater the associated energy expenditure **[55]**, since the influence of the number of bits is in power scale and the frequency is in multiplicative scale, as it can be observed through the following formula:

$$Pd_{ADC} \equiv \beta_{ADC} \left(2^b - 1\right) f_s \tag{96}$$

Above, β_{ADC} represents a constant value that adopts different values consonant the type of ADC applied. The sampling rate is measured in Hertz (Hz) and should always be greater or equal to the double of the available bandwidth, like the Nyquist-Shannon theorem evokes:

$$f_s \geq 2B \tag{97}$$

The discretization of a continuous-time analogue signal starts with the sampling operation, which consists in define how to "separate" the analogue signal into different samples at a certain rythm (sampling rate). For that, it is necessary to define a constant sampling period (T_s), described as following:

$$T_s = \frac{1}{2f_s} \tag{98}$$

Then, after the sampling, is necessary to Quantize the obtained samples (to give them a meaning) in terms of their amplitude, which will define if it is a zero or a one. The quantization process is sequential between the different samples of the sampled signal and is done by discretizing the signal with a number of quantization levels.

The quantization represents the sampled values of the amplitude by a finite set of levels, which means converting a continuous-amplitude sample into a discrete-time signal as we can see in $Fig.5.6$.

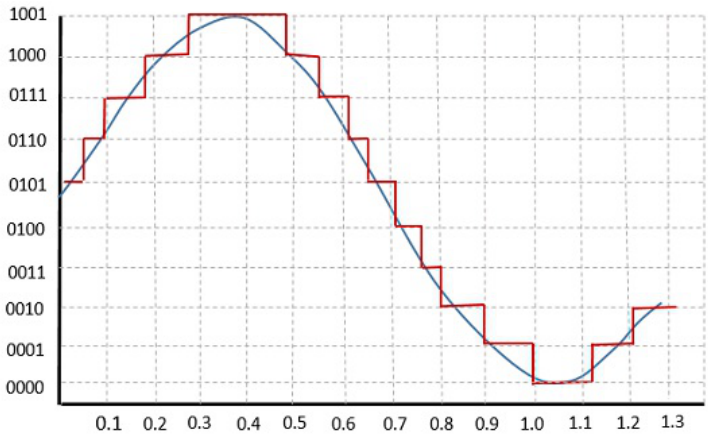

Fig. 5.6: Quantization process.

(Source: [56])

In $Fig.5.6$ is possible to observe the quantized signal (in red) that comes from the original analog signal (in blue).

Both sampling and quantization, result in the loss of information from the original signal.

The quality of a Quantizer output depends upon the number of quantization levels used. The discrete amplitudes of the quantized output are called as representation levels or reconstruction levels. The spacing between the two adjacent representation levels is called a quantum or

step-size. Any two adjacent quantized values are separated by a fixed spacing value (Δ), given by:

$$\Delta = 2\frac{S_M}{2^b} \tag{99}$$

where $S_M$corresponds to the maximum voltage value (in Volt) that the ADC is prepared to deal with, ie, the Clipping Level. The number of Quantization levels (Q) depends intirely in the number of bits of resolution (b), by the following formula:

$$Q = 2^b \tag{100}$$

which can be translated to:

$$b = \log_2(Q) \tag{101}$$

The Massive-MIMO system considered in this work, can be regarded as a scenario where T single-antenna MTs communicate with an R-branch BS. Between each pair of antennas, a frequency-selective multipath channel is considered. Then, the associated channel to the k_{th} subcarrier is represented by the $R\times T$ matrix, bellow:

$$H_k = \begin{bmatrix} H_k^{(1,1)} & H_k^{(1,2)} & \cdots & H_k^{(1,T)} \\ H_k^{(2,1)} & \cdots & \vdots & H_k^{(2,T)} \\ \vdots & \vdots & \ddots & \vdots \\ H_k^{(R,1)} & \cdots & \cdots & H_k^{(R,T)} \end{bmatrix} \tag{102}$$

The average power of the different considered multipath rays, is normalized to guarantee that the expected value overall the channel is:

$$\mathbb{E}\left[\left|H_k^{(r,t)}\right|^2\right] = 1 \tag{103}$$

At the n_{th} time instant, T QPSK symbols in the form $s_n = \pm\sigma_s \pm j\sigma_s$ are transmitted in parallel throughout the channel. Decomposing this simbols in the absolute value, we obtain:

$$\begin{aligned} &|s_n| = \sqrt{\left(\sigma_{s_n}^2 + \sigma_{s_n}^2\right)} \Leftrightarrow \\ &\Leftrightarrow |s_n| = \sqrt{\left(2\sigma_{s_n}^2\right)} \Leftrightarrow \\ &\Leftrightarrow |s_n|^2 = 2\sigma_{s_n}^2 \end{aligned} \tag{104}$$

It should be noted that these signals do not obey to a Gaussian Distribution. The data stream transmitted and associated to the t_{th} transmit antenna is represented by the block:

$$s_n^{(t)} = \left[s_0^{(t)}\ s_1^{(t)}\ s_2^{(t)}\ \cdots\ s_{N-1}^{(t)}\right]^T \tag{105}$$

Considering the frequency domain version of the transmitted signal $s_n^{(t)}$, it can be described by:

$$S^{(t)} = \left[S_0^{(t)}\ S_1^{(t)}\ S_2^{(t)}\ \cdots\ S_{N-1}^{(t)}\right]^T \tag{106}$$

where N represents the number of symbols to transmit, referent to a certain data stream.The data symbols associated to the k_{th} subcarrier are represented by the $T\times1$ block:

$$S_k = \left[S_k^{(1)}\ S_k^{(2)}\ S_k^{(3)}\ \cdots\ S_k^{(T)}\right]^T. \tag{107}$$

Then, considering the channel model represented in (102), the received signal associated to the kth subcarrier is given by:

$$Z_k = \left[Z_k^{(1)}\ Z_k^{(2)}\ Z_k^{(3)}\ \cdots\ Z_k^{(R)}\right]^T \tag{108}$$

which can be decomposed in:

$$Z_k = H_k S_k + N_k = W_k + N_k \tag{109}$$

where N_k represents the Aditive White Gaussian Noise (AWGN):

$$N_k = \left[N_k^{(1)}\ N_k^{(2)}\ N_k^{(3)}\ \cdots\ N_k^{(R)}\right]^T \tag{110}$$

The TD version of the received signal, which obeys to a Gaussian Distribution independently of the combination between Tx and Rx, is described by:

$$\begin{gathered} z_n = h_n * s_n + v_n \Leftrightarrow \\ \Leftrightarrow z_n = w_n + v_n \end{gathered} \tag{111}$$

Where the noise samples to the r_{th} antenna at the n_{th} TD are described as below:

$$v_n(r) = [v_0(r)v_1(r)\cdots[v_{N-1}(r)]^T \tag{112}$$

The real and imaginary parts of this noise samples have variance σ_n^2.

It should be noted again that, although the TD transmitted samples $s_n^{(t)}$ are not Gaussian, the samples $w_n^{(r)}$ are approximately Gaussian due to the frequency selective behaviour of the channel.

Therefore we have a Normal distribution described by:

$$w_n^{(r)} \sim \mathcal{N}(0, 2\sigma_w^2) \tag{113}$$

Hence, the TD received samples, which are the received (w_n) with the addiction of the noise (v_n), associated to each reception branch $z(r)$, are:

$$z(r) = [z_0(r) z_1(r) \cdots [z_{N-1}(r)]^T \quad (114)$$

This means that the received signal has an approximate Gaussian distribution with zero mean and variance $2\sigma_z^2$, such that:

$$z_n^{(r)} \sim \mathcal{N}(0, 2\sigma_z^2) \quad (115)$$

The average power for the received samples $z(r)$, i.e.: the expected value of z_n, is given by:

$$P_z = \mathbb{E}[|z_n|^2] = 2\sigma_{z_n}^2 \quad (116)$$

Then, taking into account (112), the SNR can be defined as:

$$SNR = \frac{\sigma_s^2}{\sigma_n^2} \quad (117)$$

It should be noted that, for the system in study, we consider that each receiver branch has two ADC. One ADC does the conversion for the in-phase component information and the other works for the in-quadrature component information. Each ADC is modeled by the nonlinear function $f(\cdot)$ that represents a uniform, mid-rise quantization process, with normalized clipping level $sMnorm = \frac{S_M}{\sigma_z}$ and different types of resolution consonant the elected number of bits (b), being σ_z the variance of the input signal.

It is important to note that, in the simulations done for this work where we employ the ADCs to simulate the impact of non-linear effects, the quantizers are defined with a certain number of bits of resolution.

Thus, consonant the defined number of resolution bits, we use an optimum clipping level with the objective of do the maximization of the $SQNR(dB)$ **[57]**, being this optimum clipping level dependent of this defined number of resolution bits, as refered in **[50]**.

In $Fig.5.7$, the number of bits is represented by m (in place of b). This figure shows the Signal to Quantization Noise Ratio (SQNR) in function of the normalized clipping level $\left(A_M / \sigma_y^{(r)}\right)$ and is possible to observe the evolution of the optimum clipping level, with the increase in the number of bits.

The saturation level which maximizes the $SQNR(dB)$, for a certain number of bits, is correspondent with the higher amplitudes of the blue lines **[57]**.

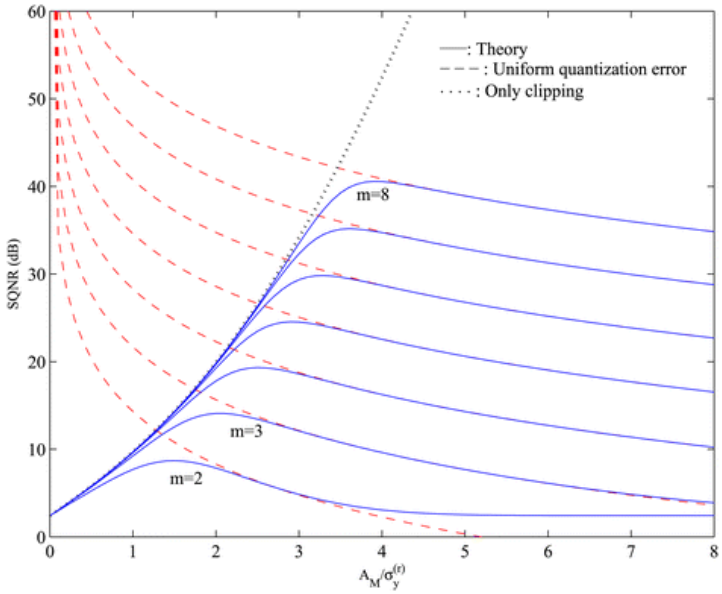

Fig. 5.7: SQNR (dB) as a function of the normalized clipping level employing different number of resolution bits.

(Source: [50])

The quantization is made separately on the real and imaginary parts of the complex time-domain samples, $z_n^{(r)}$.

Hence, at the output of the rth ADC we have, at the nth time instant:

$$y_n^{(r)} = f\left(Re\left(z_n^{(r)}\right)\right) + if\left(Im\left(z_n^{(r)}\right)\right) \tag{118}$$

The average power of the output signal, which is equal to all the reception branches, is given by:

$$P_y = \mathbb{E}[|y_n|^2] = 2\sigma_{y_n}^2 \tag{119}$$

The average power of the different multipath rays is normalized to guarantee:

$$\mathbb{E}\left[\left|H_k{}^{(r,t)}\right|^2\right] = 1 \tag{120}$$

By considering the Gaussian nature of the ADCs input, we can employ the Bussgang's theorem, which allow us to express their output as the sum of two uncorrelated components, i.e:

$$y_n^{(r)} = \alpha z_n^{(r)} + d_n^{(r)} \tag{121}$$

where α corresponds to a scale factor, given by:

$$\alpha = \frac{\mathbb{E}\left[z_n^{(r)} y_n^{*(r)}\right]}{\mathbb{E}\left[\left|z_n^{(r)}\right|^2\right]} \tag{122}$$

and where $d_n^{(r)}$ corresponds to the non-linear distortion term associated to the n_{th} time instant at the r_{th} receiver, with power:

$$P_d = \mathbb{E}[|d_n|^2] = 2\sigma_{d_n}^2 = 2\sigma_{y_n}^2 - 2|\alpha|^2\sigma_{z_n}^2 \tag{123}$$

Is important to note that the Imaginary and Real parts of the ADCs output signal are total uncorrelated and carry different data, so, in this way, we can consider that the distortion is independent.

Regarding the FD we have, for the k_{th} subcarrier of the r_{th} data stream, the following:

$$Y_k^{(r)} = \alpha Z_k^{(r)} + D_k^{(r)} \tag{124}$$

where $D_k^{(r)}$ represents the FD version of the non-linear distortion term ($d_n^{(r)}$).

Considering the expression declared in (124), It can be rewrited in the following way:

$$Y_k = \alpha Z_k + D_k = \alpha(H_k S_k + N_k) + D_k \tag{125}$$

where the data symbols received on the k_{th} subcarrier corresponds to:

$$Y_k = \left[Y_k^{(1)}\ Y_k^{(2)}\ Y_k^{(3)}\ \cdots\ Y_k^{(R)}\right]^T \tag{126}$$

The FD version of the nonlinear distortion components associated to the k_{th} subcarrier is described by:

$$D_k = \left[D_k^{(1)}\ D_k^{(2)}\ D_k^{(3)}\ \cdots\ D_k^{(R)}\right]^T \in \mathbb{C}^N \tag{127}$$

The equalization matrix used to equalize the received signals is F_k, which vary consonant the adopted equalization technique. Then, the equalized signals associated to the k_{th} subcarrier are given by:

$$\tilde{S}_k = \left[\tilde{S}_k^{(1)}\ \tilde{S}_k^{(2)}\ \tilde{S}_k^{(3)}\ \cdots\ \tilde{S}_k^{(T)}\right]^T \in \mathbb{C}^N \tag{128}$$

which can be described and decomposed, by the following set of equations:

$$\begin{gathered} \tilde{S}_k = F_k Y_k \Leftrightarrow \\ \Leftrightarrow \tilde{S}_k = \alpha F_k Z_k + F_k N_k \Leftrightarrow \\ \Leftrightarrow \tilde{S}_k = \alpha F_k H_k S_k + \alpha F_k N_k + F_k D_k \end{gathered} \tag{129}$$

Since the distortion terms are uncorrelated and the data symbols are not, the SQNR for detection purposes has a gain of R relatively to the SQNR at the ADCs output. However, as the

power of the received signal increases with T, there is a "global gain" of R/T in the SQNR for detection purposes. Then, is possible to expect that the performance penalty, associated to the non-linear distortion, can be convergent to insignificant values when considering Massive-MIMO scenarios, i.e., in scenarios where: $R \gg T$.

After the equalization process is complete, the signals are converted back to the TD by an $IDFT$ operation and, finally they are sent to the detector whose output's corresponds to the different detected data symbols, associated to the n_{th} time instant of the t_{th} antenna. The detection of the equalized symbols occurs with a Hard-Decisions process. Each of the obtained symbols is represented by $\hat{s}_n^{(t)}$and, their set, can be expressed by:

$$\hat{s}_n^{(t)} = \left[\hat{s}_n^{(1)}\hat{s}_n^{(2)}\ \hat{s}_n^{(3)} \cdots\ \hat{s}_n^{(T)}\right]^T \in \mathbb{C}^N \tag{130}$$

It should be also noted that, in the FD, the symbols corresponding to the k_{th} subcarrier of the t_{th} stream, can be denoted by $\hat{S}_k^{(t)}$, and their set, by:

$$\hat{S}_k^{(t)} = \left[\hat{S}_k^{(1)}\hat{S}_k^{(2)}\ \hat{S}_k^{(3)} \cdots\ \hat{S}_k^{(T)}\right]^T \tag{131}$$

6. Performance Results

In this section we present the performance results of the combination between the iterative techniques and the low complexity detectors, and is done an analysis and a critical comparison between some different $T \times R$ configurations.

It is important to note that the following set of experimental results, present in $section\ 6.1$, firstly do not consider neither include any type of Nonlinearity in the receiver. The analysis with the Nonlinear Distortion effects will be shown later in $section\ 6.2$.

For the first set of experiences, different simulation scenarios are considered, where the number of transmitting antenas (T) and receiving antenas (R) is sequentially changed. A different set of performance results can be obtained, representing the behaviour of the receivers for each relation between R and T. This results are compared and analyzed with the objective of get the overview conclusion about which of the different receivers is more suitable in a Massive-MIMO environment consonant the relation between T and R and another factors, e.g.: the number of iterations in the iterative algorithms. Is also made a study of impact of the Non-linear Distortion effects in the performance of the systems, due to the ADCs employed in the receiver side.

The following survey, firstly will be divided in three different aproaches that take into account, respectively:

a) the influence of increasing the iterations number (I) in the interference cancelation performance for each receiver when subjected to different $T \times R$ configurations;
b) the ratio R/T where is intended to do a comparison between different ratios in the relation $T \times R$, always with a fixed value of Tx, and to get some conclusions about the impact of the increase in the number of Rx;
c) the consequence in increasing the number of the T single-antenna MTs, for a group of simulations with a fixed number of Rx in the BS.

For the sake of simplicity, in this simulation the number of Tx for each simulation is always $T = 4$ [for the items a) and b)].

To recreate a scenario closer to the reality, where the transmission channel is subject to frequency selective fading, due to multipath propagation effects, each of the different channels (with a small correlation) generated between a empaired single-antenna Tx and a Rx antennas array, has 16 random gains, that represent the different multipath ray components, making focus on the delay-spread effect on the receivers arriving signals.

The results are presented in form of a BER in function of E_b/N_0, being Eb the average bit energy for the group of Rx (i.e., Rx multiplied by the bit energy for one single antenna) and N_0 corresponds to the unilateral Power Spectral Density (PSD) of the $AWGN$ effects.

After, in $section$ 6.2 the survey will approach the results of the introduction of the Non Linear distortion effects, doing a comparison between the performance of the NL system (with ADCs) and the system without consider the introduction of ADCs. The impact of Rx and Tx, as well as the different ADC resolution (with a certain Normalized Clipping Level associated) are studied.

6.1 Analysis in the presence of Linear Systems

6.1.1 Effect of the Iterative Interference Cancelation

Independently of the number of single-antenna MTs, henceforth (T), associated to a set of receiver antenas in the BS, henceforth (R); in a system where the spatial diversity condition $R > T$ (R being greater than value of T) is always verified, it's pressupposed, in the major of the situations, the achievement of better performances by the iterative receivers when it is performed a sequential increase in the number of iterations (I). However, although this behavior is likely most of the situations, this increase of performance may depend on the receiver in question and, as well, can vary to different behaviours depending on a bigger or smaller ratio between the number of receiver and transmiter antenas relation, i.e.: the ratio R/T, as we can observe in the different tryed simulated scenarios, whose results are shown bellow.

Results for EGC+IBDFE:

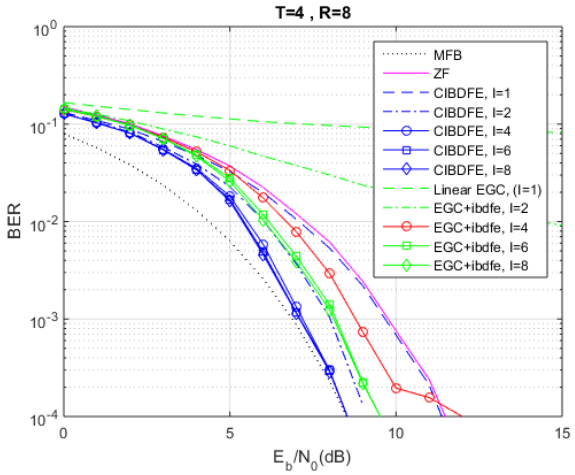

Fig. 6.1: Iterations Effect EGC+IBDFE (T=4, R=8).

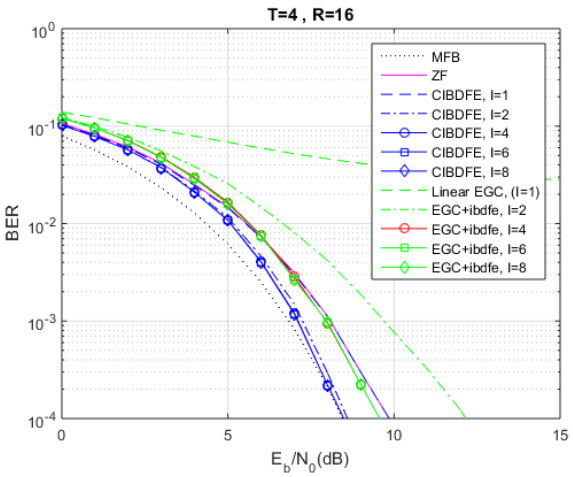

Fig. 6.2: Iterations Effect EGC+IBDFE (T=4, R=16).

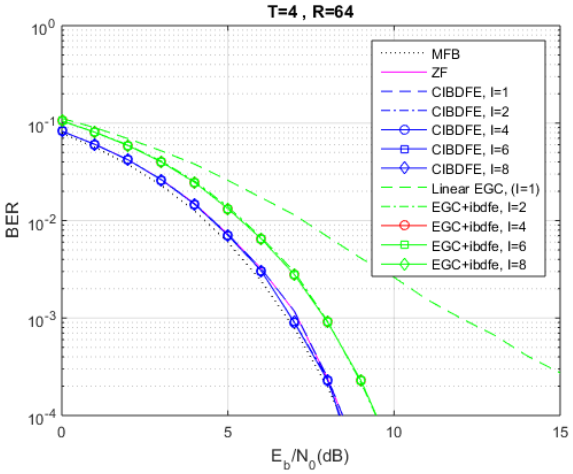

Fig. 6.3: Iterations Effect EGC+IBDFE (T=4, R=64).

As we can verify (respectively in $Fig.\,6.1$, $Fig.\,6.2$ and $Fig.\,6.3$), when the number of iterations increases, the iterative interference cancelation works in a very effective way and permits the improvement of the system performance. This performance improvement is not unlimited and tends to reach his maximum around the interval from the 4th to the 8th iteration, meaning a certain limit convergence around this values of I.

In the $Fig.\,6.1$, where is simulated a low ratio R/T, we can observe that in this scenario the system itself is more suitable to benefit of a high number of iterations, i.e.: the iterations have a big influence in the system performance. The higher the iteration índex, the higher the performance.

In another way, as we can observe in the Fig 6.3. and even in the $Fig.\,6.2$, the system performance improvements start to depend not so much in a direct relation to the number of iterations, but to the Ratio increase between R and T. This is observable since, from the 3rd iteration onwards, the other following iterations tendentially are converging the results to a limit value, so they do not really affect

the performance increase. Concluding, for a stage of low order iterations in a higher R/T relation, the performance is better comparing to the same situation in a lower R/T.

Results for MRC+IBDFE:

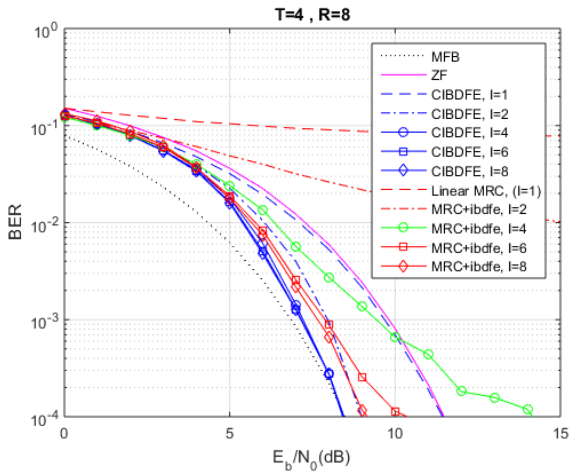

Fig. 6.4: Iterations Effect MRC+IBDFE (T=4, R=8).

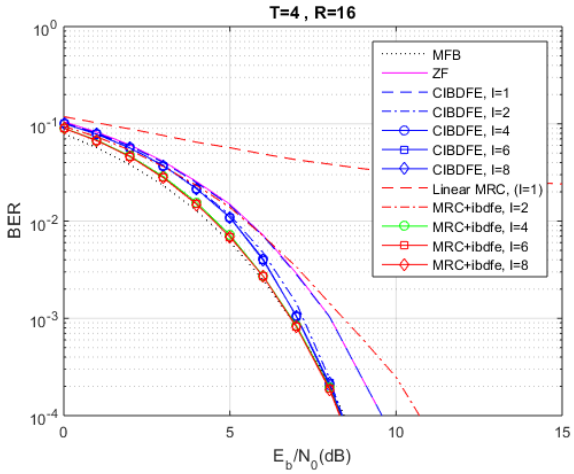

Fig. 6.5: Iterations Effect MRC+IBDFE (T=4, R=16).

As we can see above ($Fig.$ 6.4 and $Fig.$ 6.5), with the MRC detection combined with the iterative IB-DFE (as know as MRC+IBDFE), the observed effect of the increasing in the number of iterations is similar to the results obtained for the EGC+IBDFE presented previously.

Analysing the graphics, it is possible to see that, the bigger the number of iterations the bigger is the convergence of the system performance to a limit value in the case of a higher R/T ratio. In this case are needed less iterations to approach good performances. In another way, more iterations are needed to achieve a certain performance limit when using a low R/T antenna ratio.

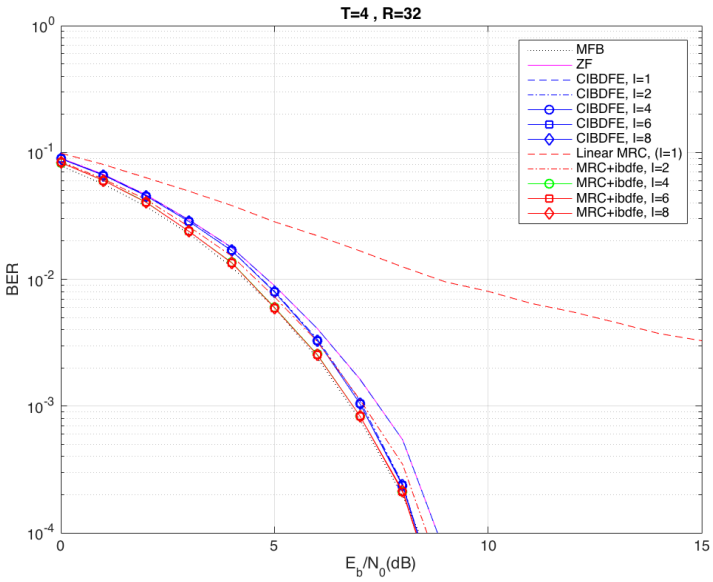

Fig. 6.6: Iterations Effect MRC+IBDFE (T=4, R=32).

In the $Fig.6.4$, the phenomenon of performance convergence (from a certain number of iterations foward) is not so observable because the ratio $R/T = 2$, represents a low ratio. However, the results in $Fig.6.6$ with respect to a $R/T = 8$ (four times higher than the previously mentioned), evidence this phenomenon of convergence, starting already from the 4th iteration onwards.

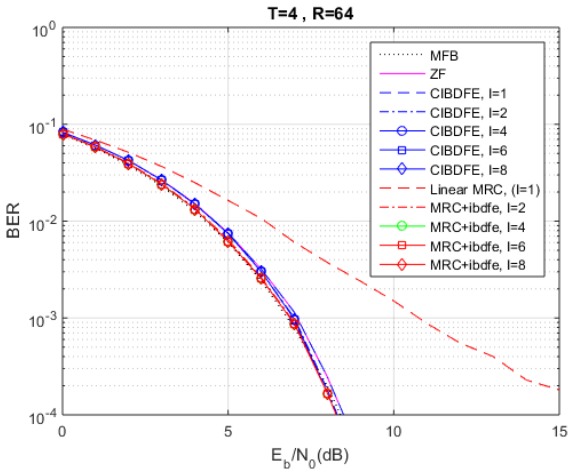

Fig. 6.7: Iterations Effect MRC+IBDFE (T=4, R=64).

The results presented above ($Fig.6.7$) are in the sequence of the ones obtained in the $Fig.6.6$ (with a ratio $R/T = 8$) and follows the same behaviour, now with a Ratio of $R/T = 16$.

The iterations number has more influence at low *SNR* values than for high *SNR* values, where the iterations influence tends to be lower, and the performance reaches a limit value.

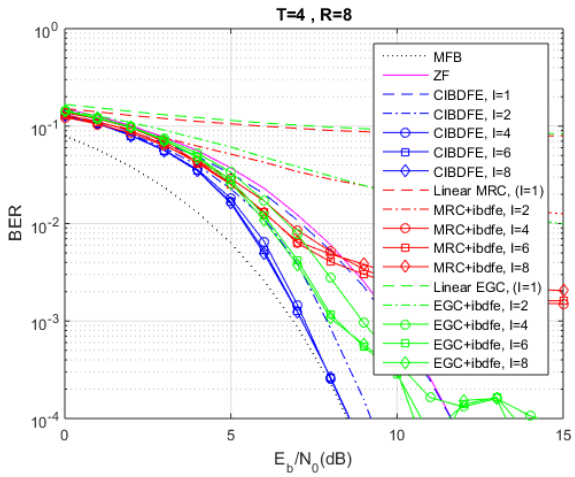

Fig. 6.8: Iterations Effect, Comparison between Receivers at low Ratio (T=4, R=8).

The $Fig.6.8$ corresponds to a general observation of the receivers' behaviour to a low antennas Ratio R/T. The results, shows us that for low R/T antennas ratio, in this case a Ratio $R/T = 2$, the *EGC+IBDFE* has better performances than the *MRC+IBDFE*.

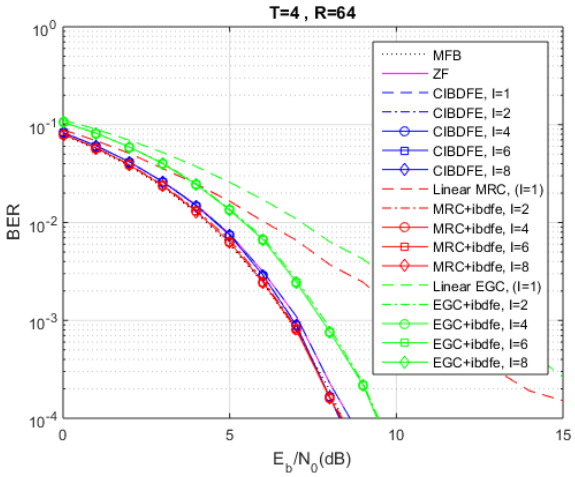

Fig. 6.9: Iterations Effect, Comparison between Receivers at high Ratio (T=4, R=64).

Contrasting with the $Fig.6.8$, the $Fig.6.9$ shows that, when doing a comparison of the MRC+IBDFE with the EGC+IBDFE for a high antenna ratio, we verify a great improvement by the MRC+IBDFE graphics performance, resulting in a lower BER much closer to the MFB, what means that the MRC+IBDFE is more appropriate to a Massive-MIMO scenario where severall receiver antenas are employed in the Base Station.

These results are due to the fact that the complexity of the EGC + IBDFE is lower than that of the MRC+IBDFE (with respect to the signal equalization process) since it only takes into account the phase of each channel for the calculations.

6.1.2 Effect of the Ratio Maintenance (with increasing T and R simultaneously)

In the following figures ($Fig.6.10$, $Fig.6.11$ and $Fig.6.12$), we can observe three different simulations whose ratio R/T is kept the same. The iterations number is set in $I = 4$.

Setting the ratio in $R/T = 2$, different configurations of $T \times R$ were experimented and it's possible to observe a sequential increase of performance for the MRC+IBDFE with the increase of the overall Tx and Rx antennas number (always with $Tx \leq Rx$).

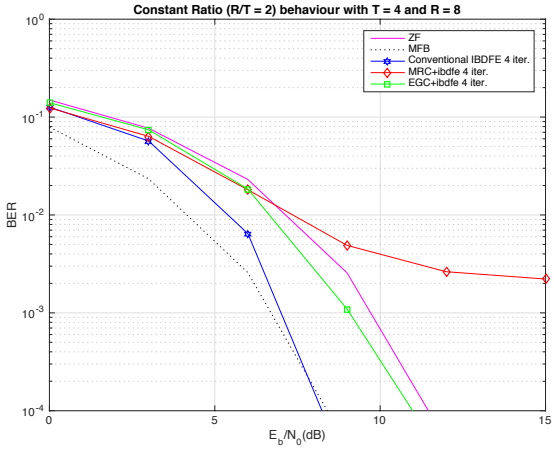

Fig. 6.10: Constant Ratio (T=4, R=8).

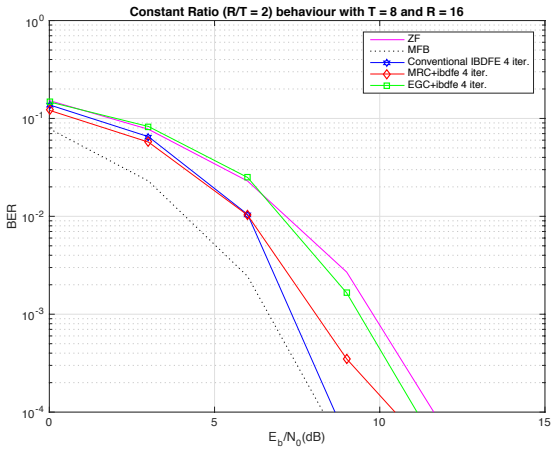

Fig. 6.11: Constant Ratio (T=8, R=16).

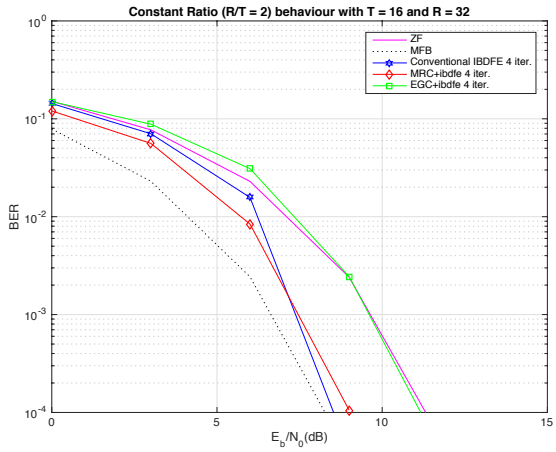

Fig. 6.12: Constant Ratio, (T=16, R=32).

The performance for the EGC+IBDFE and for the Conventional-IBDFE (CIBDFE) itself, is apparently not influenced by the number of Tx and Rx antennas involved.

Thus, in general, we can afirm that for different scenarios of $T \times R$, a constant ratio means an aproximately constant performance. Is also possible to conclude that the performance of the systems in general (MRC+IBDFE, EGC+IBDFE and CIBDFE) improves till a certain limit with a tendentialy higher value of the R/T ratio.

Despite the previous statements, in the specific case of MRC+IBDFE (for a sequence of experiments with a constant ratio), it can be noted that a higher number of Rx antenas (despite maintining the ratio constant) also means an improvement in the BER (although a small improvement), which leads the global system performance to higher levels, as it is possible to analyse and conclude doing the comparison between $Fig.\,6.11$ and $Fig.\,6.12$. Thus, once again, the MRC+IBDFE appears to be more suitable for a Massive-MIMO scenario.

6.1.3 Effect of Ratio Increasing (T fixed, R increasing)

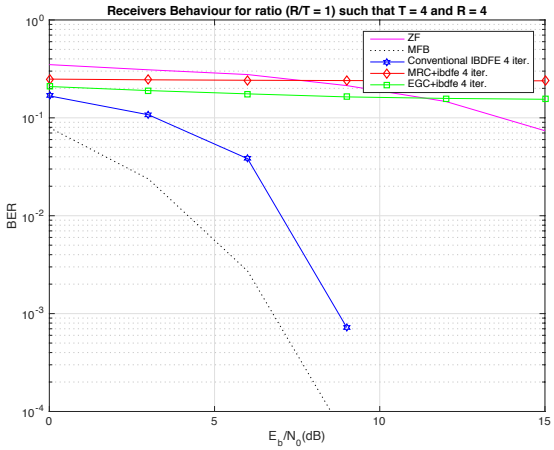

Fig. 6.13: Ratio 1 (T=4, R=4).

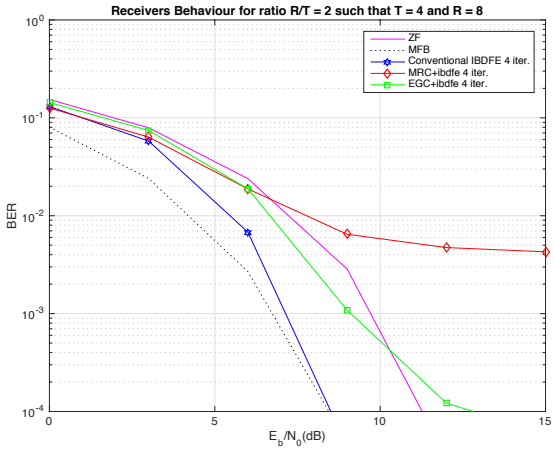

Fig. 6.14: Ratio 2 (T=4, R=8).

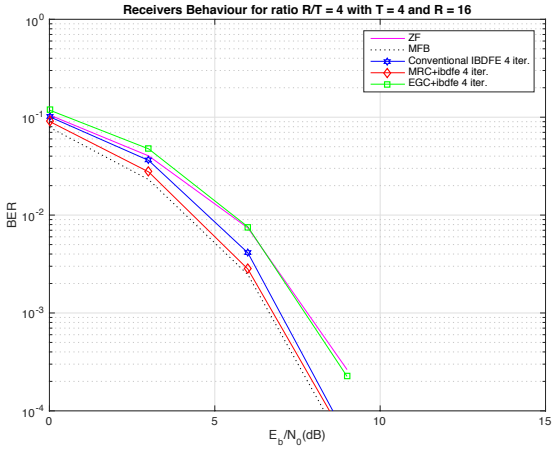

Fig. 6.15: Ratio 4 (T=4, R=16).

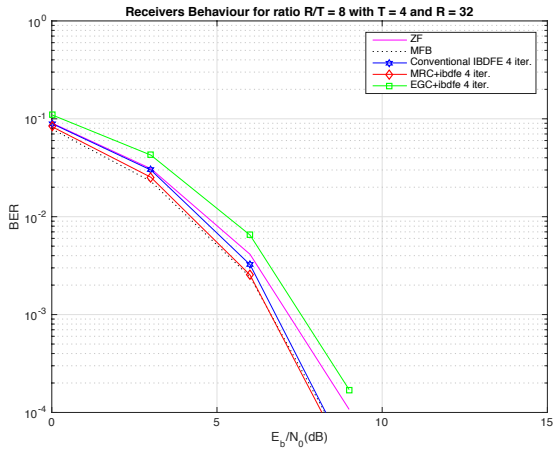

Fig. 6.16: Ratio 8 (T=4, R=32).

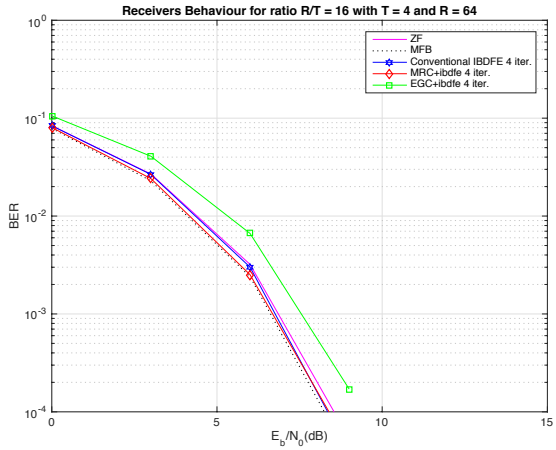

Fig. 6.17: Ratio 16 (T=4, R=64).

For a stablished value of (I) (in this case $I = 4$) and doing a direct comparison between the three diferent receivers, it's possible to affirm, by observing the evolution between the $Fig.6.13$ and the $Fig.6.17$, that the performance of the receivers is improved when the antennas ratio (R/T), has a high order. Despite that, this improvement is not unlimited and actually, his evolution tends to be convergent to a limit (like in the situation of the effect in the increasing of iterations) as we can see directly comparing the last three figures of this set of experiments, respectively $Fig.6.15$, $Fig.6.16$ and the $Fig.6.17$.

6.1.4 Effect of Decreasing the Ratio (T increasing and R fixed)

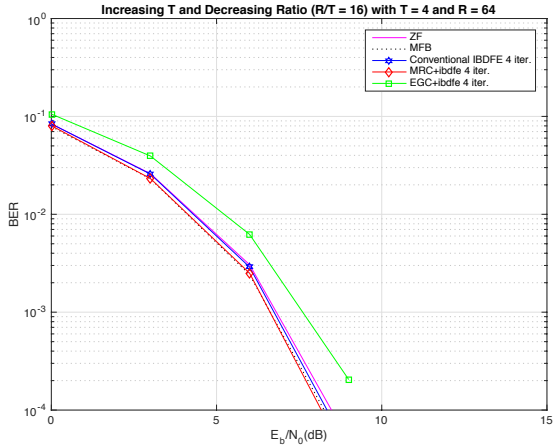

Fig. 6.18: Increasing T, Decreasing Ratio (T=4, R=64).

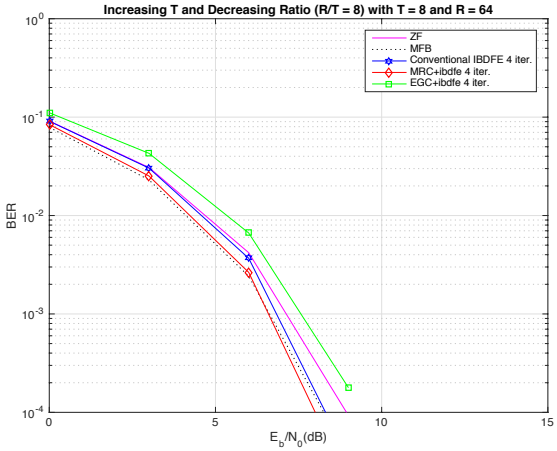

Fig. 6.19: Increasing T, Decreasing Ratio (T=8, R=64).

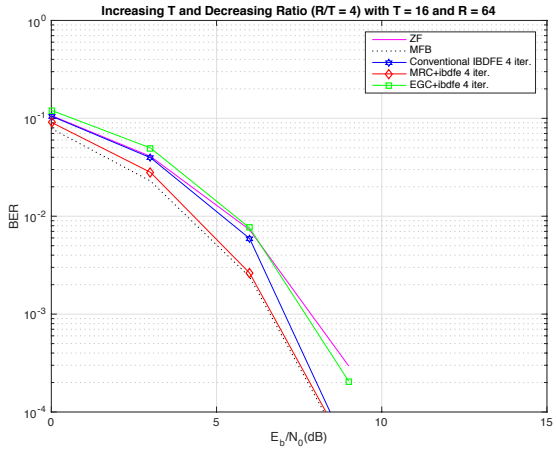

Fig. 6.20: Increasing T, Decreasing Ratio (T=16, R=64).

Assuming a fixed number of receiver antennas in the base station and vary the number of mobile terminals transmiting in the UL, it is possible to observe a sequential degradation of the performance with the increasing of devices. In a real scenario, the base stations have a fixed number of antennas and the element who vary in the communication system, is the number of mobile devices available to transmit, so, in this way and in the last case, the degradation of the system can be limited by the operator by implementing operation policies to limit the number of devices associated with a set of receivers in the *BS,* in order to offer a good quality of service *(QoS)*. Comparing the $Fig.6.20$ with $Fig.6.18$ we can conclude that lose of performance, observing the higher BER for the MRC+IBDFE ($4\ iter.$) for the higher SNR values. This effect is also very evident comparing the *Zero Forcing* receiver in the three graphics above. In the $Fig.6.20$, the ZF equalizer also has a higher BER in the higher SNR values. For the Conventional-IBDFE is also evident the increasing of degradation (clearly observable like in the *ZF*) with the R/T decreasing.

6.2 Analysis with the impact of Non-Linearities caused by Analog to Digital Conversion

In the following set of results, the Number of Iterations (I) was fixed in $I = 4$ since it is the value for which the iterative alghoritms reach a relative limit in the performance increasing due to the iterations effect, as it can be seen in the set of results of $section$ 6.1.1.

6.2.1 Comparison between the system with NL and without NL caused by the ADCs

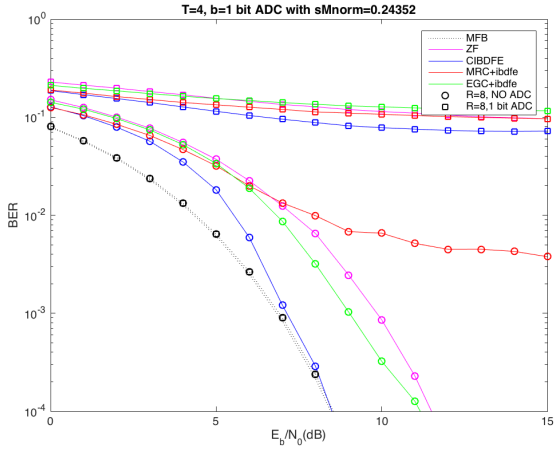

Fig. 6.21: System performance without ADCs vs with 1-bit ADCs, (T=4, R=8).

The introduction of non-linear distortion effects, caused by the employment of ADCs in the R receiving antennas, leads the system to considerable worse performances, as it can be seen in the $Fig.$ 6.21.

It is possible to verify that when we implement ADCs with a low number of bits of resolution (in this case $b = 1$) associated to a low R/T antennas ratio, the performance of the system is very poor when compared with the system without the introduced nonlinearities.

The R/T ratio, in this case is very low, with the value $R/T = 2$ demonstrating that the impact of non-linear distortion is quite large at small ratios combined with low resolutions.

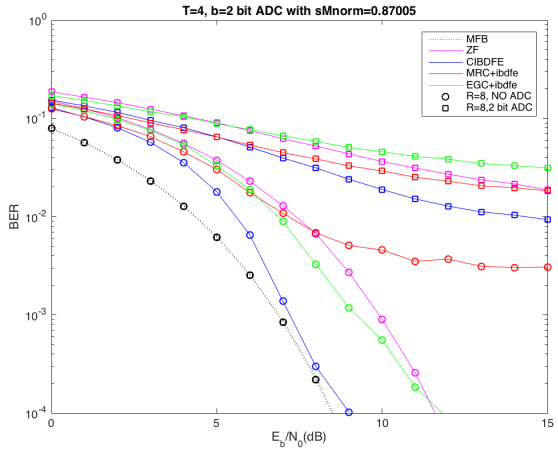

Fig. 6.22: System performance without ADCs vs with 2-bit ADCs, (T=4, R=8).

For the same Ratio, $R/T = 2$, but now considering the ADCs with one more bit of resolution ($b = 2$), the performance of the system with nonlinearities increases a little.

Despite this increase in the number of bits, the non-linear distortion imposed by the ADCs stills very visible. Then, we can conclude that the less the bits of resolution, the worse the performance of the system which includes the non-linear distortion effects.

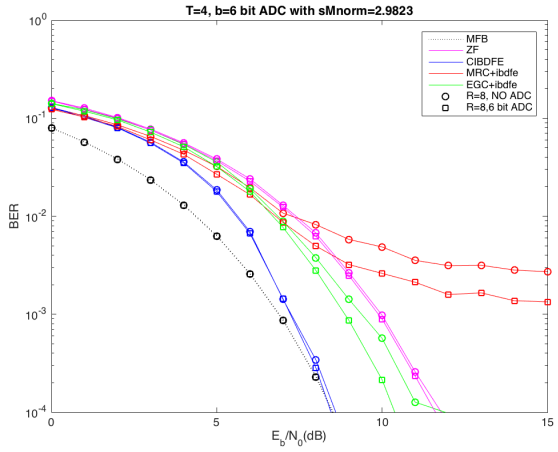

Fig. 6.23: System performance without ADCs vs with 6-bit ADCs, (T=4, R=8).

Contrasting with the $Fig.\,6.21$ and with the $Fig.\,6.22$, in the $Fig.\,6.23$, maintaining the ($R/T = 2$) and simultaneously combining this antennas configuration with a relatively high number of (b) resolution bits, the NL system tends to approach or even surpass the performances of a system without these effects of distortion. This result, is a bit strange, considering that, as we shall see below, in scenarios whose R/T ratio is greater than $R/T = 2$, the same phenomenon does not tend to occur, and, as a rule, nonlinearity systems always tend to have worse performance results than systems without their imposition (even considering high number of bits of resolution to the quantizers).

Even if the performance of systems with non-linearities tends to approximate the systems without NL, as we shall see next, they never actually exceed the performance of a system without introduced NL.

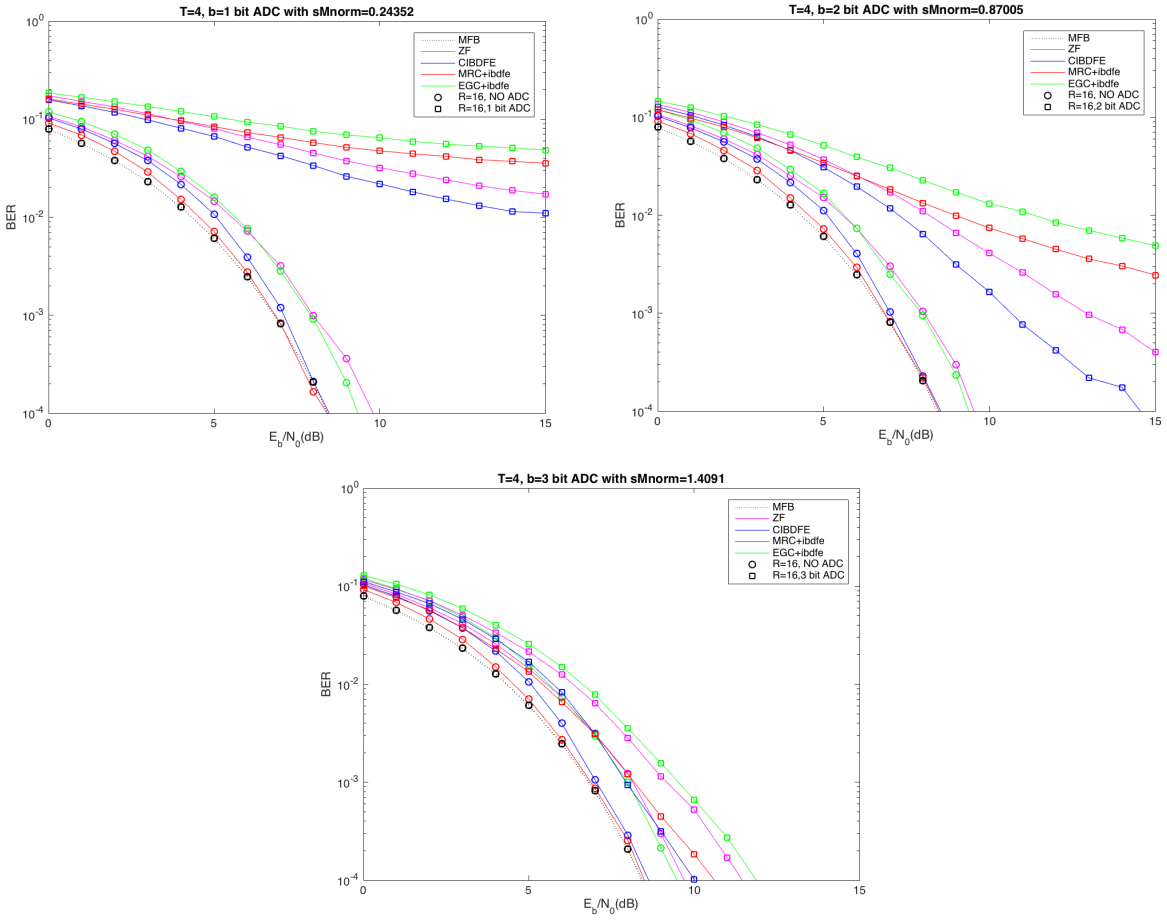

Fig. 6.24: System performance without ADCs vs with 1-bit ADCs, 2-bit ADCs and 3-bit ADCs for (T=4, R=16).

In $Fig.6.24$, for the three different graphics, considering $(R/T = 4)$ is visible the difference between the system without ADCs and the system with nonlinearities effect provoked by the ADCs implemented. We can see the performance increasing for all the equalization techniques with the successive increasing in the number of b. One can note that the deviant behaviour of the system (as we saw before in $Fig.6.23$) for this Ratio is not present anymore because the receivers are not so sub-optimal.

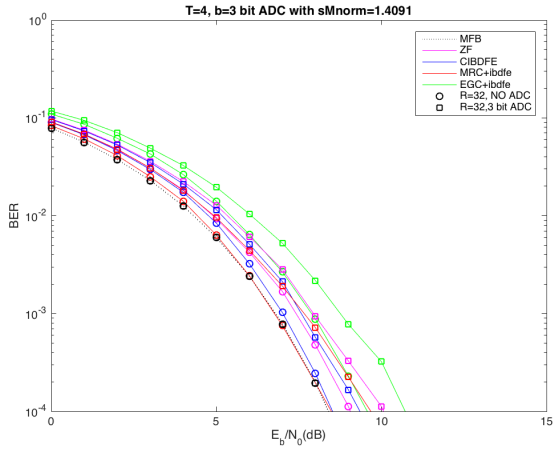

Fig. 6.25: System performance without ADCs vs with 3-bit ADCs, (T=4, R=32).

From the $Fig.6.25$ to the $Fig.6.26$ we increased the number of receivers to the double, so ($R = 32$) and, maintaining the number of bits ($b = 3$) is possible to observe that the performance of the NL system is closer to the performance of the system without NL. The R/T ratio in this case is $R/T = 8$.

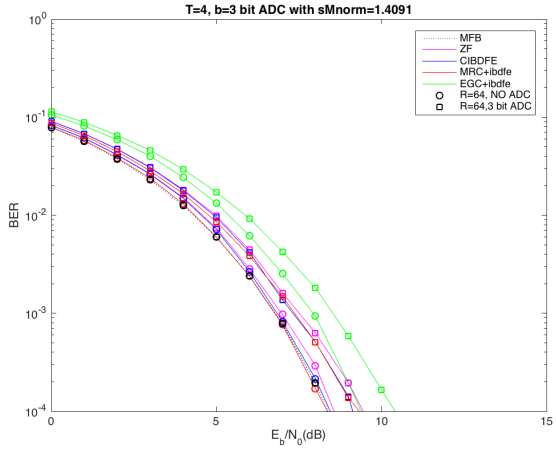

Fig. 6.26: System performance without ADCs vs with 3-bit ADCs, (T=4, R=64).

The $Fig.6.26$ outstands the Performance of the iterative equalizer MRC+IBDFE, where is possible to see the influence of a higher R/T ratio, like in the previous Figures. Despite the number of bits of resolution is the same ($b = 3$) as the ones used in the previous simulation ($Fig.6.25$), increasing the ratio from $R/T = 8$ to $R/T = 16$, brings the MRC's performance even closer to the MFB.

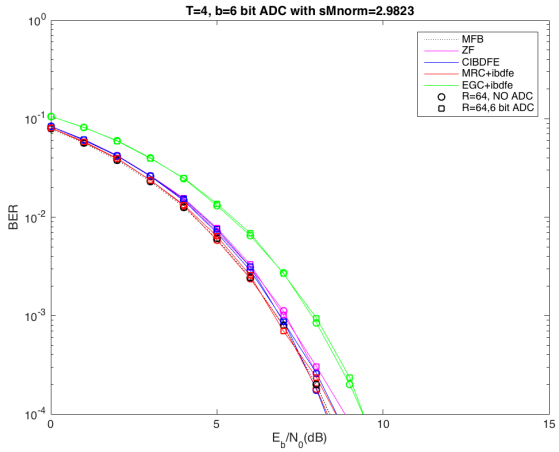

Fig. 6.27: System performance without ADCs vs with 6-bit ADCs, (T=4, R=64).

In the $Fig.6.27$ is possible to see that higher Resolution ADCs combined with higher R/T antennas ratios are a very good combination in terms of performance results, being almost all the equalization techniques with BER close to the MFB. However, the bigger the number of bits of resolution employed in the ADCs, the bigger the energy consumption as well as the implementation costs and the processment capabilities that are required. In a large MIMO scale, (Massive-MIMO), this type of implementation should be avoided because it comes impractible by the previously mentioned reasons.

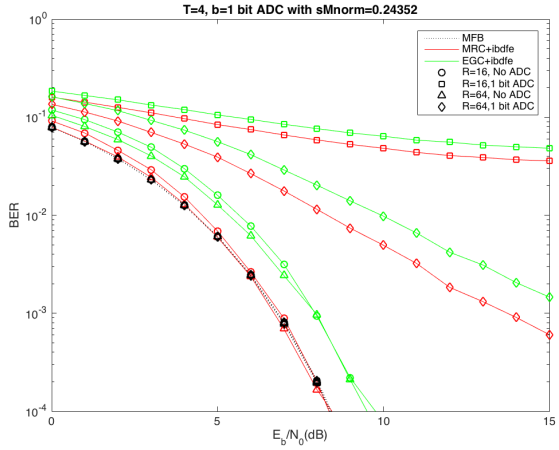

Fig. 6.28: Iterative MRC vs Iterative EGC (without ADCs vs with 1-bit ADCs), (T=4, R=16 / R=64).

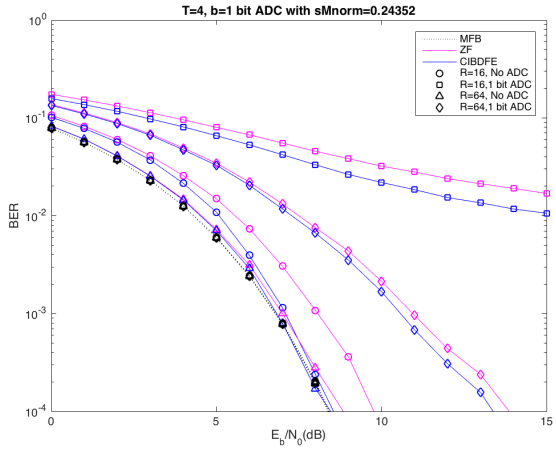

Fig. 6.29: ZF vs Conventional-IBDFE (without ADCs vs with 1-bit ADCs), (T=4, R=16 / R=64).

As we can see in the $Fig.\,6.28$ and $Fig.\,6.29$, for relatively big R/T ratios, even with just 1-bit ADC resolution is possible to achieve relatively good performances.

Specially for the low complexity iterative algorithms (the MRC+IBDFE and the EGC+IBDFE) we can consider that this results are very satisfactory because they allow us to realize that if in bigger R/T ratios (typical in Massive-MIMO) the performance tendentially will increase.

It is important to note that low complexity iterative algorithms are the most adequate in scenarios whose implementation of Antennas is quite large (case of Massive-MIMO), since, being low complexity algorithms, these techniques require less processing capacity in the receivers, which is a desirable factor for scenarios with a lot of antennas involved.

One can also note that, being these equalizers capable of achieving these performances with only 1-bit resolution ADCs, on a larger R/T ratio scale this will be quite appealing in terms of energy saving.

The Zero Forcing and the Iterative Block DFE results are the expected ones, despite the fact they are not adequate to Massive-MIMO employments because of their bigger computation complexity (due to the needed matrix inversions).

6.2.2 Studying the effect of the Antennas Ratio, in the presence of ADCs

In the $Fig.6.30$ and $Fig.6.31$ is evidenced the impact of the Ratio between the pair Transmitters + Receivers.

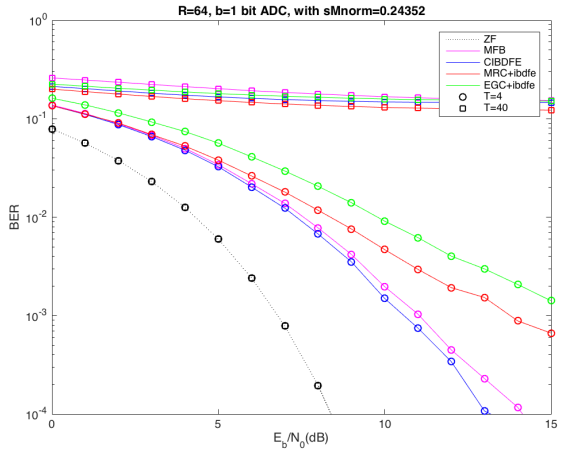

Fig. 6.30: Impact of Antennas in the performance of a NL System with 1-bit ADCs, for all the equalization techniques (T=4 / T=40, R=64).

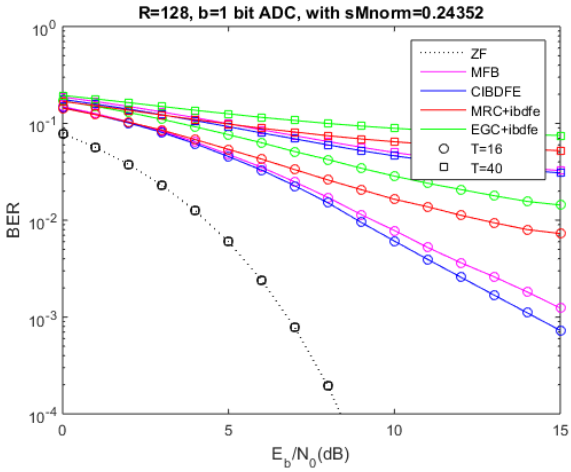

Fig. 6.31: Impact of Antennas in the performance of a NL System with 1-bit ADCs, for all the equalization techniques (T=16, T=40, R=128).

We can note that even for NL scenarios with a medium number of Mobile Terminals ($T = 16$ or $T = 40$) transmitting to a Base Station, if we have a considerable number of Receiving antennas (e.g.: $R = 128$), the global performance of the system (as a whole) is quite satisfactory for the low complexity techniques combined with low resolution ADCs.

In the following two figures ($Fig.\,6.32$ and $Fig.\,6.33$) we can observe that for a fixed value of T, and considering a sequential increase in the number of receivers, the performance increases for the NL systems considering low resolution ADCs, again highlighting the importance and the positive effect that diversity in the reception has. The diversity, in this way, turns possible to overcome the hypothetical occurrence of errors in reception. The deep fading phenomenon may occur in certain transmission channels, causing failures in the transmitted information, and thus causing them to not reach the receiver correctly. In this way, with diversity in the reception, it is possible to make the system redundant. This is a very important factor, because it allows to deal with the detection errors that can occur, ensuring, however, that the information reaches the destination.

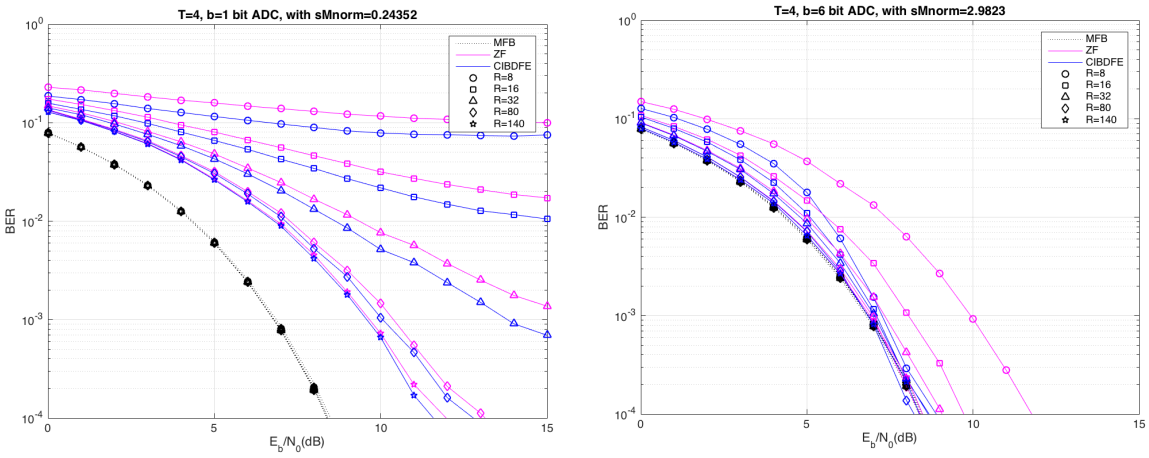

Fig. 6.32: ZF vs CIBDFE Performances in NL System with 1-bit ADCs vs 6-bits ADCs, for (T=4, increasing R).

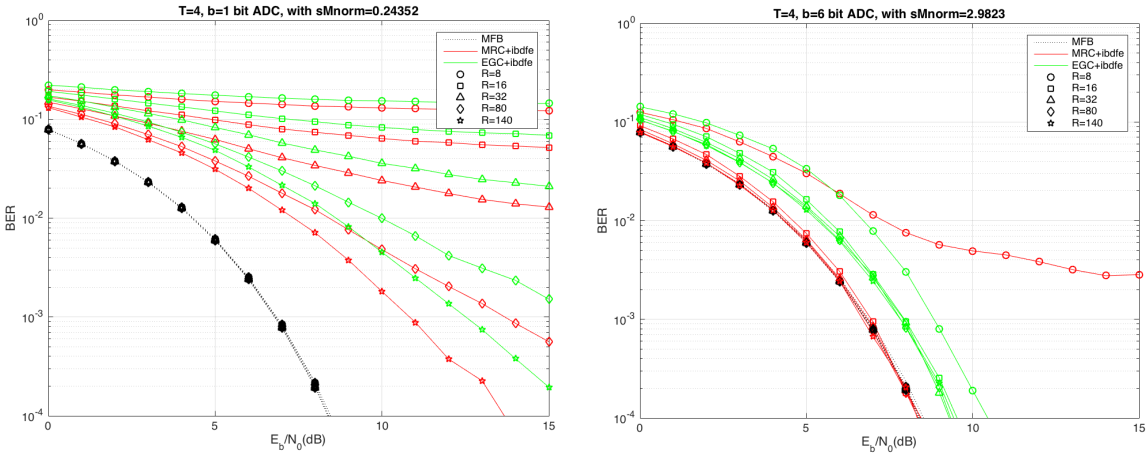

Fig. 6.33: Iterative MRC vs Iterative EGC Performances in NL System with 1-bit ADCs vs 6-bit ADCs, (T=4, increasing R).

In the $Fig.\,6.33$ is quite evident the good performances for the Iterative MRC and for the Iterative EGC when considering $R = 140$ receiving antennas and just with $T = 4$ Mobile Terminals transmitting. In all the situations, the Iterative MRC outperforms the Iterative EGC. When we implement 6-bit ADCs, the performance of the NL systems is almost equal, or at least closer, to the performance of the Linear Systems as we can see on the right side of both figures ($Fig.\,6.32$ and $Fig.\,6.33$).

6.2.3 Impact of the Number of bits of Resolution and Normalized Clipping Level

In the following set of results, we fixed the number of T Mobile Terminals as well as the number of R receiving antennas in the BS, varying the number of the used quantization bits and consequently varying the associated clipping level of each ADC in the R-branch receivers.

The main objective is to understand the impact of resolution and clipping, together, in the performance of the systems.

It is important to note that the following set of simulations take into account that for each value of (b) is associated an optimum normalized clipping level $\left(\frac{S_M}{\sigma_z}\right)$that maximizes the SQNR(dB) in the SC-FDE uplink transmissions, as described in $Fig.\,6.34$. Those correspondente values between (b) and $\left(\frac{S_M}{\sigma_z}\right)$ are described in the next figure (table):

Bits of Resolution (b)	Optimum Normalized Clipping Level $\left(\frac{S_M}{\sigma_z}\right)$
= 1	≈ 0.2435
= 2	≈ 0.8701
= 3	≈ 1.4091
= 4	≈ 1.9326
= 5	≈ 2.4549
= 6	≈ 2.9823
= 7	≈ 3.5165
= 8	≈ 4.0568

Fig. 6.34: Optimum Normalized Clipping Level for a certain number of Bits of Resolution.

The next set of simulations consider different values of (b) for two pairs of equalizers with two $R\times T$ fixed configurations.

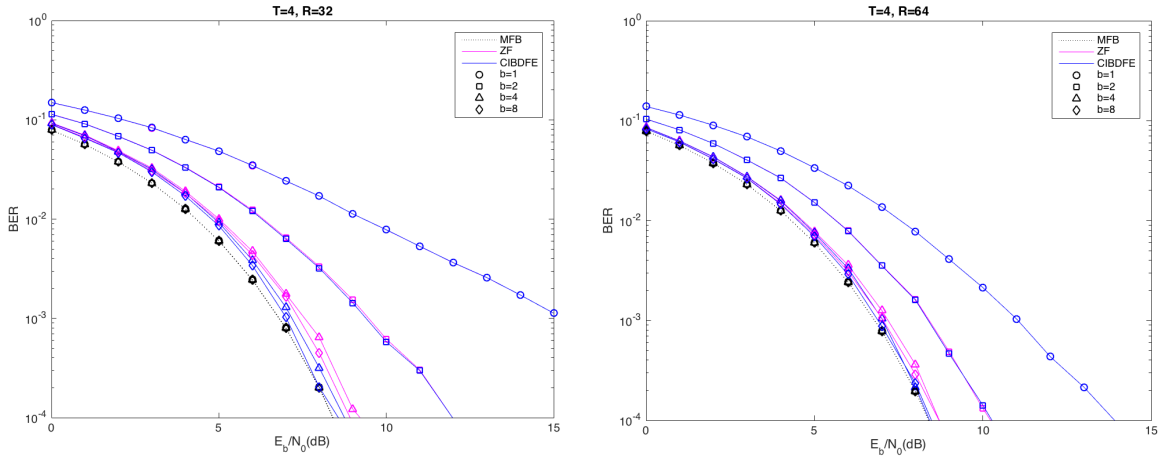

Fig. 6.35: ADCs resolution impact in the performance of NL system with ZF vs CIBDFE, for (T=4, R=32 and T=4, R=64).

Since ZF and IBDFE are very effective to combat the ISI, we can note that from the value of $b = 2$ and onwards, the performance of a $R/T = 8$ system is already pretty good.

For a bigger ratio ($R/T = 16$), and considering the ADCs with 6 bits of resolution, the system behaviour is almost equal to the performance of linear systems, with results side by side with the MFB.

It is also important to note that the ZF and CIBDFE techniques perform better than the iterative MRC and than the iterative EGC already from the $b = 1$ configuration. The $b = 1$ configuration in the ZF and CIBDFE, gives already pratically the same results than the $b = 2$ configuration for the low complexity iterative combined techniques (MRC+IBDFE and EGC+IBDFE).

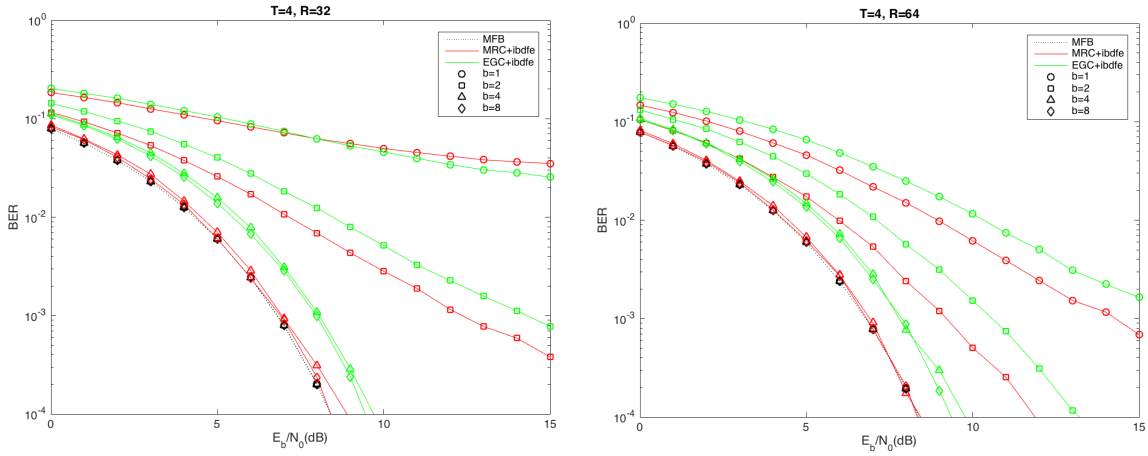

Fig. 6.36: ADCs resolution impact in the performance of NL system with Iterative MRC vs Iterative EGC, for (T=4, R=32 and T=4, R=64).

In the case of the low complexity algorithms, for low resolution ADCs with ($b = 1$), associated to low ratios, we have a big gap in the performance when compared to a higher number of bits ($b = 6$) to the same ratio. The increase in the ratio (from $R/T = 8$ to $R/T = 16$), as expected, leads to an increase in the performance, even with 1-bit resolution ADCs, as is possible to observe doing the comparison between the two graphics in the $Fig.6.36$.

Is possible to see that the difference of performance between the configuration with $b = 1$ to the configuration with $b = 2$ is considerable. However, the same not occurs when comparing the other two configurations ($b = 4$ and $b = 8$) respectively. For this last two considered configurations, the performance is practically the same.

6.2.4 Clipping Level Effect (fixing b, R and T)

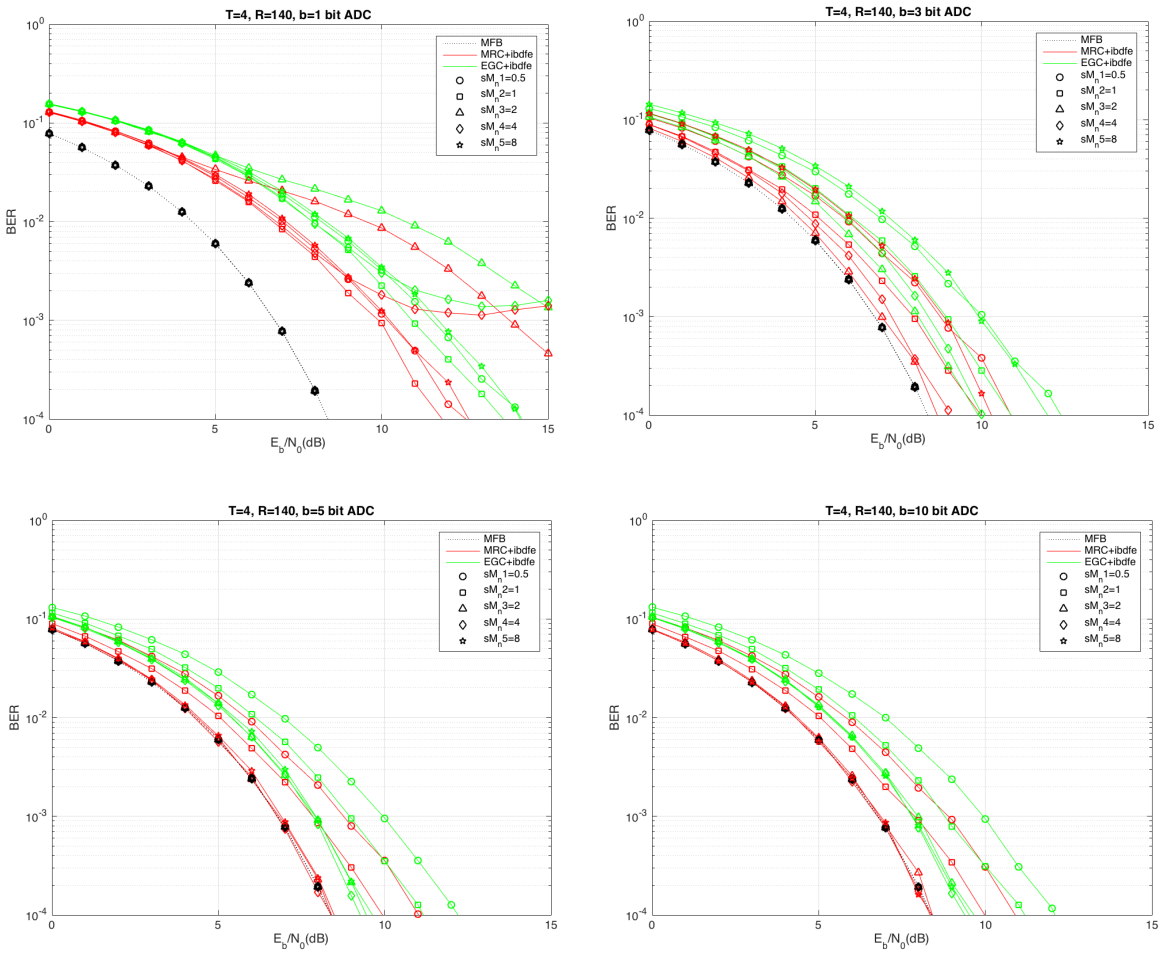

Fig. 6.37: Clipping impact in the performance of NL system with Iterative MRC vs Iterative EGC, for different resolutions (b=1, b=3, b=5, b=10) considering (T=4 and R=140).

As we can see in the set of graphics of $Fig.\,6.37$, the impact of the normalized clipping level is inferior for higher resolutions.

For a resolution of $(b = 10)$, and considering $(sM = 0.5)$ the EGC+IBDFE performs pratically the same as the ADC configuration with $(b = 1)$ and considering $(sM = 8)$. For the MRC+IBDFE it is not so evident, since from $(b = 3)$ and onwards till $(b = 10)$ the effects of clipping are pratically the same indepedently of the resolution.

The bigger the clipping level, the worst the system performs. One can note that considering higher clipping effects ($sM = 4$ and $sM = 8$), the loss of performance for the MRC+IBDFE is pratically the same considering the same number of resolution bits. In general, unless the considered situation for the low resolution ADCs $(b = 1)$, the biggest noted gap in the performance is between the values of $(sM = 1)$ to the set of ($sM = 2$, $sM = 4$ and $sM = 8$). For the low resolution ADCs $(b = 1)$, the value of $(sM = 1)$ performs better than the other clipping levels, this, for higher SNRs. In the following set of raphics ($Fig.\,6.38$), are presented the clipping effects for ZF and CIBDFE:

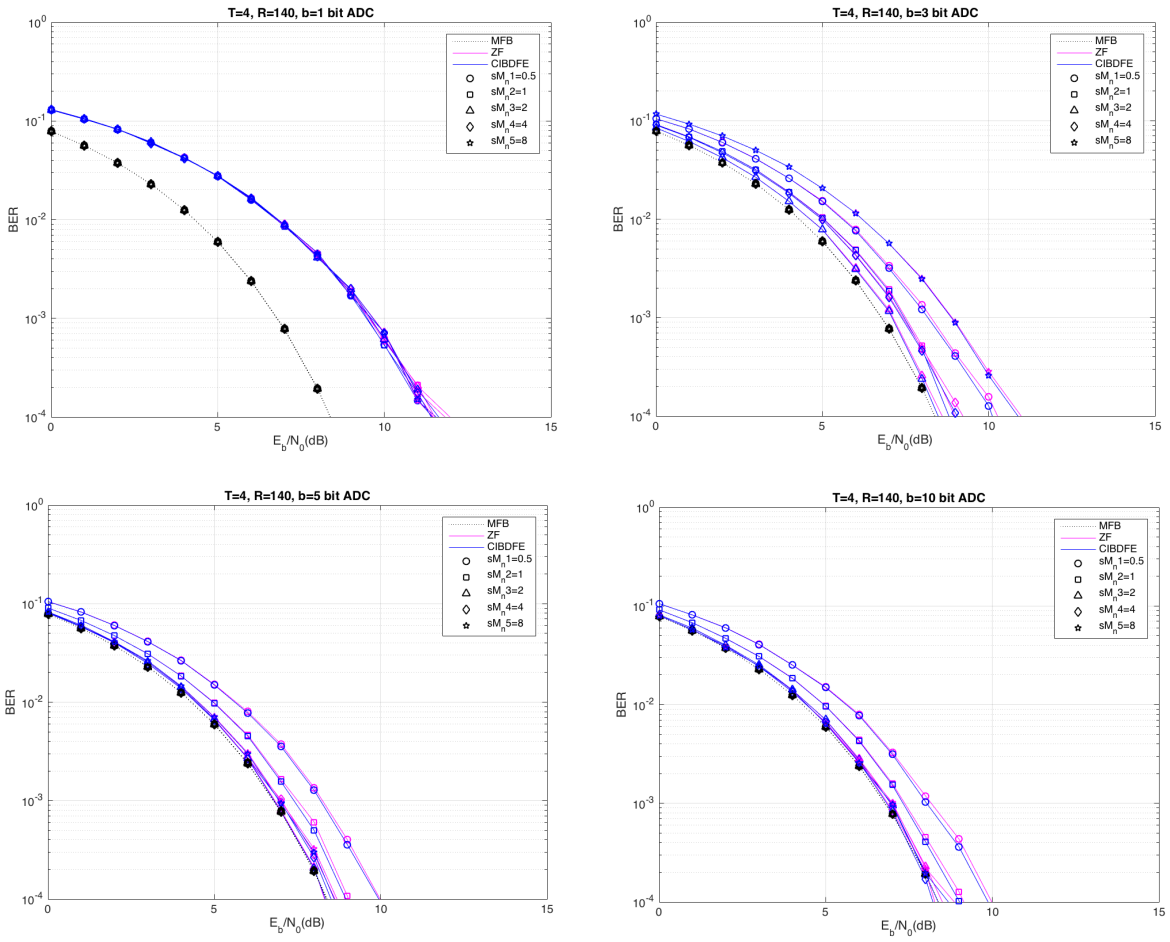

Fig. 6.38: Clipping impact in the performance of NL system with ZF vs CIBDFE, for different resolutions (b=1, b=3, b=5, b=10) considering (T=4 and R=140).

For low resolution ADCs ($b = 1$), the impact of the addopted clipping level is almost indistinguishable depending on the clipping values. The impact on the performance is very visi- ble, once again, due to the low resolution.

The results follow the expected, since for specific resolution values, the maximization of the SQNR(dB) occurs to specific intervals of values of the normalized saturation. For ($b = 3$), the optimal clipping level (which is $sM = 2$), in fact is the one who offers the best performance (as we can see in the top right of the $Fig.\,6.38$). The same occurs to the set of results for the MRC+IBDFE, where for a medium resolution value ($b = 5$), the saturation values that maximize the SQNR(dB) are respectivelly between ($sM = 2$) and ($sM = 4$) (as described in $Fig.\,5.7$).

7. Conclusions and Future Work

7.1 Conclusions

In the future 5G, and with the Massive-MIMO networks, the high number of devices in action, leads the telecommunications systems to be more complex and, as well, probably subject to high levels of interference. This type of problems need to be circumvented so we can have less degra-dation of signal and consequently a global better quality of the communication system.

With the knowledge and experience of MIMO systems employed in the 4G and taking some advantage of it, it is possible to extend and combine some already used techniques to get an aproach and predict what will be like the Massive-MIMO and its performance capabilities. In this thesis, as we saw, it is convenient not to see Massive-MIMO as an enlarged scaled-up version of MIMO systems, specially due to the undesirable complexity this would entail in terms of mathematical processing of the equalization algorithms and also because of the higher implementation costs it would entail.

As we saw, the Conventional-IBDFE, by itself, is an algorithm able to present good per-for-mance results (closer to the MFB) since his first iteration, in a MIMO scenario. When the number of iterations grows, the performance results are increased even closer to the MFB. However, despite this good results for the MIMO case, the IBDFE, by itself, is not enough, neither viable, to be aplicable in a Massive-MIMO situation due to the exponentially greater processing com-plexity with the grow of the involved antennas number.

On the other hand, the low complexity algorithms MRC and EGC, by themselves, are verified as being inefficient algorithms in the first iteration of their equalization processes. However, from the second iteration and onwards, these algorithms show remarkable improvements in their per-formance. These facts, together with their low processing complexity and the abstention of matrix inversions, makes these algorithms highly suitable and interesting to ponder for scenarios where the number of involved antennas in the transmission is larger than in the existing MIMO scenarios. The great effectiveness of the iterative algorithms (the Conventional-IBDFE with proved results in MIMO) with the low complexity detection (that do not make use of the matrix inversions during their equalization processes are plausible solutions for a Massive-MIMO situation. To deal and eliminate the residual interference in the UL branch together with a low complexity technique, arises the combination between the iterative algorithms (in this case, the IBDFE) with the simpler algorithms (as MRC or EGC).

After just some iterations, these combined techniques perform very well, and, in fact, can even perform greater than the classic linear algorithms, such as the ZF and the MMSE. The higher the ratio R/T between antennas in both sides of the communication environment, the higher will be the performance results.

In the study done for the nonlinearities effect in the systems, was possible to conclude that the implementation of higher resolution ADCs will lead to higher energy consumptions and higher implementation costs, despite the better performances it gives since the non-linear distortion is not so big as in the low resolution options. The 1-bit ADCs, by other side, being low resolution ADCs offer the ideal solution to implement in Massive-MIMO scenarios. This type of ADCs are utopic to implement if they are not combined with very big ratios. So, it is possible to conclude that, for a situation with a Massive-MIMO working network, and considering a very low the number of users inside a cell (in the order of tens), if the number of receiving antennas in the BS is very high, the transmission performance in this multi-user scenario will be great with pairs of 1-bit ADCs working on the BS. Ofcourse, if the number of users is very high, the need of more resources is expected, both at the level of the quantizers and at the level of the equalization algorithms. In this last, more iterations to perform will be needed by the low complexity iterative combined equalization solutions as MRC+IBDFE and the EGC+IBDFE. To conclude, the higher the ratio, the better the performance, so it is very important to implement large arrays of receiving antennas in the BS and combine this solution with the proposed equalization techniques and hardware elements, always considering the low implementation costs.

7.2 Future work

In this thesis, the studied themes have just boarded a small group of problems, drawbacks and possible solutions to the Massive-MIMO realization. The pointed objectives by Massive-MIMO, such as the reducing of the hardware complexity and the achievement of good solutions with low costs, are subjects to be further explored by the scientific community. In the future, deeper mathematical analysis should be done in order to better understand if it stills be possible to improve or not some performance gains as well as if it is achievable complexity decreasings in the global elements, blocks and techniques related to this engineering. The nonlinear effects due to the hardware elements can also be object of review with the developing of the materials engineering and the new concepts by the scientific research world for telecommunications. The impact in the performance can maybe be further circunmvented with the investigation of new models, specially in the way how the receiving antennas blocks are implemented in the BS.

With the new, and popular, green energies, whose are taking care of our daily life, some new solutions may be part of the telecommunication systems in the near future, specially to the Massive-MIMO, since the efficiency and power saving is crucial in this project.

The cellphone batteries and the development of new eletronic circuits and new ideas in the equalization methods, are also of great importance to implement the 5G. The study of the transmitter technologies paired with the receiver technologies should be approached to find even more cooperative solutions in the telecommunications.

Bibliography

[1] J. J. G. Andrews, S. Buzzi, W. Choi, S. V. S. Hanly, A. Lozano, A. A.C. K. Soong, and J. J. C. Zhang. "What will 5G be?" In: IEEE Journal on Selected Areas in Communications 32.6 (2014), pp. 1065–1082.

[2] G. Wunder, R. F. H. Fischer, H. Boche, S. Litsyn, and J. S. No. "The PAPR problem in OFDM transmission: New directions for a long-lasting problem." In: IEEE Signal Processing Magazine 30.6 (2013), pp. 130–144.

[3] A. A. Florea, H. Gacanin, and F. Adachi. "Performance comparison of cooperative OFDM and SC-FDE relay networks in a frequency-selective fading channel." In: 12th IEEE International Conference on Communication Systems 2010, ICCS 2010. 2010, pp. 371–375.

[4] G. Foschini and M. Gans. "On limits of wireless communications in a fading environment when using multiple antennas." In: Wireless personal communications (1998), pp. 311–335.

[5] B. Laboratories, L. Technologies, H.-k. Rd, and R. A. V. P. W. Wolniansky, G. J. Foschini, G. D. Golden. "V-BLAST: An Architecture for Realizing Very High Data Rates Over the Rich-Scattering Wireless Channel." In: International Symposium on Signals, Systems and Electronics (1998), pp. 295–300.

[6] R. Candeias, J. Guerreiro, R. Dinis, and P. Montezuma. "Performance Evaluation of Low-complexity FDE Receivers for Massive MIMO Schemes with 1-bit ADCs."

[7] Rappaport, T. S., Sun, S., Mayzus, R., Zhao, H., Azar, Y., Wang, K., Gutierrez, F. (2013). Millimeter wave mobile communications for 5G cellular: It will work! IEEE Access, 1, 335–349.

[8] http://pubs.sciepub.com/iteces/3/1/3/index.html#Figure4 (last acess, 5th of October of 2017)

[9] https://www.anandtech.com/show/4289/verizon-4g-lte-two-datacards-wifi-hotspot-massively-reviewed/2 (last acess, 18th of October of 2017)

[10] L. J. Cimini. “Analysis and Simulation of a Digital Mobile Channel Using Orthogonal Frequency Division Multiplexing.” In: Communications, IEEE Transactions on 33.7 (1985), pp. 665–675.

[11] www.researchgate.net/publication/259649471 (last acess, 1st of july of 2018)

[12] Pancaldi, F., Vitetta, G., Kalbasi, R., Al-Dhahir, N., Uysal, M., & Mheidat, H. (2008). Single-carrier frequency domain equalization. IEEE Signal Processing Magazine, 25(5), 37–56.

[13] https://www.dsprelated.com/thread/2128/cyclic-prefix-concept-in-lte (last acess, 2nd of October of 2017)

[14] https://en.wikipedia.org/wiki/Orthogonal_frequency-division_multiplexing (last acess, 5th of December of 2017)

[15] https://openclipart.org/detail/194650/multipath-propagation (last acess, 19th of October of 2017)

[16] https://www.researchgate.net/publication/220672901 (last acess, 29th of June of 2018)

[17] http://www.telecomhall.com/what-is-cp-cyclic-prefix-in-lte.aspx (last acess, 3rd of October of 2017)

[18] https://www.researchgate.net/publication/272623859 (last acess, 5th of October of 2017)

[19] https://scialert.net/fulltextmobile/?doi=jas.2014.2194.2218 (last acess, 10th of October of 2017)

[20] https://www.slideshare.net/gerti/lte-tutorial-april-2009-ver11 (last acess, 2nd of November of 2017)

[21] R. Dinis, R. Kalbasi, D. Falconer, and A. H. Banihashemi. “Iterative layered space-time receivers for single-carrier transmission over severe time-dispersive channels.” In: IEEE Communications Letters 8.9 (2004), pp. 579–581.

[22] H. G. Myung. “Introduction to single carrier FDMA.” In: European Signal Processing Conference. 2007, pp. 2144–2148.

[23] A. A. Florea, H. Gacanin, and F. Adachi. “Performance comparison of cooperative OFDM and SC-FDE relay networks in a frequency-selective fading channel.” In: 12th IEEE International Conference on Communication Systems 2010, ICCS 2010. 2010, pp. 371–375.

[24] D. Falconer, A. Benyamin-seeyar, and H. Corp. “Frequency Domain Equalization for Single-Carrier Broadband Wireless Systems.” In: IEEE Communications Magazine April (2002), pp. 58–66.

[25] https://www.mathworks.com/discovery/ofdm.html (last acess, 25th of October of 2017)

[26] http://acts.ing.uniroma1.it/courses/comelet/Slides/20071217_TEL_lecture_2.pdf (last acess, 27th of October of 2017)

[27] https://en.wikipedia.org/wiki/Single-carrier_FDMA (last acess, 6th of December of 2017)

[28] Berardinelli, G., Priyanto, B. E., Sørensen, T. B., & Mogensen, P. (2008). Improving SC-FDMA performance by turbo equalization in UTRA LTE uplink. IEEE Vehicular Technology Conference, 2557–2561.

[29] Pravin, W., and SL Badjate. " Diversity Techniques for Wireless Communication." International Journal 2013.

[30] Garg, Juhi, Priyanka Mehta, and Kapil Gupta. "A Review on Cooperative Communication Protocols in Wireless World." International Journal of Wireless & Mobile Networks 5.2 2013.

[31] https://www.nutaq.com/blog/alamouti-space-time-block-coding (last acess, 8th of March of 2018)

[32] Laneman, J. Nicholas. Cooperative diversity in wireless networks: algorithms and architectures. Diss. Massachusetts Institute of Technology, 2002. 25 architectures. Diss. Massachusetts Institute of Technology, 2002.

[33] Laneman, J. Nicholas, David NC Tse, and Gregory W. Wornell. "Cooperative diversity in wireless networks: Efficient protocols and outage behavior."Information Theory, IEEE Transactions on 50.12 2004.

[34] http://ftm.futureelectronics.com/2016/10/future-electronics-mimo-how-does-802-11-benefit-from-multiple-antenna-techniques/ (last acess, 21st of November of 2017)

[35] G. Foschini and M. Gans. “On limits of wireless communications in a fading environment when using multiple antennas.” In: Wireless personal communications (1998), pp. 311–335.

[36] http://article.sapub.org/10.5923.j.jwnc.20170701.01.html (last acess, 5th of October of 2017)

[37] S. M. Alamouti. “A simple transmit diversity technique for wireless communications.” In: IEEE Journal on Selected Areas in Communications 16.8 (1998), pp. 1451– 1458.

[38] https://www.gaussianwaves.com/2014/08/mimo-diversity-and-spatial-multiplexing/ (last acess, 19th of November of 2017)

[39] Deng, R., Jiang, Z., Zhou, S., & Niu, Z. (2018). How Often Should CSI Be Updated for Massive MIMO Systems with Massive Connectivity? 2017 IEEE Global Communications Conference, GLOBECOM 2017 - Proceedings, 2018–January (1), 1–6.

[40] Anton A. Huurdeman, The Worldwide History of Telecommunications, John Wiley & Sons, 31 july 2003, page 529.

[41] Nam, J., Ahn, J. Y., Adhikary, A., and Caire, G. (2012). Joint spatial division and multiplexing: Realizing massive MIMO gains with limited channel state information. In 2012 46th Annual Conference on Information Sciences and Systems, CISS 2012.

[42] Gutierrez-Estevez, D. M. (2017). Interference-aware flexible TDD design for massive MIMO 5G systems. IEEE Wireless Communications and Networking Conference, WCNC.

[43] https://www.researchgate.net/publication/309756148_Location-aware_channel_estimation_enhanced_TDD_based_massive_MIMO/figures?lo=1 (last acess, 9th of April of 2018)

[44] Madhow, U. (2012). Introduction to Communication Systems Simulation, 336. Retrieved from http://site.ebrary.com/lib/umanitoba/docDetail.action?docID=10160975

[45] Kajaree, D., & Behera, R. . (2017). A Survey on Web Crawler Approaches. International Journal of Innovative Research in Computer and Communication Engineering, 5(2), 1302–1309.

[46] Borges, D., Montezuma, P., Ferreira, A., & Dinis, R. (2018). Two Low Complexity MRC and EGC Based Receivers for SC-FDE Modulations with Massive MIMO Schemes. Journal of Signal Processing Systems, 90(10), 1357–1367.

[47] Rahaman, S., Shahabuddin, S., Hossain, M. B., & Shahabuddin, S. (2016). Complexity analysis of matrix decomposition algorithms for linear MIMO detection. 2016 5th International Conference on Informatics, Electronics and Vision, ICIEV 2016, (December).

[48] F. C. Ribeiro, R. Dinis, F. Cercas, and A. Silva. "Analytical performance evaluation of Base Station cooperation systems using SC-FDE modulations with iterative receivers." In: 2012 IEEE Globecom Workshops, GC Wkshps 2012. 2012, pp. 637– 641.

[49] J. G. Proakis. Digital Communications. Vol. 11. 2. 2001, pp. 55–61.

[50] F. Ribeiro, R. Dinis, F. Cercas, and A. Silva. "Receiver design for the uplink of base station cooperation systems employing SC-FDE modulations." In: EURASIP Journal on Wireless Communications and Networking 2015.1 (2015), p. 7.

[51] Dinis, R., Universidade, F. C. T., Lisboa, N. D., Desenvolvimento, I. D., Tecnologias, D. N., and Torre, Q. (2016). Low Complexity Mrc and Egc Based Receivers for Sc-Fde Modulations. (1):675–678.

[52] H. S. Lee and C. G. Sodini, "Analog-to-digital converters: Digitizing the analog world," Proc. of the IEEE, vol. 96, no. 2, pp. 323-334, Feb. 2008.

[53] Ribeiro, F.C. & Dinis, Rui & Cercas, Francisco & Silva, Adão. (2015). Receiver design for the uplink of base station cooperation systems employing SC-FDE modulations. EURASIP Journal on Wireless Communications and Networking. 2015.

[54] Wu, M., Dirk, W., Dekorsy, A., Baracca, P., Braun, V., & Halbauer, H. (2016). Hardware Impairments in Millimeter Wave Communications using OFDM and SC-FDE. Proceedings of the 20th International ITG Workshop on Smart Antennas (WSA 2016), 127–134.

[55] R. Walden. "Analog-to-digital converter survey and analysis." In: IEEE Journal on Selected Areas in Communications 17.4 (1999), pp. 539–550.

[56] https://www.tutorialspoint.com/digital_communication/digital_communication_quantization.html (last acess, 16th of August of 2018)

[57] J. Max. "Quantizing for Minimum Distortion." In: IRE Transactions on Information Theory 6.1 (1960), pp. 7–12.